PROCESS SIMULATION, INTEGRATION AND OPTIMIZATION OF BLENDING OF PETRODIESEL WITH BIODIESEL

A Thesis

by

TING WANG

Submitted to the Office of Graduate Studies of
Texas A&M University
in partial fulfillment of the requirements for the degree of

MASTER OF SCIENCE

August 2008

Major Subject: Chemical Engineering

PROCESS SIMULATION, INTEGRATION AND OPTIMIZATION OF BLENDING OF PETRODIESEL WITH BIODIESEL

A Thesis

by

TING WANG

Submitted to the Office of Graduate Studies of
Texas A&M University
in partial fulfillment of the requirements for the degree of

MASTER OF SCIENCE

Approved by:

Chair of Committee,	Mahmoud M. El-Halwagi
Committee Members,	Sam M. Mannan
	Sergiy Butenko
Head of Department,	Michael Pishko

August 2008

Major Subject: Chemical Engineering

ABSTRACT

Process Simulation, Integration and Optimization of Blending of
Petrodiesel with Biodiesel. (August 2008)
Ting Wang, B.S., East China University of Science and Technology;
M.S., National University of Singapore
Chair of Advisory Committee: Dr. Mahmoud M. El-Halwagi

With the increasing stringency on sulfur content in petrodiesel, there is a growing tendency of broader usage of ultra low sulfur diesel (ULSD) with sulfur content of 15 ppm. Refineries around the world should develop cost-effective and sustainable strategies to meet these requirements. The primary objective of this work is to analyze alternatives for producing ULSD. In addition to the conventional approach of revamping existing hydrotreating facilities, the option of blending petrodiesel with biodiesel is investigated. Blending petrodiesel with biodiesel is a potentially attractive option because it is naturally low in sulfur, enhances the lubricity of petrodiesel, and is a sustainable energy resource.

In order to investigate alternatives for producing ULSD, several research tasks were undertaken in this work. Firstly, base-case designs of petrodiesel and biodiesel production processes were developed using computer-aided tools ASPEN Plus. The simulations were adjusted until the technical criteria and specifications of petrodiesel and biodiesel production were met. Next, process integration techniques were employed to optimize the synthesized processes. Heat integration for petrodiesel and biodiesel was carried out using algebraic, graphical and optimization methods to maximize the integrated heat exchange and minimize the heating and cooling utilities. Additionally, mass integration was applied to conserve material resources. Cost estimation was carried out for both processes. The capital investments were obtained from ASPEN ICARUS Process Evaluator, while operating costs were calculated based on the updated chemical market prices. The total operating costs before and after process integration were

calculated and compared. Next, blending optimization was performed for three blending options with the optimum blend for each option identified. Economic comparison (total annualized cost, breakeven analysis, return on investment, and payback period) of the three options indicated that the blending of ULSD with chemical additives was the most profitable. However, the subsequent life-cycle greenhouse gas (GHG) emission and safety comparisons demonstrated that the blending of ULSD with biodiesel was superior.

ACKNOWLEDGEMENTS

I would like to express my sincere gratitude to my advisor, Dr. El-Halwagi, for his technical and spiritual guidance and support during my graduate years. He is the one who made me realize the fascination and meaning of chemical process engineering, and who made me more and more passionate about being a true process engineer, with his wisdom, intelligence, sincerity and selflessness. I would also like to thank my committee members, Dr. Mannan and Dr. Butenko, for their support and advice on my coursework and research. My special thanks also go to Dr. Baldwin for his help and guidance in my research work.

I would also like to extend my gratitude to my friends and colleagues for their help and support, especially to Lay, Viet, René and Grace for their technical guidance and discussions on my research, and to Eva and Buping for their advice and moral encouragement.

Finally, I am sincerely thankful and grateful to my parents who support me when I confront setbacks, encourage me when I feel hesitant and depressed, and guide me when I cannot make up my mind. It is their patience, unconditional love and support that help me get through the difficult periods of my life journey, follow my interests and fulfill my dreams.

TABLE OF CONTENTS

CHAPTER Page

LIST OF FIGURES

FIGURE Page

LIST OF TABLES

TABLE Page

TABLE Page

CHAPTER I

INTRODUCTION

1.1 Petrodiesel Basics

Diesel or diesel fuel is a fractional distillate of petroleum fuel or a washed form derived from vegetable oils or animal fats that are used as fuels in a diesel engine invented by a German engineer Rudolf Diesel. Initially diesel stood for fuel that has been developed and produced from petroleum, but nowadays alternatives such as biodiesel or biomass to liquid (BTL) or gas to liquid (GTL) diesel, which are not produced from petroleum, are being developed and utilized. Therefore, the term "petrodiesel" is used in order to distinguish from those alternative diesel fuels. Petrodiesel is a hydrocarbon mixture obtained in the fractional distillation of crude oil with a temperature between 200 °C and 350 °C and 1 atm. The fractional distillation takes place in the distillation tower followed by a hytrotreating step.

1.2 Ultra Low Sulfur Diesel (ULSD) Regulation

In December 2000, the US Environmental Protection Agency (EPA) proposed a regulation on Heavy-Duty Engine and Vehicle Standards and Highway Diesel Fuel Sulfur Control Requirements, in order to reduce emissions of nitrogen oxides (NOx) and particulate matter (PM) from heavy-duty highway engines and vehicles which are fueled by diesels. The new rule specified that the sulfur content of on-road diesel need to meet an ultra low sulfur diesel (15 parts per million) maximum requirement. In addition, the sulfur content in pipelines are expected to keep below 10 ppm, due to a tolerance requirement for testing and post logistics concerns of ULSD such as contamination from higher sulfur products in the system during production, storage and transportation. The new specification of ULSD should be effective at terminals by July 2006 and at retail

_____

This thesis follows the style of Bioresource Technology.

stations and wholesalers by September 1, 2006 (EIA, 2001). Prior to this new stringent regulation for on-road diesel, there was only a low sulfur diesel (LSD) requirement with a sulfur content limit of 500 ppmw. This dramatic decrease of sulfur content from 500 ppmw to 15 ppmw poses a major challenge for ultra low sulfur diesel production. It also provides the driving force of technology innovation in petrodiesel production as well as alternative fuels identification and development.

1.3 Desulfurization of Petrodiesel

Since the essence of producing diesel that meets the new ultra low sulfur diesel (ULSD) regulation is to remove the sulfur components and to keep the sulfur content below the designated value, various desulfurization technologies or other alternative technologies which can help reduce the cost of desulfurization have been recently investigated. Desulfurization processes can be classified into two main parts: hydrodesulfurzation (HDS)-involved technologies and physico-chemical-involved sulfur removal technologies, based on the characteristics of the key physico-chemical process used for sulfur removal, as shown in Figure 1.1. The most developed and commercialized technologies are the processes which convert sulfur compounds with sulfur elimination in the presence of catalysts. Such catalytic conversion technologies include conventional hydrotreating, hydrotreating with advanced catalysts and/or reactor design, and a combination of hydrotreating with some additional chemical processes. The second desulfurization technologies mainly involve the application of physico-chemical processes to separate and/or to transform sulfur compounds from refinery streams, which are different from catalytic HDS in nature. These technologies include distillation, alkylation, oxidation, extraction, adsorption or a combination of these processes (Babich et al., 2003).

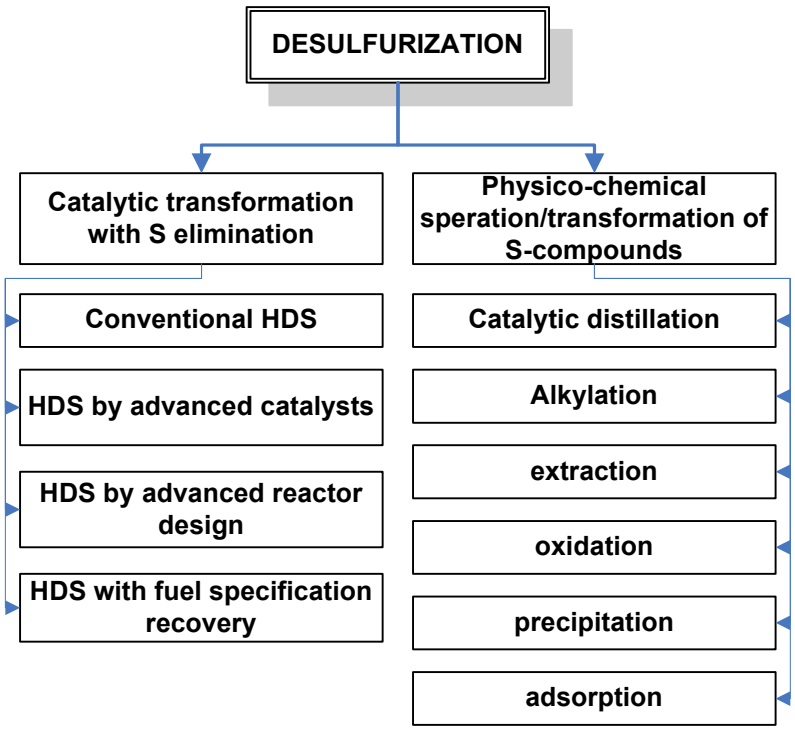

Figure 1.1 Desulfurization technologies classified by nature of a key process to remove sulfur (Babich et al., 2003)

Being driven by the EPA ULSD rule, a few new technologies which can help reduce the cost of diesel desulfurization have been identified and developed. These include sulfur adsorption, biodesulfurization, desulfurization by extractive photochemical oxidation, desulfurization by precipitation, and sulfur oxidation (EIA, 2001; Lee et al., 2003; Babich et al., 2003). However, they are still in the experimental phase of development and are unlikely to have significant effects on ULSD production in the very near future. In addition, although some other techniques have been developed to produce diesel fuel from natural gas and organic fats such as the Fisher-Tropsch diesel and biodiesel technology, they are still not cost-competitive. Refineries currently producing ULSD in limited quantities significantly rely on enhanced hydrotreating technology, which is the major method to produce ULSD at this time (EIA, 2001).

Conventional hydrotreating is a commercially proven refining process that inputs feedstock together with hydrogen through a hydrotreater to separate sulfur and other undesirable impurities from hydrocarbon molecules in the presence of catalysts. Various distillate streams in a refinery can be hydrotreated such as the straight-run streams directly following crude oil distillation, the streams coming out of the fluid catalytic cracking (FCC) unit, and the heavier streams that go through a hydrocracker. It is reported that over half of the streams used to produce low sulfur diesel (LSD, 500 ppmw) consist of straight-run distillate streams, which are the easiest and least expensive to treat (EIA, 2001; Lee et al., 2003).

There are two major distinct routes for sulfur removal by hydrotreating. The first route is direct hydrogenolysis. Almost all the simpler sulfur compounds such as mercaptans, sulfides, disulfides, thiophenes, and a majority of benzothiophenes (BT) and unsubstituted dibenzothiophenes are removed by this route. The Co/Mo HDS catalysts are the most effective in removing sulfur via this route, even under mild pressures. The second route needs to go through an aromatic saturation by partial hydrogenation of aromatic rings in the dibenzothiophene (DBT) molecules before the sulfur are removed by hydrogenolysis. This route is more effective with Ni/Mo catalysts and much slower than the direct hydrogenolysis route. Furthermore, the second route is heavily affected by hydrogen partial pressure and susceptible to thermodynamic equilibrium limitation (Hu et al., 2002).

The reactivity of sulfur compounds in hydrodesulfurization (HDS) has the following order (from most to least reactive): thiophene > alkylated thiophene > benzothiophenes (BT) > alkylated BT > dibenzothiophenes (DBT) and alkylated DBT without substituents at the 4 and 6 positions > alkylated DBT with one substituent at either the 4 or 6 position > alkylated DBT with alkyl substituents at the 4 and 6 positions. 4, 6-dimethyl-dibenzothiophene is one of the most unreactive and refractory sulfur compounds in the diesel range (Babich et al., 2003). Hu et al. (2002) indicated that

almost all of the remaining sulfur belongs to the dibenzothiophene (DBT) class when sulfur content in the diesel goes below 100 ppmw. Therefore, more and more unreactive and refractory sulfur compounds must be converted in order to achieve ULSD levels.

1.4 Revamping of Petrodiesel Production

Currently, some technologies have been demonstrated to be capable of producing diesel with a sulfur content of less than 10 ppm. Moreover, currently there exist some refineries which can produce diesel with sulfur in the 10 ppm range on the industry scale. However, the number of the refineries that can produce ULSD is quite limited and the emerging and promising technologies are either in the experimental stages or expensive to employ, which prevents ULSD from being produced on a large scale. Therefore, revamping and reconstruction of the main units or plants play a crucial role in widespread production of ULSD (EIA, 2001). Furthermore, revamping the existing units can also improve profitability and limit capital cost by maximizing the utilization of the existing facilities. Consequently, most refiners are considering revamps on existing hydrotreating units to meet the new ULSD regulation. Palmer et al. (2004) reported that 75-80 % of all ULSD refinery projects in US are hydrotreating units retrofitting.

Currently, there are widespread studies of ULSD on laboratory, pilot plant, and industry scales. Knudsen et al. (2008) reviewed several important factors governing the production of ultra low sulfur diesel, especially the factors affecting the kinetics of desulfurization reaction with the inhibiting effect of certain nitrogen-containing components of diesel fuel. They illustrated the effect of catalyst choices on required catalyst volume, hydrogen consumption and product properties with a few cases studies. The advantages of revamps versus grassroots units were also discussed based on the case study results. Li et al. (2001) discussed the revamp options in details followed by the test run and case study results. With the comparison of the case studies, they concluded that the unit can produce ULSD with less than 10 ppm sulfur with a typical feedstock combination of straight run gas oil (SRGO) and fluid catalytic cracking (FCC LCO) by

substituting two small reactors with a larger reactor and proper changes of operation conditions. Palmer et al. (2004) not only gave a brief review on the theoretical fundamentals of retrofitting for ULSD production, but also identified the capital investment costs for revamping an existing diesel hydrotreater to meet the ultra low sulfur diesel standard. The base case was a typical plant that was commissioned in the early nineties to produce the low sulfur diesel (LSD). Revamp options were evaluated for hydrotreaters originally designed with and without recycle gas amine scrubbing (Palmer et al., 2001). Ackerson et al. (2004) discussed the kinetics and hydrogen requirement limits to ULSD production and the impact these limits have on the design of a conventional unit revamp. They also showed the advantages of the new IsoTherming technology in overcoming the challenges of ULSD production in the most cost-competitive way, and concluded that refiners can minimize the capital cost with the new IsoTherming technology. Bharvani et al. (2002) studied the limits on existing equipments, the costs for replacement and unit design parameters and showed that the revamp of an existing hydrotreater for ULSD production is a feasible option and should be seriously considered since it is an effective utilization of existing assets.

Other than the revamp studies, investigation for grassroots hydrotreater that can produce ULSD were also widely performed. Harwell et al. (2003) presents a comprehensive overview of design considerations for grassroots ULSD hydrotreaters. Engineering aspects such as an appropriate operating pressure level that satisfies reaction conditions and the practical limits of piping mechanical design were discussed, followed by process simulations for different process configurations, and capital costs and life cycle costs estimations for three cases.

The revamp options for ULSD production include (Li et al., 2001)

- Use of improved catalyst
- Adjustment of feed end point and feed composition
- Improvement of reactor efficiency

- Increase of operating temperature
- Increase of hydrogen-to-oil ratio
- Removal of H_2S from the treat gas
- Increase of hydrogen partial pressure

1.4.1 New Improved Catalysts

Recent developments for hydrotreating catalysts have significantly improved sulfur removal abilities. There are several major catalyst manufacturers which can provide catalysts with enhanced desulfurization activity.

With the development of the new catalyst manufacturing technology, Akzo Nobel introduced new highly active CoMo and NiMo catalysts which are called STARS (Super Type II Active Reaction Sites) commercially. Under normal hydrotreating operating conditions, STARS can reduce the sulfur in the streams down to 2–5 ppm, and can improve the cetane number and density of diesel fuels. Other highly active hydrotreating catalysts from Akzo Nobel, the so-called NEBULA catalysts (NEBULA, NEw BULk Activity) are reported to be applicable in diesel hydrotreating both at mild conditions and at high pressure. The hydrogen consumption is relatively high than STARS and the NEBULA catalysts have already been applied in two commercial plants (Babich et al., 2003). The NEBULA catalysts not only provide high activity in hydrodesulfurization (HDS), but also in hydrodenitrogenation (HDN) and aromatics saturation (HDA) (Courier 11 and 4). In reactor volume-limited units, a combination of STARS and NEBULA catalysts may allow the refiners to produce ULSD while still maintaining the expected cycle length.

The CENTINEL catalysts introduced by Criterion Catalysts and Technologies are claimed to possess both superior hydrogenation activity and selectivity. CoMo CENTINEL catalysts are more effective at lower hydrogen pressures and for high sulfur

content streams, while NiMo CENTINEL catalysts are preferred for low sulfur content (below 50 ppm) under higher H2 pressures (Babich et al., 2003).

Catalysts TK 573 and TK 574 from Haldor Topsoe AS, Lyngby, Denmark are also reported to enhance desulfurization activity by 25-75 % more than the catalysts used in the 1990s (Li et al., 2001).

1.4.2 Adjustment of Feed End Point and Feed Composition

Theoretically sulfur in the higher boiling range is more difficult to convert. Therefore lowering the end point of the feedstock is an efficient way to help meet the ULSD specification by cutting out big portion of the refractory sulfur compounds contained in high end point streams and highly aromatic feedstocks such as light cycle oil (LCO) and coker LGO. The feedstock straight-run (SR) kerosene and light gas oil (LGO) has lower end point and is thus easier to produce ULSD when combined with the utilization of high activity catalysts. However, there are several challenges associated with this option that need to be taken into account. The first one is that the removal of these heavier fractions can decrease the amount of ULSD produced significantly. The other one is that refiners have to find a home for the high end point materials (Li et al., 2001; Bharvani et al., 2002).

1.4.3 Improvement of Reactor Efficiency

Improved vapor-liquid contacting or longer residence time in the hydrotreating reactors can significantly decrease the temperature required to achieve the same level of desulfurization and in turn to enhance desulfurization. The decrease of liquid hourly space velocity (LHSV) or the increase of vapor-liquid contact time can greatly reduce the product sulfur content. The reduction of the liquid hourly space velocity (LHSV) can be achieved by adding more catalysts. The additional amount of catalyst volume depends on the characteristics of the feedstock such as the distribution and composite of the sulfur in the compounds. Significant increases of catalyst volume (e.g., 5-10 times of the

existing size) may be required if the feedstock contains a large amount of light cycle oil (LCO) (Li et al., 2001; Bharvani et al., 2002).

1.4.4 Increase of Operating Temperature

Increasing the reactor operating temperature significantly influences the desulfurization capability. The product sulfur content greatly decreases with the operating temperature. However, this option has limited effectiveness due to the mercaptan equilibrium and a shorter catalyst life cycle length (Bharvani et al., 2002).

1.4.5 Increase of Hydrogen-to-Oil Ratio

Increasing the treat gas rate (hydrogen-to-oil ratio) can enhance the desulfurization activity of the catalysts by reducing the inhibition effect of hydrogen sulfide and ammonia. The treat gas rate primarily depends upon the existing hydraulics or compressor capacity in the plants or units (Bharvani et al., 2002).

1.4.6 Removal of H_2S from the Treat Gas

The catalyst desulfurization activity can be improved by the removal of H_2S from the treat gas (recycle gas plus make-up gas). The recycle hydrogen stream can be scrubbed to remove H_2S (Li et al., 2001). If the hydroprocessing unit does not have a recycle gas scrubber, the highly concentrated H_2S would inhibit the desulfurization reaction. The reactor temperature must then be increased significantly to offset the hydrogen sulfide inhibition effect (Bingham et al., 2000).

1.4.7 Increase of Hydrogen Partial Pressure

Increasing the hydrogen partial pressure not only improves sulfur removal capabilities, but also extends the catalyst life cycle length (Bharvani et al., 2002).

Since every refiner might use different feedstock and possess different processing facilities and equipments, the revamp options to produce ULSD are site-specific and

unique. In many cases, in order to meet the refiners' needs with the lowest capital investment, a combination of these revamp options is usually employed (Li et al., 2001).

1.5 Lubricity and Cetane Issues of ULSD

Although it has been reported that revamping the existing diesel plants was feasible on both pilot-plant and industrial scales (Li et al., 2001; Bharvani et al., 2002; Ackerson et al., 2004; Palmer et al., 2004), there exist other challenges other than the desulfurization technologies, such as the lubricity and cetane issues.

1.5.1 Lubricity

Currently, the lubricity issue is phenomenal and critical for ultra low sulfur diesel (ULSD) fuels, due to the increasing failure or damage of engine parts such as fuel pumps and injectors caused by low sulfur diesel (LSD) fuels and especially the recent ultra low sulfur diesel (ULSD) fuels, as specified by the regulations of EPA. The reason for the poor lubricity of LSD and ULSD is not the removal of the sulfur compounds themselves but rather that polar compounds with other heteroatoms such as oxygen and nitrogen are also reduced or removed during the desulfurization processes (Knothe et al., 2005). Therefore, in order to enhance the lubricity, LSD and ULSD requires additives or blending with another fuel of sufficient lubricity.

Diesel fuel and other fluids are tested for lubricity using a device called a "High Frequency Reciprocating Rig" or HFRR. Currently, the HFRR method is the internationally accepted, standardized method to evaluate the lubricity of the test fluids. It uses a ball bearing that reciprocates or moves back and forth on a metal surface at a very high frequency for a duration of 90 minutes. The machine does this while the ball bearing and metal surface are immersed in the treated diesel fuel. At the end of the test the ball bearing is examined under a microscope and the "wear scar" on the ball bearing is measured in microns. The lubricating ability of the fluid reduces as the wear scar increases (Spicer, 2007).

The US standard for diesel fuels (ASTM D 975) requires that the diesel fuel should produce a wear scar less than 520 microns, whereas the Engine Manufacturers Association (EMA) had requested a standard of a wear scar less than 460 microns for diesel fuels. It is suggested by most experts that a 520 micron standard is adequate, but also that the lower the wear scar the better (Spicer, 2007).

1.5.2 Cetane Number

Cetane number is a direct indication of the readiness of auto-ignition of a fuel when the fuel is injected into a diesel engine (Gerpen, 2008). The number is a measure of the ignition delay which is the period that occurs between the start of fuel injection and the start of combustion. Good quality combustion occurs with rapid ignition followed by smooth and complete fuel burn. A fuel with higher cetane number has shorter ignition delay, leading to a complete and better quality of combustion. Conversely, low cetane number fuels are slow to ignite and hence poor combustion occurs. These poor combustion characteristics can give rise to excessive engine noise and vibration, increased exhaust emissions and reduced vehicle performance together with increased engine stress. Excessive smoke and noise are also crucial issues associated with diesel vehicles, particularly under cold starting conditions (BP, 2008).

1.6 Blending of ULSD with Biodiesel

Blending of biodiesel into ULSD can solve or at least mitigate the lubricity and cetane issues of ULSD, which is quite promising and attractive. As a matter of fact, biodiesel has already been widely produced and used as an effective blending additive and an alternative fuel as well (DOE, 2006).

1.6.1 Biodiesel Basics

Biodiesel is a fuel that is derived from organic fats such as vegetable oils, animal fats or waste cooking greases or oils. The biodiesel production processes convert oils and fats

into chemicals called long chain mono alkyl esters, or biodiesel (DOE, 2006). As an alternative diesel fuel, it is gaining more and more attention. The production and usage of biodiesel have increased significantly in many countries around the world. Biodiesel offers many advantages as follows (DOE, 2006):

- Little or no engine modifications are required when it is used in most engines as an alternative fuel or blending additive.
- It reduces greenhouse gas (GHG) emissions.
- It reduces tailpipe emissions or air toxics such as carbon monoxide (CO), hydrocarbons (HC) and particulate matter (PM).
- It is nontoxic, biodegradable and renewable.
- It is made domestically in US from either agricultural or recycled resources, leading to less dependence on crude oil import.
- It is easy to use if guidelines are followed.
- It has a much higher flash point compared to petrodiesel, giving rise to better stability than petrodiesel.

Biodiesel can be used in several different ways. The first way is to add 1 % to 2 % biodiesel as a lubricity additive into ULSD which possesses poor lubricity due to the removal of the polar compounds during the desulfurization process. The second way is to blend up to 20 % biodiesel with other diesel fuels (B20) which can be used in most applications that use diesel fuel. Pure biodiesel (B100) can also be used with proper precautions taken. The letter "B" represents biodiesel, and the numbers following the "B" indicate the percentage of biodiesel in a gallon of fuel. The other blending fuels of the gallon can be diesel, kerosene, jet A, JP8, heating oil, or any other distillate fuel. Hence B100 stands for pure biodiesel, and B20 indicates the blend of 20% biodiesel with 80% other fuels (DOE, 2006).

1.6.2 Effect of Biodiesel on Petrodiesel Lubricity and Cetane Number

Based on comprehensive literature reviews, it has been demonstrated that biodiesel is a very effective lubricant, which is crucial for ULSD with poor lubricating properties. The US Department of Energy (DOE, 2006) reported that 2 % biodiesel is adequate enough to restore sufficient lubricity to dry fuels such as kerosene or Fischer-Tropsch diesel. 2% biodiesel blended fuels (B2) are commonly used for the purpose of improving lubricity properties instead of using other additives in some vehicles (DOE, 2006). It was also reported by Knothe et al. (2005) that neat biodiesel has naturally greater lubricity than petrodiesel, especially ultra low sulfur diesel (ULSD), and that adding biodiesel at low blend levels (1 %-2 %) can help ULSD regain adequate lubricity. Such effectiveness was reported for even lower (<1 %) blend levels or higher (10 %-20 %) levels as well. Knothe et al (2005) indicated that the lubricity of low-level blends (1 %-2 %) of biodiesel with low-lubricity petrodiesel is mainly due to the existence of free fatty acid (FFA) and monoacylglycerol contaminants in the biodiesel. Hu et al. (2005) demonstrated that methyl esters and monoglycerides are the main components which decide the lubricity of biodiesels meeting the international standards. Free fatty acids (FFA) and diglycerides can also affect the lubricity of biodiesel, but not so much as monoglycerides do, but triglycerides almost have no effects on the lubricity of biodiesel itself.

Generally, the cetane number of biodiesel is observed to be quite high. Gerpen (2008) summarized the cetane values of biodiesel derived from different feedstocks and found that the soybean-based methyl esters have cetane numbers varying between 45 and 67. Petrodiesel normally has lower cetane number than biodiesel. In the United States, No. 2 diesel fuel usually has a cetane number between 40 and 45 (Gerpen, 2008). The cetane number of biodiesel depends on the distribution of fatty acids in the feedstocks. The longer the fatty acid carbon chains and the more saturated the molecules, the higher the cetane number. Biodiesel produced from unsaturated vegetable oils such as soybean oil normally have a lower cetane number (Gerpen, 2008; DOE, 2006). Since biodiesel tends

to have higher cetane numbers than diesel, it would therefore improve the lubricity of the petrodiesel and operation of the engine when blending into the petrodiesel with poor lubricating properties (Department of the Environment and Heritage, 2004).

1.6.3 Challenges in Blending ULSD with Biodiesel

Although biodiesel is technically competitive with petrodiesel and requires no or little modification of diesel engines for application (Knothe et al., 2005), biodiesel faces some technical challenges or hurdles when blended into petrodiesel due to the following drawbacks or constraints of biodiesel itself.

- Nitrogen oxide (NOx) emission

Biodiesel has been shown to increase nitrogen oxide (NO_X) emissions in many engines by engine stand tests (DOE, 2006). The emissions of PM, CO, HC greatly decrease with the percentage of biodiesel, however, the emission of NO_X increases steadily. Although biodiesel itself does not contain nitrogen, NO_X is created in the engine when the nitrogen in the intake air reacts with oxygen at the high in-cylinder combustion temperatures. It is reported that the soybean-based biodiesel produces the highest NO_X increase (DOE, 2006), and pure biodiesel (B100) is estimated to produce between 10 % and 25 % more nitrogen oxide tailpipe-emissions than petrodiesel (wikipedia explanation of ultra low sulfur diesel, 2008).

- Cold flow properties of biodiesel

Another critical drawback of biodiesel is its less favorable cold flow properties compared to petrodiesel. Unlike gasoline, biodiesel can start to freeze or gel when the temperatures get colder. If the fuel begins to gel, it can clog filters and eventually it become so thick that it can not be pumped from the fuel tank to the engine (DOE, 2006). The temperature at which pure biodiesel starts to gel varies significantly and depends on the mixtures of esters and therefore the feedstock oil used to produce the biodiesel. For example, biodiesel produced from low erucic acid varieties of canola seed (RME) starts to gel at approximately -10 ^{o}C, and the biodiesel produced from tallow tends to gel at around 16 ^{o}C (wikipedia explanation of ultra low sulfur diesel, 2008).

- Prices

The biodiesel retail price is always higher than that of petrodiesel. The size of the cost difference depends on the size of the biodiesel producers, their feedstock costs, transportation costs, production incentives, tax incentives, and other local variables. Although biodiesel is currently more expensive than petrodiesel, this difference is believed to be diminished with the development of biorefineries, the rising costs of crude oil and government tax subsidies (wikipedia explanation of ultra low sulfur diesel, 2008). Based on the EIA ULSD price and DOE biodiesel price reports, in October 2007, the biodiesel and ULSD retail prices (after tax) are $3.39 and $ 3.05, respectively; in January 2008, they are $ 3.69 and $ 3.32 and in May 2008, they are $ 5.05 and $ 4.50, respectively.

- Energy content

Biodiesel contains 8 % less energy per gallon or 12.5 % less energy per pound than typical No. 2 diesel in the United States (DOE, 2006).

- Biological solvent

Biodiesel is derived from biological resources such as vegetable oils and animal fats or grease, which renders the biological nature of biodiesel. Microorganism can grow in biodiesel with a higher chance than in petrodiesel. In blends over 20 % biodiesel, biodiesel has a biological solvent effect, which may release deposits accumulated on tank walls and pipes from previous diesel fuel. The release of deposits may clog filters and thus precautions should be taken when using biodiesel fuels (Meadbiofuel, 2008).

- Contamination by water

Water is the major source of biodiesel contamination. Biodiesel leaving a production facility might be water-free, but water is introduced when the humidity in the air enters fuel tanks though vents and seals, and contacts with biodiesel in the existing distribution and storage network. Furthermore, there may be water residual that resulted from storage tank condensation and processing units (Gerpen et al., 1996; wikipedia explanation of ultra low sulfur diesel, 2008).

Water in the fuel generally causes four problems. First of all, water can cause corrosion of major fuel system parts such as fuel pumps and injector pumps. The most direct form of corrosion is rust, but water can become acidic with time and the resulting acid corrosion can attack fuel storage tanks. The second major problem associated with water contamination is that water can accelerate microbial growth. The microbe colonies can plug up a fuel system. Some of the organisms can convert the sulfur in the fuel to sulfuric acid which can corrode metal fuel tanks. Thirdly, water reduces the heat of combustion of the bulk fuel, which means more smoke and less energy content when biodiesel is combusted. Furthermore, water freezes to form ice crystals near 0 ^{o}C (32 ^{o}F). These crystals provide sites for nucleation and accelerate the gelling of the residual fuel (Gerpen et al., 1996; wikipedia explanation of ultra low sulfur diesel, 2008).

1.7 ASTM Biodiesel and Diesel Standards

The American Society for Testing and Materials International (ASTM) specification for biodiesel (B100) is ASTM D6751, which is summarized in Table 1.1. This specification is to ensure the quality of biodiesel to be used as a blend stock at 20% and lower blend levels. Any biodiesel used in the United States for blending should meet this standard before blending (DOE, 2006).

Table 1.1 ASTM biodiesel standard (ASTM D6751) (NBB, 2007)

Property	Test Method	Limits	Units
Flash point	ASTM D93	130 min.	°C
Water and Sediment	ASTM D2709	0.050 max.	% vol.
Kinematic Viscosity, 40°C	ASTM D445	1.9-6.0	mm²/sec
Sulfated Ash	ASTM D874	0.020 max.	% mass
Sulfur (S15)	ASTM D 5453	0.0015 max. (15)	% mass (ppm)
Sulfur (S500)	ASTM D5453	0.05 max. (500)	% mass (ppm)
Copper Strip Corrosion	ASTM D130	No. 3 max.	
Cetane Number	ASTM D613	47 min.	
Cloud Point, °C	ASTM D2500	report	°C
Carbon Residue	ASTM D4530	0.050 max.	% mass
Acid Number	ASTM D664	0.80 max.	mg KOH/g
Free Glycerin	ASTM D6584	0.020	% mass
Total Glycerin	ASTM D6584	0.240	% mass
Phosphorous Content	ASTM 4951	10 max	ppm
Distillation, T90 (90%)	ASTM D1160	360 max	°C

The US standard for petrodiesel is ASTM D975, as summarized in Table 1.2, and no specific standards are available for ULSD currently. However, the Engine Manufacturers Association (EMA) recommends that all ULSD fuels distributed in North America meet the requirements of ASTM D975. Furthermore, the following additional performance requirements are also recommended by Engine Manufacturers Association (2008):

- Cetane. Using ASTM D 613, ULSD fuel should have a minimum cetane number of 43. Although ASTM D975 currently requires a minimum cetane number of 40, EMA has asked ASTM to revise the standard to require a minimum cetane number of 43. EMA suggest that such an increase will improve the other technical performances of ULSD, such as white smoke, engine starting and engine combustion noise.

- Lubricity. As mentioned in section 1.5, ASTM D975 currently requires lubricity specified as a maximum wear scar diameter of 520 micrometers using the HFRR test method (ASTM D6079) at a temperature of 60°C. However, fuel injection equipment manufacturers have required that ULSD fuels have a maximum wear scar diameter of 460 micrometers, based on testing conducted on ULSD fuels. EMA also recommends that the lubricity specification be consistent with the fuel injection equipment manufacturers' recommendation.

Table 1.2 ASTM D975 diesel fuel specification (sources: Biodiesel Association of Canada, 2008)

Property	Test Method	Limits	Units
Flash point	ASTM D93	52 min.	^{o}C
Water and Sediment	ASTM D2709	0.050 max.	% vol
Kinematic Viscosity, 40^{o}C	ASTM D445	1.9 - 4.1	mm²/sec
Ash	ASTM D482	0.01 max.	% mass
Sulfur (Grade No. 2)	ASTM D129	0.50 max.	% mass
Sulfur(Grade No. 2-Low Sulfur)	ASTM D2622	0.05 max.	% mass
Copper Strip Corrosion	ASTM D130	No. 3 max.	
Cetane Number	ASTM D613	40 min.	^{o}C
Pour point	ASTM D97	—	^{o}C
Cloud Point, ^{o}C	ASTM D2500	Depends on location	% mass
Density, 15^{o}C	ASTM D1298	—	kg/m^3
Ramsbottom Carbon Residue	ASTM D524	0.35 max.	mg KOH/gm
Cetane Index	ASTM D976	40 min.	
Aromaticity	ASTM D1319	35 max.	% vol
Distillation T90 (90%)	ASTM D86	282-338	^{o}C
Lubricity, HFRR @60^{o}C	ASTM D6079	520 max.	microns

1.8 Biodiesel Production Processes

1.8.1 Transesterification

Transesterification, a catalyzed chemical reaction involving vegetable oil and an alcohol to yield fatty acid alkyl esters, or biodiesel and glycerol, is the most common way to produce biodiesel on the industrial scale. Triglycerides, as the main component of vegetable oil, consist of three long chain fatty acids esterified to a glycerol backbone. One mole of triglycerides react with three moles of an alcohol (e.g., methanol) can produce three moles of fatty acid alkyl esters (e.g. fatty acid methyl esters or FAME) with one mole of byproduct glycerol. The reaction is reversible, as shown below in Figure 1.2. Transesterification reactions can be alkali-catalyzed, acid-catalyzed or enzyme-catalyzed. The first two types have gained more attention than the last one, as the enzyme-catalyzed system requires a much longer reaction time than the former two systems. Currently, the enzyme-catalyzed transesterification has only been carried out on the laboratory scale (Zhang et al., 2003).

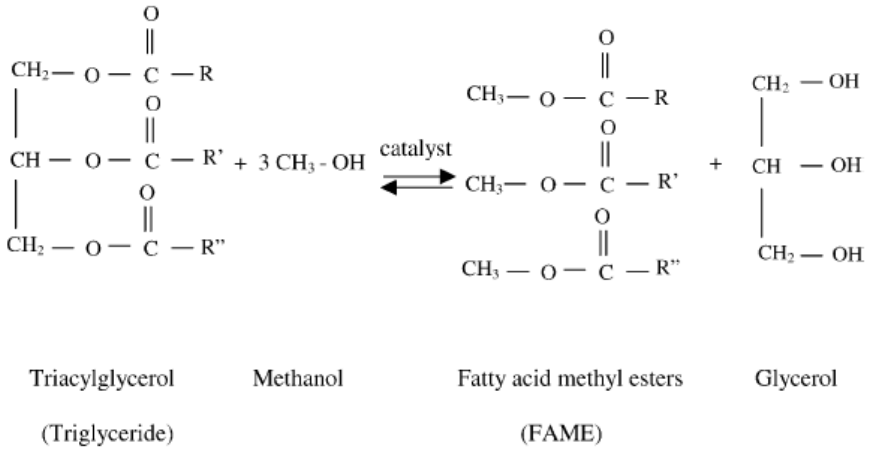

Figure 1.2 A schematic representation of the transesterification of triglycerides (vegetable oil) with methanol to produce fatty acid methyl esters (biodiesel) (Zhang et al., 2003)

1.8.2 Feedstocks for Biodiesel Production

The primary feedstocks for the production of biodiesel include vegetable oils, animal fats and greases, recycled or waste oils and greases. These materials contain triglycerides, free fatty acids, and other contaminants depending on the degree of pretreatment implemented on these materials. The other major feedstock is the primary alcohol which is used to form the ester, as biodiesel is a mono alkyl fatty acid ester. Although other alcohols, such as ethanol, isopropanol, and butyl, can be used, methanol is the most commonly applied due to its low cost. Excessive methanol is needed in order to facilitate the reversible transesterification to shift far to the right (Zhang et al., 2003). The most common catalysts used are strong bases such as sodium hydroxide (NaOH) and potassium hydroxide (KOH). After transesterification, the base catalyst will be neutralized with a strong acid to avoid the formation of soaps and emulsions, the presence of which would prevent subsequent biodiesel and glycerol purification and recovery (Zhang et al, 2003; Gerpen et al., 2004).

1.8.3 Effect of Free Fatty Acid

Many feedstocks with low costs such as the waste cooking oils or greases are available for biodiesel production. However, many of these feedstocks contain large amounts of free fatty acids (FFAs). The existence of excess free fatty acid gives rise to lower conversion of transesterification, because the excess free fatty acids will react with alkali catalysts to produce soaps that inhibit the reaction. The formation of soaps promotes the emulsification and leads to difficulties in the separation of the glycerol and ester phases and subsequent purification and recovery of biodiesel and glycerol. Soap formation also produces water that can hydrolyze the triglycerides and contribute to the formation of more soap (Gerpen et al., 2004). Therefore, to keep the free fatty acid level as low as possible is crucial and pretreatment step is necessary for feedstocks with high FFA levels such as waste cooking oils. Typically for a base-catalyst transesterification, a free fatty acid (FFA) value lower than 3% is recommended (Meher et al., 2006). The ranges of FFA for commonly used biodiesel feedstocks are shown in Table 1.3.

Table 1.3 Ranges of free fatty acids (FFAs) for commonly used biodiesel feedstocks (Gerpen et al., 2004)

Feedstocks	Free Fatty Acid (FFA) amount
Refined vegetable oils	< 0.05 wt%
Crude vegetable oil	0.3-0.7 wt%
Restaurant waste grease	2 - 7 wt%
Animal fat	5 – 30 wt%
Trap grease	40 -100 wt%

Studies of acid-catalyzed transesterification are very limited and no industrial biodiesel processes are reported nowadays simply due to the fact that the acid-catalyzed transesterification possesses relatively slower reaction rate than the alkali-catalyzed transesterification. However, acid-catalyzed transesterification is not sensitive to free fatty acid amounts in the feedstocks. This advantage makes the acid-catalyzed systems a potential scheme to produce biodiesel. Zhang et al. (2003) demonstrated that the acid-catalyzed process using waste cooking oil is technically feasible with less complexity than the base-catalyzed process using waste cooking oil and therefore it would be a competitive alternative or supplement to the base-catalyzed biodiesel production processes.

1.8.4 Catalyst Selection

Catalysts used for the transesterification of triglycerides can be categorized into alkali, acid, enzyme or heterogeneous catalysts, among which alkali catalysts like sodium hydroxide, sodium methoxide, potassium hydroxide, and potassium methoxide are more effective. If the oil has high free fatty acid content and more water, acid catalyzed transesterification is suitable. The acids could be sulfuric acid, phosphoric acid, hydrochloric acid or organic sulfonic acid. As the catalysts in the base-catalyzed transesterification, sodium hydroxide (NaOH) or potassium hydroxide (KOH) are the most commonly used, typically with a concentration range of 0.4 to 2 wt % of oils.

Refined and crude oils with 1 % either NaOH or KOH catalyst resulted in good conversion (Haas et al., 2006; Meher et al., 2006).

1.8.5 Multiple-Stage Transesterification Systems

As mentioned in the section 1.8.1, the transesterification reaction is reversible and equilibrium would eventually be achieved. After the transesterification in one stage, the biodiesel contains unreacted oils in the terms of glycerides. In the final equilibrium of the transesterificaiton reaction there are considerate amounts of triglycerides, diglycerides, and monoglycerides. In order to obtain higher conversion of the feedstocks and to produce as much biodiesel as possible, the equilibrium can be shifted to the right using a multistage transesterification process (Encinar et al., 2007). Furthermore, the multiple-stage transesterification can lead to the reduction of excess alcohol (Wimmer, 1995). Therefore, multi-stage transesterification and multi-step operating units are widely studied and implemented for both batchwise and continuous biodiesel production processes. Several patents were also drawing attention on the multi-stage transesterification of organic oils or fats to produce biodiesel fuel.

Connemann et al. (1998) reported that most biodiesel plants in the world within the capacity range of 500-10,000 tons/yr are built as two-step batchwise operating units, each step consisting of a reactor vessel and a settling tank, so-called mixer or settler systems. Ma et al. (1999) mentioned in the biodiesel production review paper that Zhang studied the transesterification of edible beef tallow with a free fatty acid amount of 0.27 wt %. Transesterification was carried out with 6:1 molar ratio of methanol to tallow, 1 wt% NaOH dissolved in the methanol at 60 °C for about 30 min. After the separation of glycerol in the settling tank, the second transesterification of the unreacted tallow was carried out again using 0.2 % NaOH and 20 % methanol at 60 °C for about 1 h. The mixtures were washed with distilled water until the wash water was clear. In addition, the well-known Henkel transesterification technology contains two tube reactors followed by settling vessels with the operating pressure of 4-5 bars and the temperature

of 70-80 ^{o}C (Connemann et al., 1998). Two sequential transesterification reactions of soybean oils with methanol, catalyzed by sodium methoxide (NaOMe), were modeled by Haas et al. (2006). These continuous reactions were conducted in stirred tank reactors at 60 ^{o}C. The first reactor was continuously fed with soybean oil and 1.78 wt % sodium methoxide. Product was removed from the reactor with a flow rate equals to the input flow rate of reactants and catalyst in order to obtain a residence time of 1 h and to maintain steady state in the stirred reactor. After the first transesterification reaction, continuous centrifugation is employed to separate the byproduct glycerol from the glycerol-rich phase and the removed glycerol is subsequently sent to the glycerol recovery unit. The methyl ester phase, which contains unreacted methanol, soybean oil and catalyst, is fed into a second stirred tank reactor for further transesterification with the addition of sodium methoxide and methanol. Again, the second reaction is conducted at the same temperature with a discharge rate of products equals to the input rate. An overall conversion of 99 % of the feedstock was used with assuming transesterification efficiency in both reactors is 90 %. Tapasvi et al (2005) modeled a two-stage continuous biodiesel production process with a base catalyst followed by ester washing, methanol recovery and glycerol refining. An overall transesterification efficiency of 98 % was assumed, and the methanol to triglyceride mole ratio of 6:1 was used. Encinar et al. (2007) studied the transesterification reaction of used frying oil with ethanol, using various base catalysts such as sodium hydroxide, potassium hydroxide, sodium methoxide, and potassium methoixde. Ethanol/oil molar ratio (6:1-12:1), catalyst concentration (0.1-1.5 wt %) and temperature (35-78 ^{o}C) were used as the operation variables. They demonstrated that the two-stage transesterification is better than the one-stage process by reporting the yields of ethyl esters 30 % higher than those in one-stage transesterification.

CHAPTER II

PROBLEM STATEMENT

The problem to be addressed in this work is stated as follows:

Given a refinery with a certain production and characteristics of low-sulfur diesel (LSD), it is desired to upgrade the diesel production to ultra-low sulfur diesel (ULSD) of certain production and characteristics (e.g., sulfur content, cetane number, etc.). Potential alternatives are to be considered. These include retrofitting of the refinery (e.g., addition of hydrotreating units), usage of special additives or blending with biodiesel are also considered, assessed, and screened.

The questions to be addressed include:

- How should the refinery be retrofitted to meet ULSD regulations?
- How should the special additives be used to provide required characteristics of the ULSD?
- What is the optimal design of a biodiesel facility?
- What is the optimal blending strategy of petrodiesel with biodiesel?

The specific tasks of this work include

- Development of base-case designs of biodiesel and petrodiesel production processes
- Optimization of biodiesel and petrodiesel production processes
- Techno-economic evaluation of biodiesel and petrodiesel production processes
- Identification of optimum blending strategy of petrodiesel with biodiesel
- Analysis of the impact of greenhouse gas policies on the process design and blending characteristics

In order to achieve the abovementioned objectives, the work being carried out includes:

- Process synthesis with the base-case flowsheets

- Base-case process simulations and sensitivity analysis using computer-aided tools
- Mass and heat integration of biodiesel and petrodiesel processes
- Cost estimation of biodiesel and petrodiesel production processes
- Blending optimization of three blending options
- Economic evaluation and comparison of the optimum blends of each blending option
- Life-cycle greenhouse gas emission assessment and safety comparison of the three blending options

CHAPTER III

APPROACH AND METHODOLOGY

3.1 Approach

Three blending options are investigated in this work. The first option is to blend low sulfur diesel (LSD) with biodiesel, the second one is to blend ultra low sulfur diesel (ULSD) with biodiesel, and the third one is the blending of ULSD with commercial chemical additives. The three options are shown in Figure 3.1. For each alternative, an approach is developed. Figures 3.2a, 3.2b, 3.2c show schematically the approach for each option. After all the blending options are optimized, the three options are compared from economic, safety and environmental perspectives.

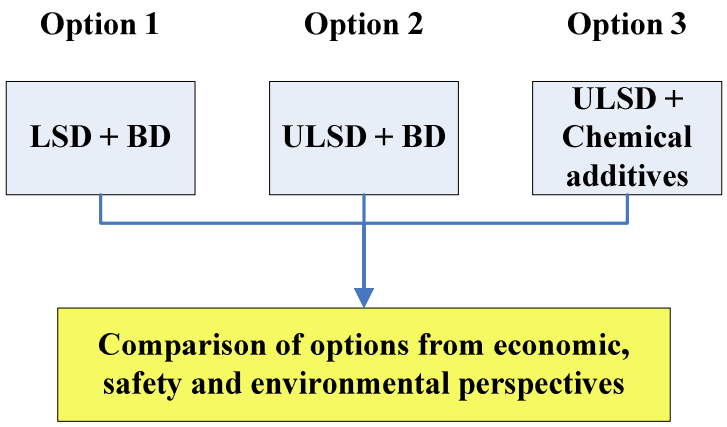

Figure 3.1 Overall blending options in this work

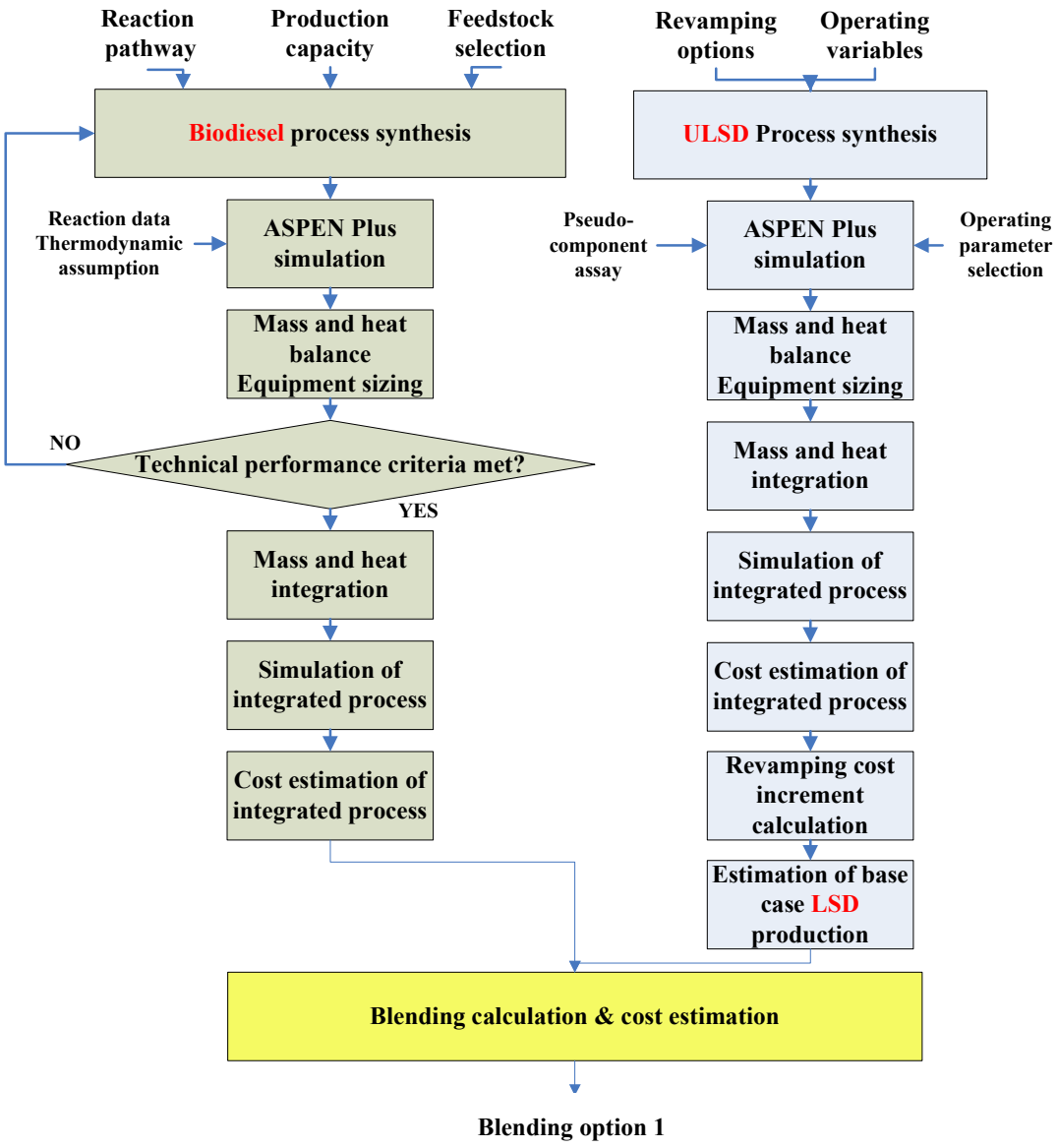

(a)

Figure 3.2 Approaches for (a) blending option 1; (b) option 2; (c) option 3

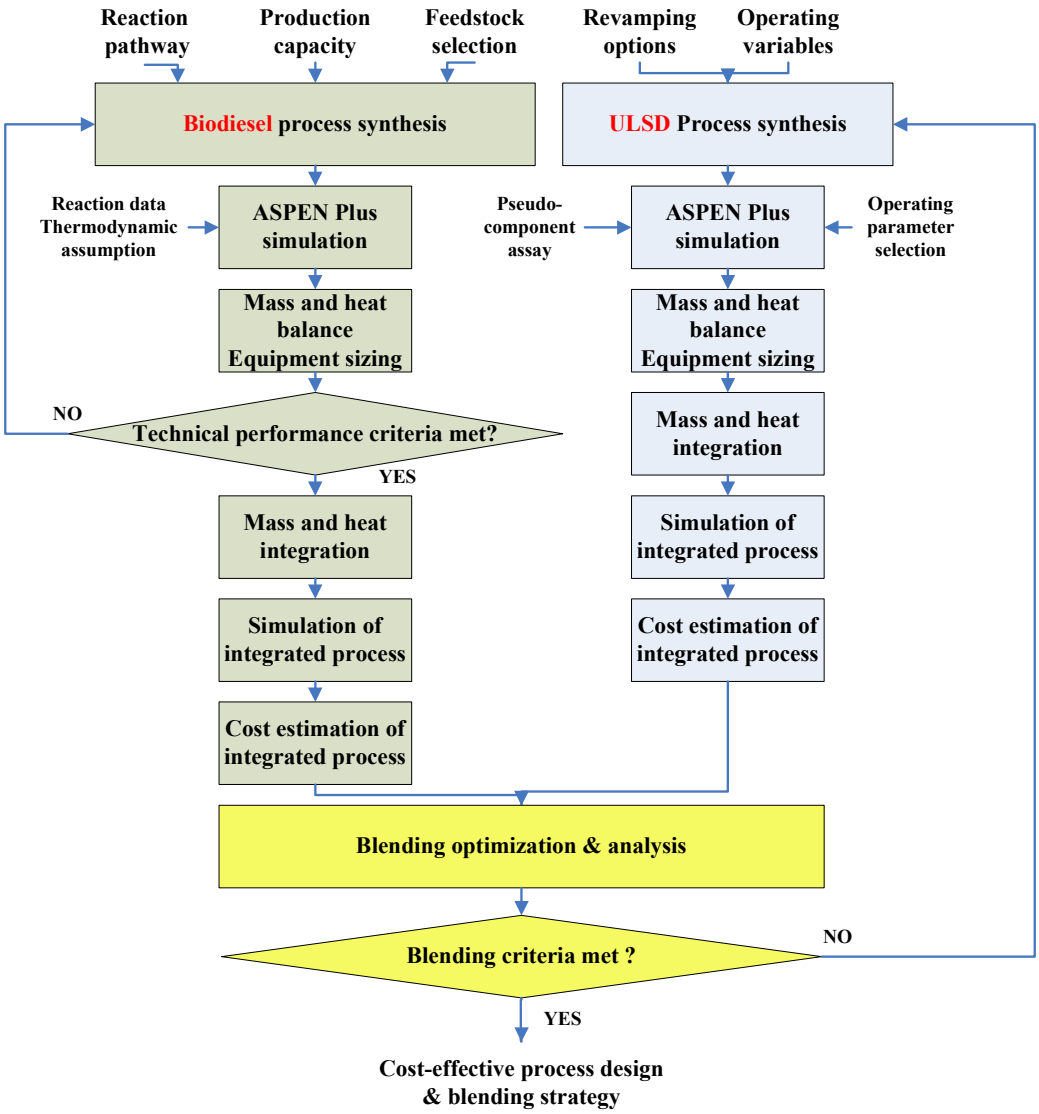

(b)

Figure 3.2 Continued

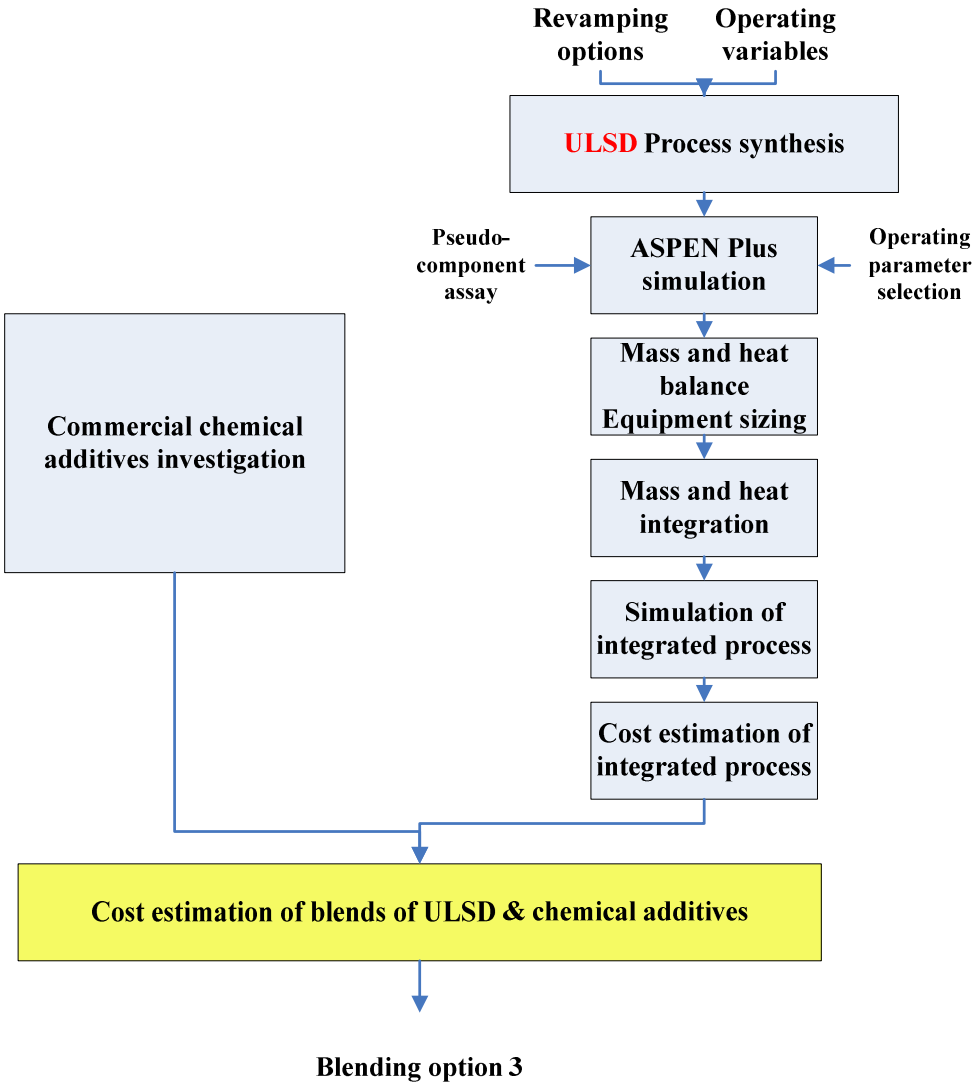

(c)

Figure 3.2 Continued

3.2 Methodology

3.2.1 Process Synthesis

Process synthesis involves incorporating and combining individual process elements into an interactive and connected process in order to achieve certain specification or meet the requirements. With process synthesis, the individual units (reactors, flashes, heat exchangers, etc.) are sequenced and connected, the options of chemicals or agents are enumerated and considered, the operating parameters (pressure, temperature, etc.) are optimized and the flowsheets of the system are generated. In process synthesis, the process inputs and outputs are specified, while the process layouts and components of the flowsheets are unknown. In order to meet the specified output requirements given the inputs, the process layouts and components need thorough consideration and revision. The process synthesis problem is illustrated in Figure 3.3 (El-Halwagi, 2006).

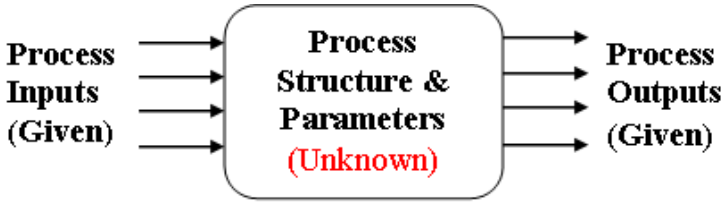

Figure 3.3 Process synthesis problems (El-Halwagi, 2006)

Various methods can be employed for process synthesis including total enumeration of all the alternatives in an explicit space, a coordinated search in the space of design decisions, evolutionary methods, superstructure optimization, targeting, problem abstraction, and combinations of these (Westerberg, 2004).

3.2.2 Process Analysis

While process synthesis involves combining individual process elements into an incorporated whole, process analysis involves the decomposition of the whole into its constituent elements for individual performance assessment. Hence, process analysis can be contrasted or complemented with process synthesis. Once an alternative is generated or a process is synthesized, its detailed characteristics (e.g., flow rates, compositions, temperature, and pressure) are investigated using analysis techniques. These techniques include mathematical models, empirical correlations, and computer-aided process simulation tools. In addition, process analysis may involve predicting and validating performance using experiments on the lab and pilot-plant scales, and even actual runs of existing facilities. Thus, in process analysis problems, the process inputs and the process layouts and components are specified while the outputs of the process are to be determined, as illustrated in Figure 3.4 (El-Halwagi, 2006).

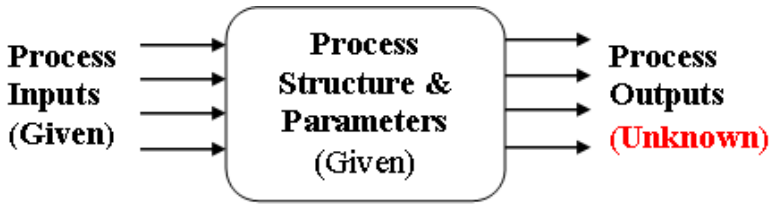

Figure 3.4 Process analysis problems (El-Halwagi, 2006)

3.2.3 Process Integration

With the increasing awareness of the environmental and energy problems associated with manufacturing facilities, a considerate amount of efforts has been put into the process industry in order to mitigate the detrimental environment impact, to conserve resources, and to lessen the pressure on energy utilization. These efforts have gradually

shifted from a unit-based approach to a holistic methodology, requiring in-depth understanding and appreciation of the integrated nature of the process. Furthermore, enumeration of possible alternatives using a unit-based approach is time-consuming and cumbersome. What is worse, an optimum process strategy might not be identified through enumeration and brainstorming, and a small change in a unit or a stream can lead to major implications on the operability and profitability of the process. Therefore, a systematic and generally applicable methodology is imperative to deal with the increasing practical environment and energy problems, and to meet the specification that the conventional enumeration methods can not reach. Process integration design methodology is brought and applied to solve the abovementioned challenges (Dunn and El-Halwagi, 2003).

Process integration is “a holistic approach to process design and operation that emphasizes the unity of the process”, which involves the activities as follows (El-Halwagi, 2006):

- Task identification

Task identification is the first step in process synthesis. In this step, the overall goal is specified and the tasks for the goal are identified and described. The actionable task should be defined in such a way as to capture the essence of the original goal.

- Targeting

Targeting refers to “the identification of performance benchmarks ahead of detailed design”. In this way, one can identify the ultimate solutions without specifying the details.

- Generation of alternatives (synthesis)

Since there are a number of alternative options and solutions to reach the target or the defined task, the deployment of a framework that is comprehensive enough to contain all configurations of interest and represent alternatives is inevitable.

- Selection of alternatives (synthesis)

Once the framework with the right level has been generated to embed the appropriate alternatives, the identification of the optimum solutions from among the possible options is important. The selection and extraction of the optimum solutions can be accomplished with the help of certain techniques such as graphical, algebraic, and mathematical optimization techniques.

- Analysis of selected alternatives

Process analysis techniques are applied to assess the selected alternatives. The evaluation may include prediction of performance, techno-economic assessment, safety review, environmental impact assessment, etc.

Process integration can be broadly classified into mass integration and energy integration. Mass integration is "a systematic methodology that provides a fundamental understanding of the global flow of mass within the process and employs this understanding in identifying performance targets and optimizing the allocation, separation, and generation of streams and species". The other important category of process integration is energy integration involving the general allocation, generation, and exchange of energy throughout the process (Dunn and El-Halwagi, 2003).

3.2.4 Graphical Method in HENs

Energy integration deals with all forms of energy such as heating, cooling, power generation/consumption, pressurization/ depressurization, and fuel. Increasing heat recovery in chemical processes is one of the major areas in energy integration. Industrial heat exchange networks, "HENs", play an important role in increasing the heat recovery. An HEN is a network composed of one or more heat exchangers that help achieve the goal of conserving energy. Therefore in most chemical process industries, the synthesis and analysis of cost-effective HENs that can transfer heat among the hot and cold streams before the external utilities are used is necessary. The application of heat integration can result in the simultaneous reduction of heating and cooling duties of the

external utilities (El-Halwagi, 2006; Dunn and El-Halwagi, 2003). Figure 3.5 illustrates the synthesis of a heat exchange network (HEN).

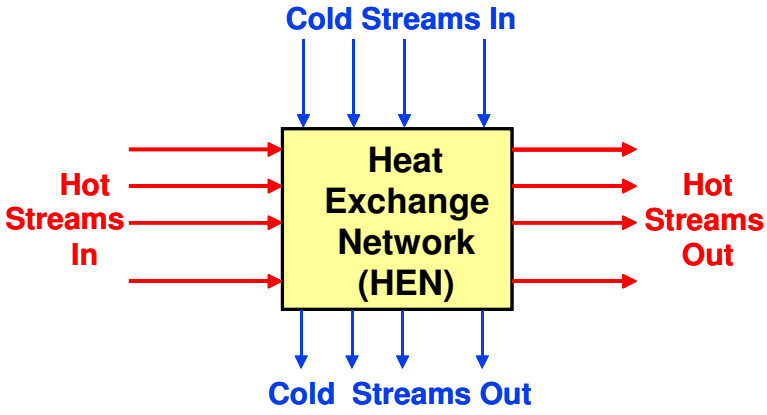

Figure 3.5 Heat exchange network (HEN) synthesis (El-Halwagi, 2006, 2008)

Various methods have been developed for the synthesis of HENs. One of the major methods is thermal pinch analysis, which is a very useful graphical technique. This method can be used to figure out the minimum utility targets ahead of synthesizing the networks (El-Halwagi, 2006).

In order to construct the thermal pinch diagram, the heat enthalpy of each hot and cold stream needs to be calculated. The heat loss from the u th hot stream

$$HH_u = F_u C_{p,u}(T_u^s - T_u^t) \qquad u = 1, 2, \ldots, N_H$$

where

HH_u - heat loss from the u th hot stream

$F_u C_{p,u}$ - heat capacity (flow rate × specific heat) of each process hot stream

T_u^s - supply (inlet) temperature of hot stream

T_u^t - target (outlet) temperature of hot stream

The heat gain by the v th cold stream

$HC_v = f_v C_{p,v}(t_v^s - t_v^t)$ $\quad v=1, 2, \ldots, N_C$

where

HC_v - heat gain by the vth cold stream

$f_v C_{p,v}$ - heat capacity (flow rate × specific heat) of each process cold stream

t_v^s - supply (inlet) temperature of cold stream

t_v^t - target (outlet) temperature of cold stream

After the heat enthalpy of each hot and cold stream are calculated, the enthalpy exchanged by each process hot and cold stream versus its temperature are then plotted on the same diagram. The enthalpy exchanged by the hot stream is plotted with the hot temperature scale T, while enthalpy exchanged by the cold stream is plotted with the cold temperature scale t. $T = t + \Delta T^{\min}$ is used to make sure that the heat-transfer considerations of the second law of thermodynamics are satisfied. For a given pair of corresponding temperatures (T, t), it is thermodynamically and practically feasible to transfer heat from any hot stream with temperature greater than or equal to T to any cold stream with temperature less than or equal to t (El-Halwagi, 2006). Then a hot composite stream and a cold composite stream can be created using the graphical superposition diagonal rule. The cold composite stream can be moved up and down which indicates different heat exchange decisions. The optimal situation is obtained when the cold composite stream is slid vertically until it touches the hot composite stream while lying completely to the left of the hot composite stream at any horizontal level. The point where the two composite streams touch is the "thermal pinch point", as shown in Figure 3.6. In this situation, the integrated heat exchange was maximized and the minimum heating and cooling utility was attained.

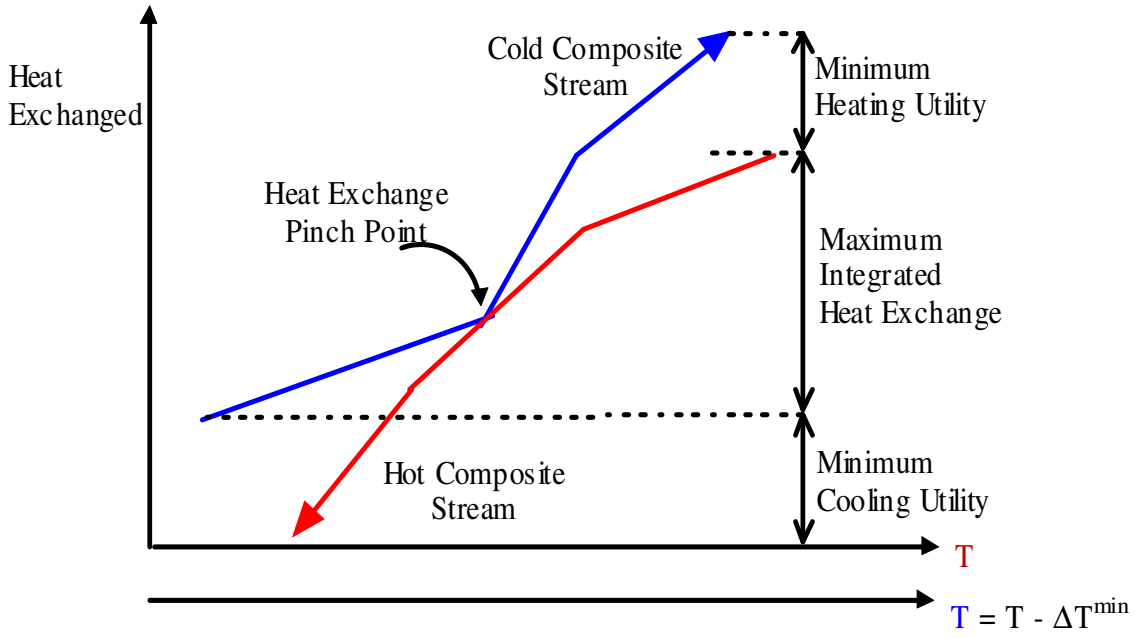

Figure 3.6 Thermal pinch diagram (Myint, 2007)

3.2.5 Algebraic Method in HENs

Graphical method gives vivid illustration for the minimum heating and cooling utility and the maximum integrated heat exchange, while algebraic method provides more insights of the heat exchange between the hot and cold streams by providing quantitative data.

The algebraic method involves the construction of temperature-interval diagram (TID), table of exchangeable heat loads (TEHL) and cascade diagram. In TID, horizontal lines define the series of temperature intervals. Heads of vertical arrows represent target temperatures of the streams and tails represents the supply temperature of the stream. It is thermodynamically feasible to transfer heat from the hot stream to the cold stream within each interval and heat from a hot stream in an interval can also transfer to any

interval below it. Figure 3.7 shows a schematic representation of temperature-interval diagram (TID).

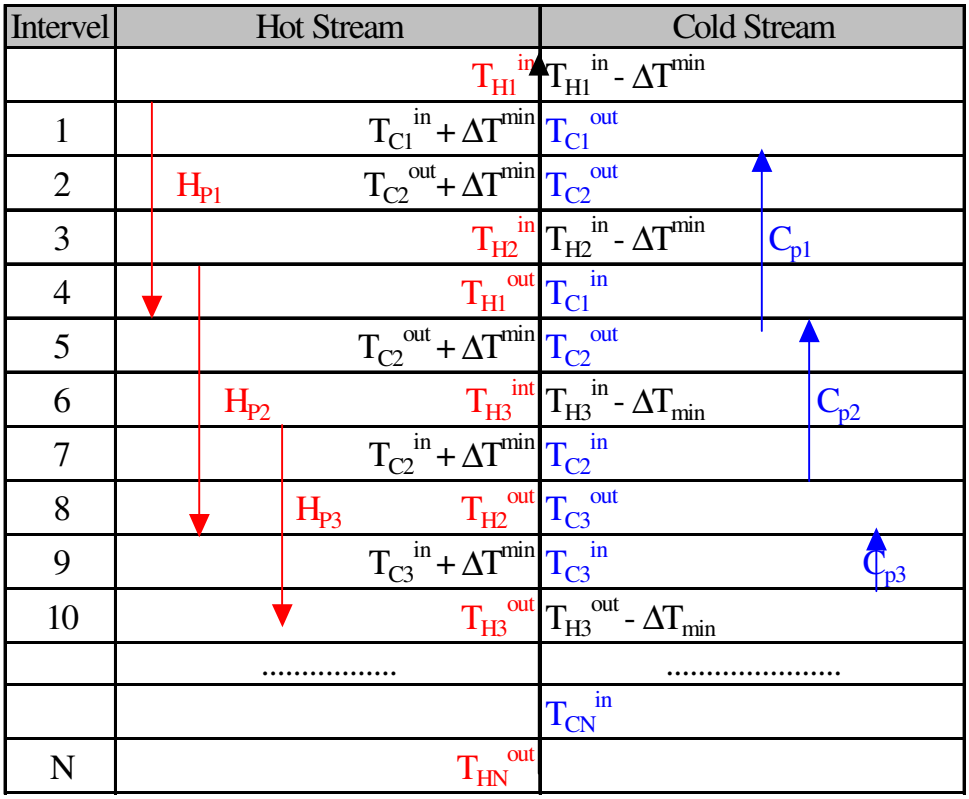

Figure 3.7 Temperature-interval diagram (El-Halwagi, 2006)

After that, a table of exchangeable heat loads (TEHL) is constructed in order to determine the heat exchange loads of the process streams in each temperature interval. The exchangeable load of the u th hot stream which passes through the z th interval is calculated by

$$HH_{u,z} = F_u C_{p,u} (T_{z-1} - T_z)$$

where

T_{z-1}, T_z - the hot-scale temperature at the top and the bottom lines defining the z th interval.

The exchangeable capacity of the v th cold stream which passes through the z th interval is calculated by

$$HC_{v,z} = f_v C_{p,v}(t_{z-1} - t_Z)$$

where

t_{z-1}, t_z - the cold-scale temperature at the top and the bottom lines defining the z th interval.

After that, the total load of hot (cold) process streams with the z th interval is calculated by summing up the individual loads of the hot (cold) process streams that pass through that interval, as shown below.

$$HH_z^{Total} = \sum_{\substack{u \text{ passes through interval } z \\ where u=1,2,.....,N_H}} HH_{u,z}$$

$$HC_z^{Total} = \sum_{\substack{v \text{ passes through interval } z \\ and v=1,2,....,N_C}} HC_{v,z}$$

Within each temperature interval, it is thermodynamically and practically feasible to transfer heat from a hot process stream to a cold process stream. In addition, it is feasible to pass heat from a hot process stream in an interval to any cold process stream in lower interval. Therefore, the following heat balance equation is obtained for the z th interval:

$$r_z = HH_Z^{Total} + HHU_z^{Total} - HC_Z^{Total} - HCU_z^{Total} + r_{z-1}$$

where

r_{z-1}, r_z - the residual heats entering and leaving the z th interval. Figure 3.8 shows a schematic representation of the heat balance around the z th interval.

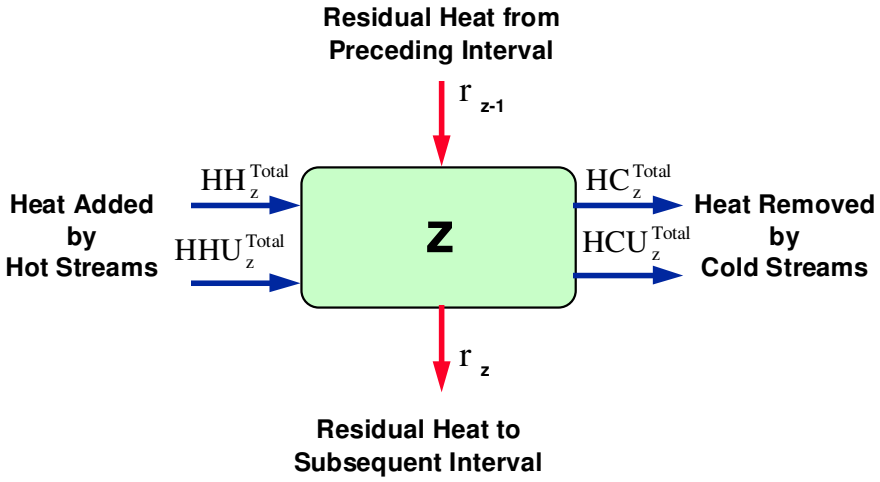

Figure 3.8 Heat balance around a temperature interval (El-Halwagi, 2008)

A cascade diagram is constructed by adding all the intervals together. Only when all the $r_z's$ are non-negative is the HEN thermodynamically feasible. A negative r_z indicates that the residual heat is flowing upwards and thus thermodynamically infeasible. The constructed cascade diagram can be revised by adding a hot load equal to the most negative residual heat. Once this hot load is added, the load is identified as the minimum heating utility, the load leaving the last temperature interval is the minimum cooling utility, and a zero residual heat suggests the thermal pinch diagram. Figure 3.9 illustrates the constructed and revised cascade diagram with the thermal pinch point, the minimum heating and cooling utilities identified.

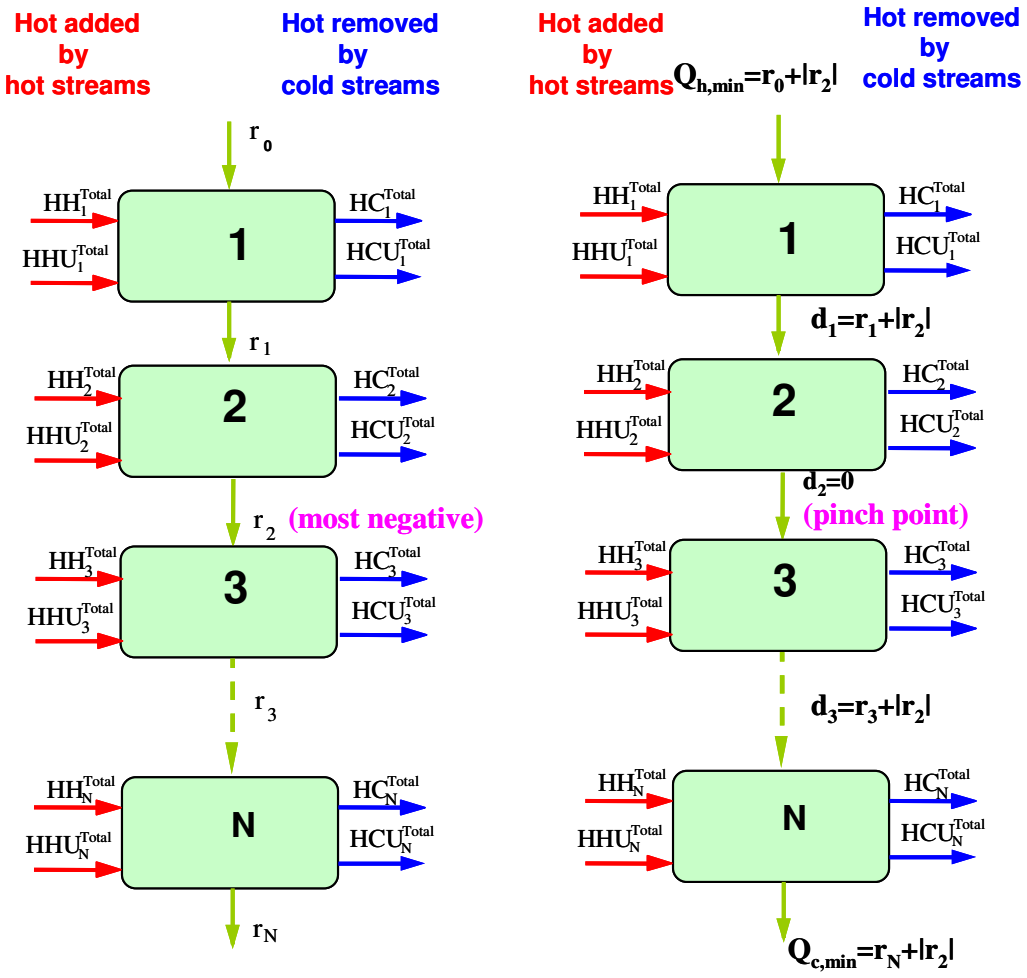

Figure 3.9 Cascade diagram for HENs (El-Halwagi, 2006)

CHAPTER IV

CASE STUDY

4.1 Biodiesel Process Description

A continuous (instead of batch) process for biodiesel production was selected in this work because of the following advantages (Anderson et al., 2003):

- better heat economization
- better product purity from phase separation by removing only the portion of the layer furthest from the interface
- better recovery of excess methanol in order to save on methanol cost
- minimal operator interference in adjusting plant parameters
- higher production capacity or lower capital costs per unit of biodiesel produced

There are three basic routes for the biodiesel production. The first route is base catalyzed transesterification of the oil with alcohol, the second is direct acid catalyzed esterification of the oil with methanol, and the third one is conversion of the oil to fatty acids, and then to alkyl esters with acid catalysts (National Biodiesel Board, 2008). The first route is the most widely used and economic in industrial biodiesel production nowadays (Zhang et al., 2003). Therefore, the base catalyzed transesterification route will be investigated in details in this work. A pretreatment step is needed to the alkali-catalyzed process using waste cooking oil in order to reduce the content of FFAs to at most 1wt% (the pretreatment steps are shown in yellow in schematic process block diagram in Figure 4.1), and the pretreatment cost of waste cooking oil would offset the savings of waste oil over vegetable oil (Zhang et al., 2003). Therefore, only refined vegetable oil will be used as feedstock for our biodiesel production and the pretreatment step would not be considered. In this work, soybean oil was chosen as the feedstock for the following reasons:

- made domestically from either agricultural or recycled resources, lessening the dependence on the crude oil import

- Expandable harvest areas (Myint, 2007)
- Cheapest feedstock among the vegetable oils, which is a crucial factor in determining the feedstocks, as the dominant factor in biodiesel product cost is the feedstock cost, with capital cost contributing only about 7 % of the final product cost (Gerpen et al., 2004)
- High quality (low free fatty acids, high purity)
- Plenty of experimental studies of biodiesel production on the laboratory scale and kinetics data of transesterification (Freedman et al., 1986; Noureddini et al., 1997)

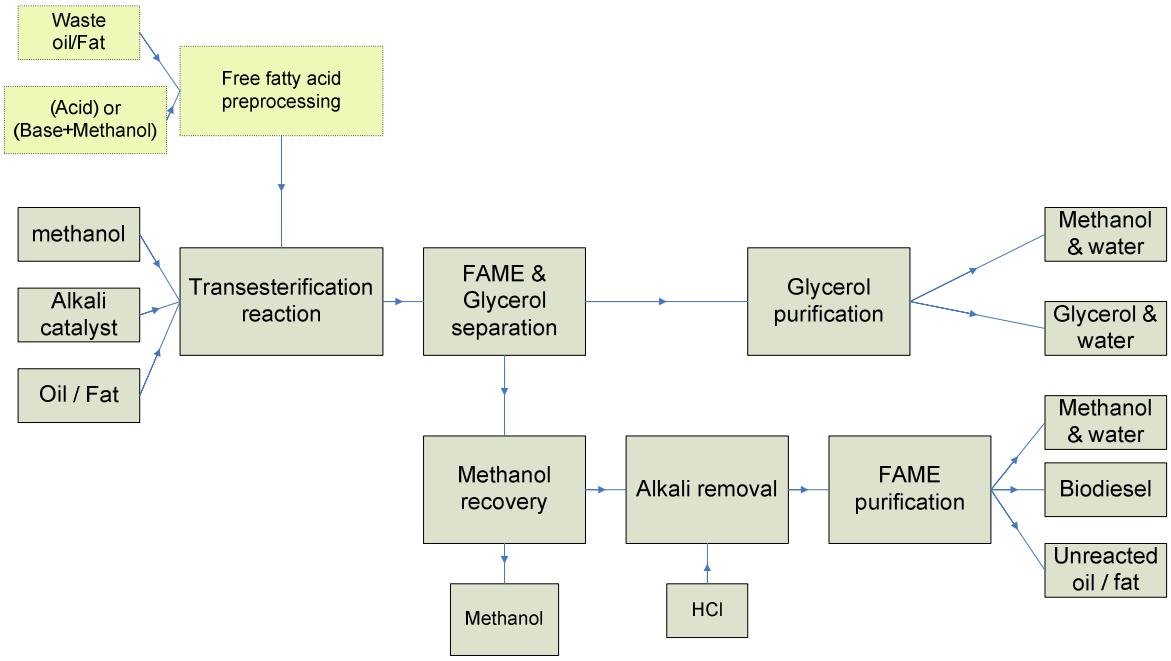

Figure 4.1 Schematic process block diagram of biodiesel production (If waste oil or acid catalysts are used, the free fatty acid pretreatment steps are needed as highlighted in yellow with dot lines)

In general, the biodiesel process in this work consists of six sections:

- Two-stage transesterification
- FAME & glycerol separation
- Methanol recovery
- Alkali removal
- Water washing (FAME purification)
- Glycerol purification

4.1.1 Two-Stage Transesterification

In this work, it is assumed that soybean oil consists of pure triolein which is a triglyceride in which all three fatty acid chains are oleic acid. This molecule has a molecular weight that is very close to that of soybean oil (Gerpen et al., 2004). Furthermore, only trioleic acid's (triolein, $C_{57}H_{104}O_6$) thermodynamic data is available in ASPEN Plus simulation software (Myint, 2007). The reaction between the triolein and methanol is shown in Figure 4.2. It is shown that one molecule of triolein reacts with three molecules of methanol to produce three molecules of methyl oleate, the biodiesel product, and one molecule of glycerol (Gerpen et al., 2004).

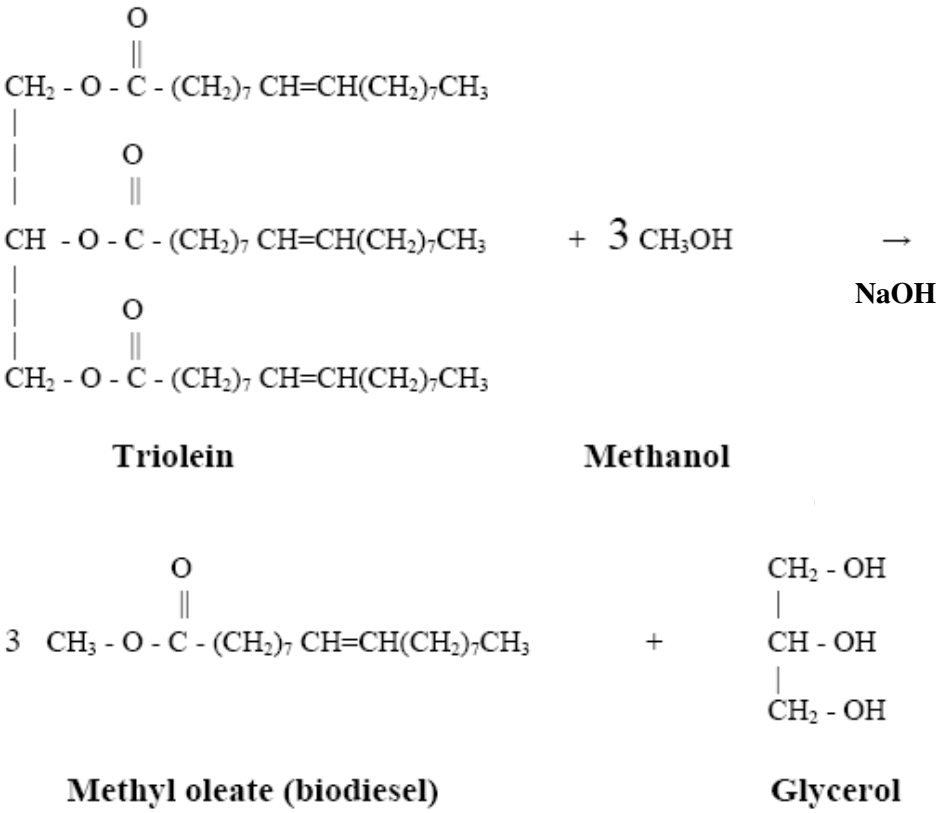

Figure 4.2 Reaction between triolein and methanol (Gerpen et al., 2004)

Based on several studies of alkali-catalyzed transesterfication on the laboratory scale, a reaction is suggested to be carried out at the temperature near the boiling point of the alcohol (for example, 60 ^{o}C for methanol). For maximum conversion to the ester, a molar ratio of alcohol to triglyceride of 6:1 is used in the first reactor in our case. This ratio is confirmed to be the optimal molar ratio based on comprehensive literature reviews (Ma et al., 1999; Zhang et al., 2003; Tapasvi et al., 2005; Meher et al., 2006; Myint, 2007). Sodium hydroxide (NaOH) is used as the base catalyst for our biodiesel production, due to its low cost, a lot of kinetics studies on the laboratory scale and a widespread application in large-scale biodiesel processing. In the first reactor, sodium hydroxide with a concentration of 1.0 wt % of the feed soybean oil was used. In the

second reactor, the concentration of NaOH used is 0.2 wt % of the unreacted triolein from the first transesterification based on the suggestion of patents given by Wimmer (1995) and Tanaka et al.(1981). Methyl, rather than ethyl, ester production was modeled because methyl esters are predominantly produced on the industrial scale and methanol is much more cost-effective than ethanol. Furthermore, the downstream unreacted methanol is of great ease to recover (Haas et al., 2006). A triolein purity of 99.95 wt % was assumed. The rest 0.05 wt % consists of free fatty acid (FFA).

Two sequential transesterification reactions are employed in order to achieve higher conversion of the soybean oil. 99.5 wt % conversion of the feedstock is assumed as suggested by Tanaka et al. (1981). Therefore, the conversion of the feedstock in the first reactor (R-101 on the Process Flow Diagram shown in Figure 4.3) is set at 95 wt %, and the conversion of the unreacted triolein in the second reactor (R-102) is 90 wt %. The reaction products biodiesel and glycerol from the first reactor are separated in decanter D-001 with the byproduct glycerol sent to a distillation column T-001 for purification. The unreacted triolein is transesterified in the second reactor, followed by a further separation of glycerol from biodiesel in Decanter D-002.

4.1.2 FAME & Glycerol Separation

The transesterification products (Fatty acid methyl esters or FAME, and glycerol) are first cooled to 25 ^{o}C from 60 ^{o}C, and pumped to a decanter (D-001 on the Process Flow Diagram shown in Figure 4.3) where FAME and byproduct glycerol are separated. The biodiesel and glycerol from the second reactor are further separated in D-002. FAME and glycerol are separated at 25 ^{o}C and atmospheric conditions simply because of their immiscibility and gravity difference. The glycerol phase is much denser than biodiesel phase and the two can be gravity separated with glycerol drawn off the bottom of the settling vessel.

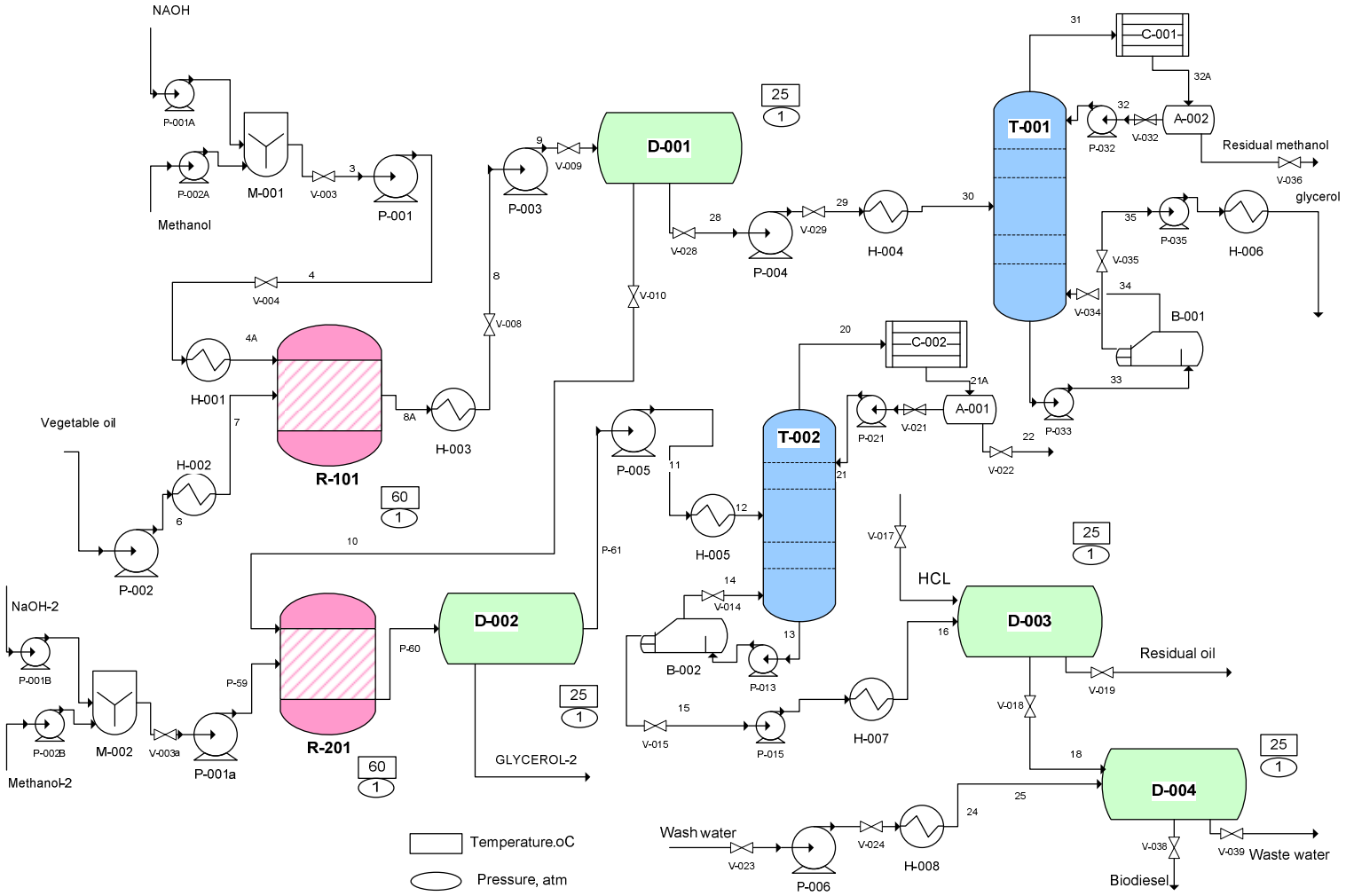

Figure 4.3 Process flow diagram of biodiesel production

4.1.3 Methanol Recovery

The lighter products, which mainly consist of FAME or biodiesel and is separated from the decanter (D-002), is first heated to 60 ^{o}C and then sent to a distillation column (T-002) with theoretical stages of 6, a total condenser and a kettle reboiler. In this distillation column, methanol are separated and recovered from the biodiesel phase through the overhead as a vapor. A reflux ratio of 1.5 is used to obtain a good separation between methanol and other components.

4.1.4 Alkali Removal

The bottom effluents from the distillation column (T-002) are cooled to 25 ^{o}C and then sent to another decanter (D-003), where the excess sodium hydroxide is neutralized with hydrogen chloride. Other than removing any residual catalyst sodium hydroxide, hydrogen chloride is also added in order to split any soap that may have formed during the reaction shown in Figure 4.4. The purpose of the neutralization before water washing step is to reduce the water required for subsequent FAME purification and minimize the chances of emulsion formation when the wash water is added to the FAME.

Figure 4.4 Reverse saponification (Myint, 2007)

4.1.5 Water Washing (FAME Purification)

Once separated from other components such as sodium hydroxide and triolein in decanter D-003, FAME (the biodiesel) is purified by washing gently with warm water to remove residual catalyst, salts, methanol, free glycerol and soaps. 99.65 wt% purity of

biodiesel is required to achieve in order to meet ASTM D 6751 of biodiesel specification. The waste water coming from the water washing unit can then be recycled by pumping through pump P-006.

4.1.6 Glycerol Purification

The glycerol stream separated from decanter D-001 is heated to 60^{o}C and then set to glycerol distillation column (T-001) with theoretical stages of 3, a total condenser and a kettle reboiler. The residual FAME goes through the overhead of the column in terms of vapor, while the glycerol goes through the bottom, cooled and then kept for commercialized use.

4.2 Process Simulation and Design of Biodiesel Production

Both NRTL and RK-Soave thermodynamic properties were used in the simulation. Although some thermodynamic data of triolein is available in ASPEN Plus, certain crucial thermodynamic properties are not included such as the ideal gas heat capacity of triolein. Therefore, these thermodynamic properties which are not given by ASPEN Plus have to either be entered by a user-defined method or estimated by Aspen upon providing the molecular structure of the compounds (Myint, 2007). The molecular structure of triolein was downloaded and exported as the MDL file online (PubChem CID: 5497163) and then imported to ASPEN. The molecular structure of triolein can also be constructed by ISIS draw and imported to APSEN as well (Myint, 2007). The same simulation results were obtained using both molecular structure construction methods. Properties of these compounds were then estimated by Aspen's UNIFAC group contribution factor method based on the provided molecular structures. It is expected that there are some deviations between the actual thermodynamic data and the estimated one based on the imported molecular structure, as ASPEN can not distinguish the cis and trans of the compounds (Myint, 2007).

Na+ and OH- ions were used instead of NaOH solid form based on the Myint's simulation experiences on biodiesel production (Myint, 2007). Similarly, for HCl, H+ and Cl- ions were used instead of the HCl provided in the ASPEN Plus built-in properties. Electrolytes property method was used when Na+, OH-, H+ and Cl- ions were involved.

Feed wash water amount was determined by performing the water sensitivity analysis with the methyl oleate purity higher than 99.65 wt%, which is required by ASTM D 6751 for biodiesel purity. Moreover, sensitivity analysis of distillate mass flow rate in distillation column T-001 was performed in order to guarantee that the purity of glycerol is higher than 90 % (Myint, 2007) and the temperature of glycerol is lower than its decomposition temperature 554^{o}F (290 ^{o}C given by Material Safety Data Sheet of glycerol, available at http://avogadro.chem.iastate.edu/MSDS/glycerine.htm). Similarly, sensitivity analysis of distillate mass flow rate in column T-002 was performed as well in order to keep the biodiesel stream temperature below its decomposition temperature 482 ^{o}F (250 ^{o}C).

4.3 Calculation of Feed Streams of Biodiesel Production

The flow rates of the feed streams were calculated and shown in Table 4.1.

Table 4.1 Input calculations of the feed streams for an overall conversion of 99.5%

final product	**methyl oleate**		
	specific gravity	0.872	lb/lbmol
	molecular weight	296.494	lb/gal
	density	7.265	lb/gal
	production	5000.000	gal/hr
	total flow rate	36323.399	lb/hr
		122.510	lbmol/hr
first reactor (95% conversion)	**triolein (99.95 wt% purity)**		
	molecular weight	885.449	lb/lbmol
	total flow rate	36357.005	lb/hr
		41.100	lbmol/hr
	FFA (oleic acid, 0.05 wt%)		
	molecular weight	282.467	lb/lbmol
	total flow rate	18.178	lb/hr
		0.064	lbmol/hr
	methanol (6:1)		
	molecular weight	32.042	lb/lbmol
	total flow rate	7901.597	lb/hr
		246.600	lbmol/hr
	NaOH (1 wt% of triolein)		
	molecular weight	39.997	lb/lbmol
	total flow rate	363.570	lb/hr
		9.090	lbmol/hr
second reactor (90% conversion)	**unreacted triolein**		
	molecular weight	885.449	lb/lbmol
	total flow rate	1816.900	lb/hr
		2.052	lbmol/hr
	methanol (20 wt% of unreacted triolein		
	molecular weight	32.042	lb/lbmol
	total flow rate	363.400	lb/hr
		11.341	lbmol/hr
	NaOH (0.2 wt%)		
	molecular weight	39.997	lb/lbmol
	total flow rate	3.634	lb/hr
		0.091	lbmol/hr

4.4 ULSD Process Description

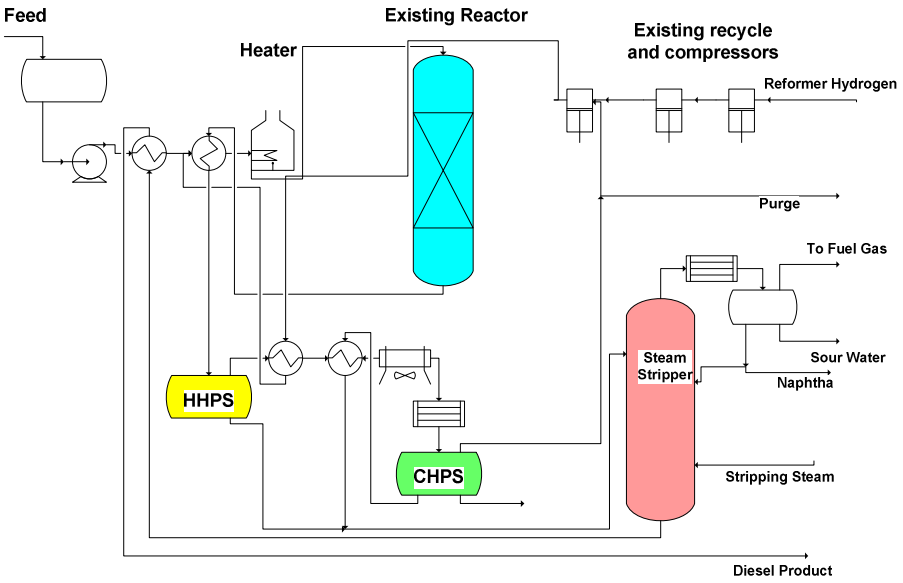

Figure 4.5 Base case process flow diagram (Palmer et al., 2001)

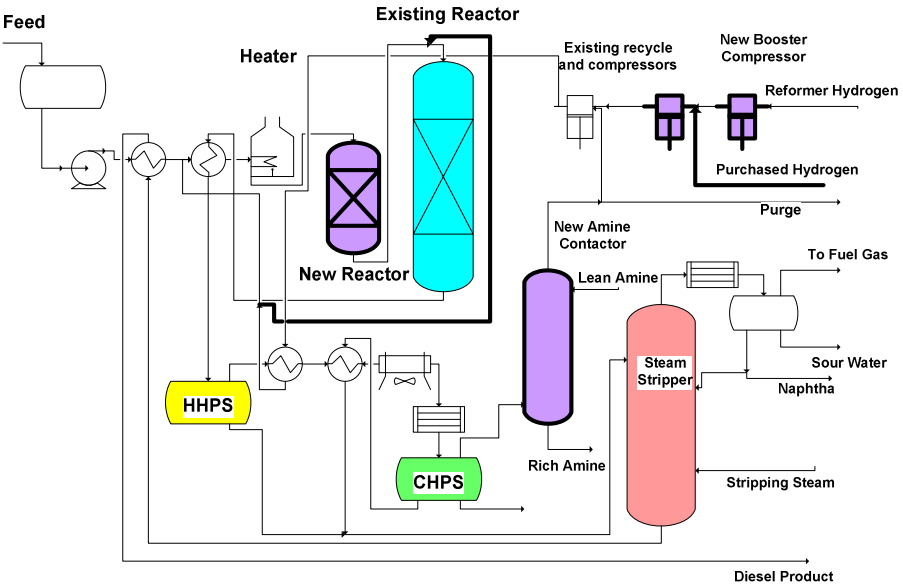

Figure 4.6 Revamped process flow diagram (Palmer et al., 2001)

4.4.1 Base Case Description

The basic case for our case is a typical low sulfur diesel (LSD) production process that was commissioned in the early nineties to meet the 500 ppmw sulfur requirements. The feed for the base case is a combination of straight run gas oil (SRGO) and fluid catalytic cracking light cycle oil (FCC LCO) (Palmer et al., 2001).

The untreated diesel feed is preheated by the diesel stripper bottoms and heated by the fire heater before pumped into the hydrotreater. In the hydrotreater, sulfur compounds are removed from the feed by catalytic reaction with a hydrogen stream composed of recycle and make-up hydrogen. Leaving the reactor, the effluent is cooled by cross exchange with the feed before entering the hot high-pressure separator (HHPS). The function of the HHPS is to remove unwanted gas (hydrogen sulfide, ammonia, carbon monoxide, etc.) and obtain a stream that is highly pure in diesel and naphtha. Liquid from the HHPS proceeds to the steam-stripping column. Vapor from the HHPS is partially condensed by heat exchange with the treat gas and cold high-pressure separator (CHPS) liquid, followed by air and water coolers. Hydrocarbon liquid from the CHPS is preheated by the HHPS vapor, and then sent to the stream-stripping column. Leaving the diesel stripper, the hydrocarbon liquid was separated in terms of naphtha from overhead of the column and diesel from the bottom. Vapor from the cold separator is sent to the recycle compressor. Figure 4.5 shows the simplified base case process flow diagram.

4.4.2 Revamp Case Description

In our case, a combination of revamp options is applied in order to meet the ultra low sulfur diesel (ULSD) specification at the lowest capital expenditure. Figure 4.6 shows the simplified revamp case process flow diagram. The revamps include

- New amine scrubbers added on the recycle gas
- New reactor added
- New compressors
- Purchased H2 with purity of 99.9%

- Criterion's DC-2118 catalysts with enhanced activity used

The revamps made in this study are based on the following assumptions (Palmer et al., 2001)

- Minimum catalysts cycle life of one year and particularly, a cycle life of 2.5 year used based on the specification provided by Fluor Daniel.
- Utility systems such as steam, cooling water and pressure relief system have sufficient capacity for the revamp.
- The refinery has excess amine regeneration capacity.
- Sufficient space around the existing hydrotreater is available for a new hydrotreater and other newly added equipments.

4.5 ULSD Process Simulation and Design

ULSD production for our case was designed with a feed capacity of 70,000 BPSD or 980 million gallon per year (MMGPY).

4.5.1 Pseudocomponents

The Petroleum Assays method in ASPEN Plus was used to specify the diesel and naphtha from the hydrotreater, with the true boiling point distillation curve information of diesel and naphtha given by Fluor Daniel. The pseudocomponents were generated with divided cuts for a more realistic distillation simulation based on the input information and built-in Assay Libraries (Aspentech, 2001; El-Halwagi, 2007).

4.5.2 Start-of-Run (SOR) and End-of-Run (EOR)

At start-of-run (SOR) the catalyst activity typically indicates activity of a new catalyst, while EOR suggests the minimum required catalyst activity at end-of-run (CDTECH, 2008). The production of ULSD involves both the direct and indirect removal of sulfur. For simple compounds such as sulfide, the sulfur atom is directly removed by cleavage. However, for more complex sulfur species, hydrogenation is inevitable to gain access to

the sulfur atoms before the removal of sulfur. Direct sulfur removal is kinetically limited, so reaction rates increase with increasing temperature. The hydrogenation step is equilibrium-limited and reaction rates decline as temperature increases, so indirect sulfur removal dictates EOR conditions (NPRA, 2007). Since almost all of the remaining sulfur belongs to the dibenzothiophene (DBT) class when the diesel sulfur level goes below 100 ppmw (Hu et al., 2002), indirect sulfur removal dominates during the desulfurization, EOR is determined to be more limiting. Therefore, in our study, all the EOR specifications given were used for process simulation rather than the SOR specifications.

4.5.3 Reactor Simulation

The hydrotreater was not simulated by ASPEN Plus in our case for the following reasons:

- Kinetics data of hydrodesulfurization with updated catalysts for ULSD production was not sufficient, thus the RStoic reactor model can not be used. Existing improved catalysts for ULSD production such as STARS and NEBULA were tested in pilot plants with various kinds of feedstocks (Courier 4 and 11). The sulfur concentrations of the effluents after the desulfurization were detected by analytical techniques such as gas chromatograph with a mass selective detector (GC-MS) and gas chromatograph with a flame ionization detector (GC-FID) (Hu et al., 2002). Few kinetics details of the hydrodesulfurization with the new improved catalysts were given by literatures. Furthermore, the sulfur distributions in the feed they tested with were unknown (Courier 4 and 11; Hu et al., 2002), and a lot of compounds in the desulfurization processes contain sulfur such as benzothiophenes, benzothiophenes and 4, 6-dimethyl-dibenzothiophene (Hu et al., 2002; Babich et al., 2003), stoichiometric information for desulfurization of all the sulfur-contained compounds and the percentage of all the parallel reactions were needed.

- The pseudocomponents can not be specified if RYield reactor model was used. RYield reactor model was considered to deloyed, as the information regarding the reactor yields for both SOR and EOR was given. However, the pseudocomponents can not be specified in the RYield model. In the other word, the naphtha and diesel yields given by Fluor Daniel can not be input in ASPEN Plus, although other compounds such as H_2S, NH_3, C1-C4 hydrocarbons can be specified.

Since the desulfurization in the hydrotreater can not be simulated by ASPEN Plus, the final sulfur content in ULSD can not be investigated by the simulation. In our work, the final sulfur concentration in ULSD was specified as 8 ppm, which was given by the revamp case study result by Palmer et al.(2001). The 8 ppm sulfur concentration was demonstrated to be able to achieve by various pilot studies and industrial trials (couriers 4 and 11, 2008). 8 ppm is specified in the pipelines rather than the regulated 15 ppm due to a tolerance requirement for testing and post logistics concerns of ULSD such as contamination from higher sulfur products in the system during production, storage and transportation.

4.5.4 Removal of H_2S in the Amine Scrubber

MDEA (methyldiethanolamine) amine system utilizing 45 wt % with a pickup of 0.4 mol/mol was used based on the information given by Fluor Daniel.
Methyldiethanolamine (MDEA) is chosen due to its high selectivity in removal of H_2S. It is a tertiary amine and can selectively remove H_2S to meet requirements under moderate or high pressures. The high selectivity of MDEA in removal of H_2S can be explained by the fact that CO_2 hydrolyzes much slower than H_2S. The selective removal of H_2S using MDEA renders some benefits as follows (GPSA, 1998):

- Reduced solution flow rate resulting from a reduction in the amount of acid gas removed.
- Smaller amine regeneration unit.

- Higher H_2S concentrations in the acid gas giving rise to less problems in sulfur recovery.

4.5.5 Determination of Operating Parameters

The operation conditions and parameter ranges for the main units and streams were obtained based on comprehensive literature search (Palmer et al., 2001; Bharvani et al., 2002; Harwell et al., 2003; Baldwin, 2008) and specifications from Fluor Daniel. The operation condition ranges were listed in Table 4.2. The minimum conditions meet the ranges given were selected in order to minimize the costs associated with heating and cooling, pressurization and feed raw materials.

Table 4.2 Operating parameter ranges for main units and streams of ULSD

	target conditions	sources	comments
main equipments			
hytrotreater	708 ^{o}F, >725 psia	Palmer, 2001; Bharvani, 2002	
HHPS	500-550 ^{o}F, 950-1150 psia	Bharvani, 2002; Harwell, 2003	
CHPS	110 ^{o}F, 650 psig-1000 psia	Bharvani, 2002; Harwell, 2003	
diesel stripper	140 ^{o}F -700 ^{o}F, distillation curves should match	Bharvani, 2002; Harwell, 2003	
amine contactor 1	H_2S < 5 ppmw	Bharvani, 2002	sensitivity analysis needed
amine contactor 2	H_2S <10^{-5} lbmol/hr	Bharvani, 2002	sensitivity analysis needed
main streams			
feed stream	708 ^{o}F, 800 psia	Palmer,2001; Bharvani, 2002	
lean amine (45 wt%)	110 ^{o}F-140 ^{o}F, <250 psig, at least 10 ^{o}F higher than minimum	Fluor Daniel, 2005; Baldwin, 2008	sensitivity analysis performed for stream amount
H_2 circulation/H_2 consumption	5:1 minimum	Fluor Daniel, 2005	

4.6 Calculation of Feed Streams for ULSD Production

The input calculations of the feed streams for ULSD production is shown in Table 4.3. It is shown that the streams for reactor inlet and outlet achieved mass balance.

Table 4.3 Input calculations of the feed streams for ULSD production

feed		
flow rate	70,000	BPSD
	891,059	lb/hr
Gravity	30.77	API
diesel		
EOR yield	95.15	wt%
flow rate	847843	lb/hr
naphtha		
EOR yield	4.78	wt%
flow rate	42593	lb/hr
H2 (99.9mol%)		
H2 consumption	1.39	wt%
H2 circulation/H2 consumption	5	
flow rate of consumed H2	12398.1	lb/hr
flow rate of H2 leaving the reactor	49542.8	lb/hr
reactor inlet		
feed	891059	lb/hr
pipeline H2 (99.9 mol%)	61991	lb/hr
total	953050	lb/hr
reactor outlet		
vapor	62614	lb/hr
diesel	847843	lb/hr
naphtha	42593	lb/hr
total	953050	lb/hr

4.7 Heat Transfer Area Estimation

After the performance of ASPEN Plus simulation, the simulation results were sent to the linked ASPEN ICARUS process evaluator for fixed capital investment (FCI) and equipment cost estimation. Heat transfer areas of the heat exchangers needed to be specified manually for the estimation. However, the heat transfer areas of the heat exchangers using the simplest model HEATER were not given by ASPEN Plus. Therefore, the heat transfer areas need to be estimated. The estimation methods were as follows:

- ASPEN Plus simulation was first carried out for the complete flowsheet.
- The same heat exchangers model HEATER was then used with specifying the input streams which should be exactly the same with the corresponding ones in the complete flowsheets. Utilities should be specified as well for the HEATER model in order to calculate the utility flow rate. The selection and operating parameters of utilities and heat exchangers were based on the heuristics by Seider et al. (2004). Based on the suggestion of Heuristic 27, a water inlet temperature of 90 ^{o}F and a maximum water outlet temperature of 120 ^{o}F were assumed when using cooling water to cool or condense a process stream. Moreover, a 5-psi pressure drop in heat exchanger was assumed based on the Heuristic 31. The utility flow rates and heat duty were obtained after performing simulation for the additional heat exchangers.
- Two-stream heat exchangers model HEATX for counter-current shell and tube heat exchangers were added. Utility flow rates and heat duty obtained from previous simulation with the simple HEATER model were specified for the new HEATX model. After performing simulation for the new heat exchangers with the more complex models, the heat transfer areas were attained.

For the heat transfer area estimation of the biodiesel process, the input stream compositions and the heat duty calculated for the newly-added heat changers were exactly the same with those for the original heat exchangers in the flowsheet. However,

when it came to the estimation for the ULSD process, the input stream needed to be estimated due to the fact that the pseudocomponents from the stream table can not be specified in the input stream. Hydrocarbon molecules with similar molecular weights to pseudocomponents in the input streams were used to substitute the pseudocomponents. This assumption was made based on the fact that the pseudocomponents were hydrocarbons and hydrocarbons with similar molecules normally have similar properties such as boiling point, vapor pressure, and volatility, etc. For pseudocomponents without similar molecular-weight hydrocarbons, the mixtures of two hydrocarbons were used, as shown in Table 4.4.

Table 4.4 Estimation and substituted molecules for pseudocomponents

	pseudocomponents average molecular weight	**substitute hydrocarbons**
HE-0001	32.5	methane (41.1 mol%) propane (58.9 mol%)
HE-0002	9.5	hydrogen (46.4 mol%) methane (53.6 mol%)
HE-0003	203.0	phenyl-naphthalene MW =204.26
HE-0004	210.7	pentadecane MW =212.41
HE-0005	37.1	ethane (50 mol%) propane (50 mol%)

Since the substituted hydrocarbons were used to estimate the pseudocomponents, the input stream specifications for the newly-added heat exchangers were no longer the same, and thus the heat duties of the new heat exchangers deviated from those of original ones. The simulated heat transfer areas were adjusted by assuming that the heat transfer areas are proportional to the heat duty. Since

$A_0 = Q_T / U\Delta T_m$

Where A_0 is the heat transfer area, Q_T is the heat duty, U is the constant mean overall heat transfer coefficient, and ΔT_m is the mean temperature difference (Perry, 1997). The assumption $A_0 \propto Q_T$ is reasonable for the estimation and adjustment of the heat transfer areas. The heat transfer areas estimation results for biodiesel and ULSD production were summarized in Table 4.5 and Table 4.6.

Table 4.5 Heat transfer areas estimation for biodiesel process

HEX #	heat duty (Btu/hr)	utility	utility flow rate (lb/hr)	area (ft2)
1	43852	hot water	2188	9
2	849733	hot water	42397	94
3	3197	hot water	160	1
4	-1440578	cooling water	36089	299
5	308685	hot water	15402	34
6	358507	hot water	17888	40
7	1138071	hot water	56784	127
8	-7999257	cooling water	200394	440
9	1174737	hot water	58613	131
10	-1187033	cooling water	29737	182
11	-998961	cooling water	25026	65

Table 4.6 Heat transfer areas estimation for ULSD process

HEX #	expected heat duty (Btu/hr)	actual heat duty (Btu/hr)	utility	utility flow rate (lb/hr)	area (ft^2)	adjusted area (ft^2)
HE-0001	-111576084	-73762112	Cooling water	2468223	1000	1512
HE-0002	-142625321	-103571646	Cooling water	3465707	5145	7085
HE-0003	-172709725	-135360208	Cooling water	4529414	7924	10110
HE-0004	-193577134	-227390232	Cooling water	7608916	11968	10188
HE-0005	-168418	-251041	Cooling water	8400	18	12

CHAPTER V

RESULTS AND ANALYSIS

5.1 Distillation Curves

The distillation curve is a graphical description of the boiling temperature of a fluid mixture as a function of the volume fraction distilled. This volume fraction is usually expressed as a cumulative percent of the total volume. The distillation curve is a direct indication of the fluid volatility. For the crude petroleum, the distillation curve can be divided into different regions that contain butanes and lighter, gasoline, naphtha, kerosene, gas-oil, and residue. One can gain the insights of the volatility of each cut by the temperature range of each of these cuts or regions and thus identify the relative difference between light crude and heavy crude from the distillation curves (Bruno et al., 2006).

For our case, the distillation curves of ULSD and naphtha were obtained from the ASPEN Plus simulation results for the diesel stripper unit, and presented by the boiling temperature as a function of vapor fraction distilled, as shown in Figure 5.1. The red curves were the expected distillation curves specified by Fluor Daniel, while the green curves were the actual simulation results. It was shown that the actual distillation curve of ULSD crossed over the expected ULSD curve. Since the petrodiesel were the mixtures of distillation fractions from crude oil within certain temperature range, it is reasonable that the simulated and expected curves crossovers but not overlaps. The crossover of the simulated and expected ULSD distillation curves indicated the similar distillation temperature range and similar volatilities of the simulated and expected ULSD. The actual and expected distillation curve trends of the naphtha were very similar with the actual one slightly below the expected curve, which indicated that the actual naphtha simulated by ASPEN Plus had lower boiling temperature and higher volatility, due to the existence of the lighter impurities. Since the major goal of the simulation is to produce ULSD with high purity and to avoid the loss of diesel (diesel flow rate of 847843 lb/mol from reactor vs. diesel flow rate of 847844 lb/mol from the

diesel stripper) during the separation, the presence of lighter impurities and slightly lower distillation curve is not important. The naphtha from the overhead of the diesel stripper will be sent to other units for further purification. The simulated and expected diesel densities results were very close, indicating that the simulation results were acceptable and the ULSD and naphtha specifications were met, as shown in Table 5.1.

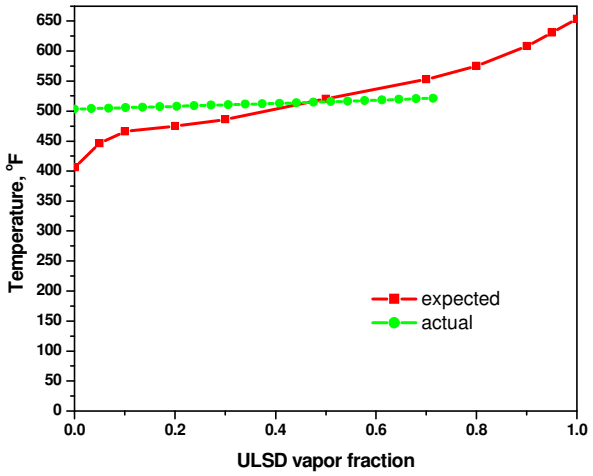

(a)

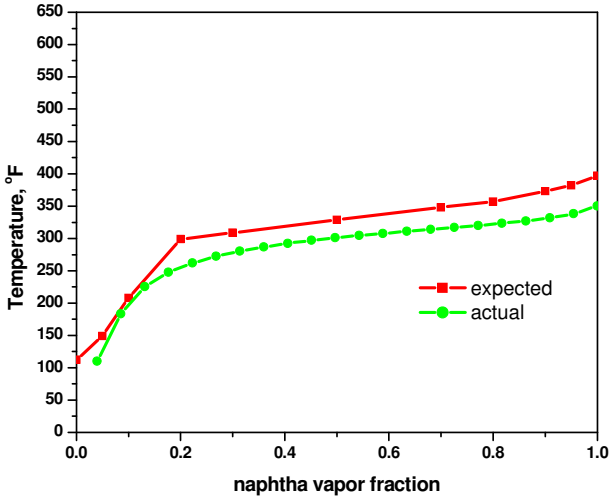

(b)

Figure 5.1 Distillation curves. (a) ULSD (b) naphtha

Table 5.1 Simulated and expected densities at 110 ^{o}F for ULSD and naphtha

		Density (lb/ft^3)	API	S.G.
ULSD	**simulated**	52.04	36.3	0.843
	expected		33.8	0.856
naphtha	**simulated**	45.02	62.4	0.730
	expected		58.0	0.747

5.2 Process Integration

In order to determine the minimum heating and cooling utility for the biodiesel and ULSD production, heat integration were carried out using both algebraic and graphic methods for biodiesel and ULSD production.

5.2.1 Heat Integration for Biodiesel Production

Heat integration was performed for the biodiesel plant with a production capacity of 40 million gallons per year (MMGPY) or 5000 gallons per hour based on 8000 operating hours per year. The cold and hot streams of biodiesel production with expected total heating and cooling utilities are shown in Table 5.2. The heat capacity was calculated by net duty / (target temperature-supply temperature).

Table 5.2 Cold and hot streams of biodiesel production

	supply temp, ^{o}F	**target temp, ^{o}F**	**net duty (Btu/hr)**	**heat capacity (Btu/hr.^{o}F)**
cold streams				
HEX1	134	140	43852	7309
HEX2	77	140	849733	13488
HEX3	130	140	3197	320
HEX5	77	140	308685	4900
HEX6	77	140	358507	5691
HEX7	77	140	1138071	18065
HEX9	77	140	1174737	18647
MET-DIST1(reboiler)	467	468	8437044	8437044
MET-DIST2(reboiler)	390	391	5308149	5308149
total heating utility			**17621975**	
hot streams				
HEX4	140	77	-1440578	22866
HEX8	467	77	-8080031	20718
HEX10	140	77	-1187033	18842
HEX11	390	77	-1537263	4911
MET-DIST1(condenser)	62	61	-1660378	1660378
MET-DIST2(condenser)	62	61	-4104335	4104335
REACT1	140	139	-3571716	3571716
REACT2	140	139	-442118	442118
total cooling utility			**-22023452**	

The temperature-interval diagram (TID) was constructed based on the cold and hot streams of biodiesel production, as shown in Figure 5.2. Cascade diagram of biodiesel production was then developed, as shown in Figure 5.3. The pinch point was found between the 4th and 5th interval with the most negative residual heat -12357085 Btu/hr. Since no heat should be passed through the pinch, the cascade diagram was revised by adding the residual heat 12357085 Btu/hr to each residual heat. The minimum heating and cooling utility were determined to be 12357085 Btu/hr and 16758563 Btu/hr, respectively. These results were consistent with those resulted from heat integration

using the graphic method shown in Figure 5.4 and from LINGO linear programming with the set formulations shown in Appendix B. It was indicated from Figure 5.4 that the integrated heat exchange was maximized at 5.26 MMBtu/hr. After heat exchange, the heating and cooling utility was reduced by 29.9% and 23.9% shown in Table 5.3.

intervals	hot streams	°F	°F	cold streams
		478	468	
1		477	467	
2		467	457	
3		401	391	
4		400	390	
5		390	380	
6		150	140	
7		144	134	
8		140	130	
9		139	129	
10		87	77	
11		77	67	
12		62	52	
13		61	51	

Figure 5.2 Temperature-interval diagram (TID) of biodiesel production HEN

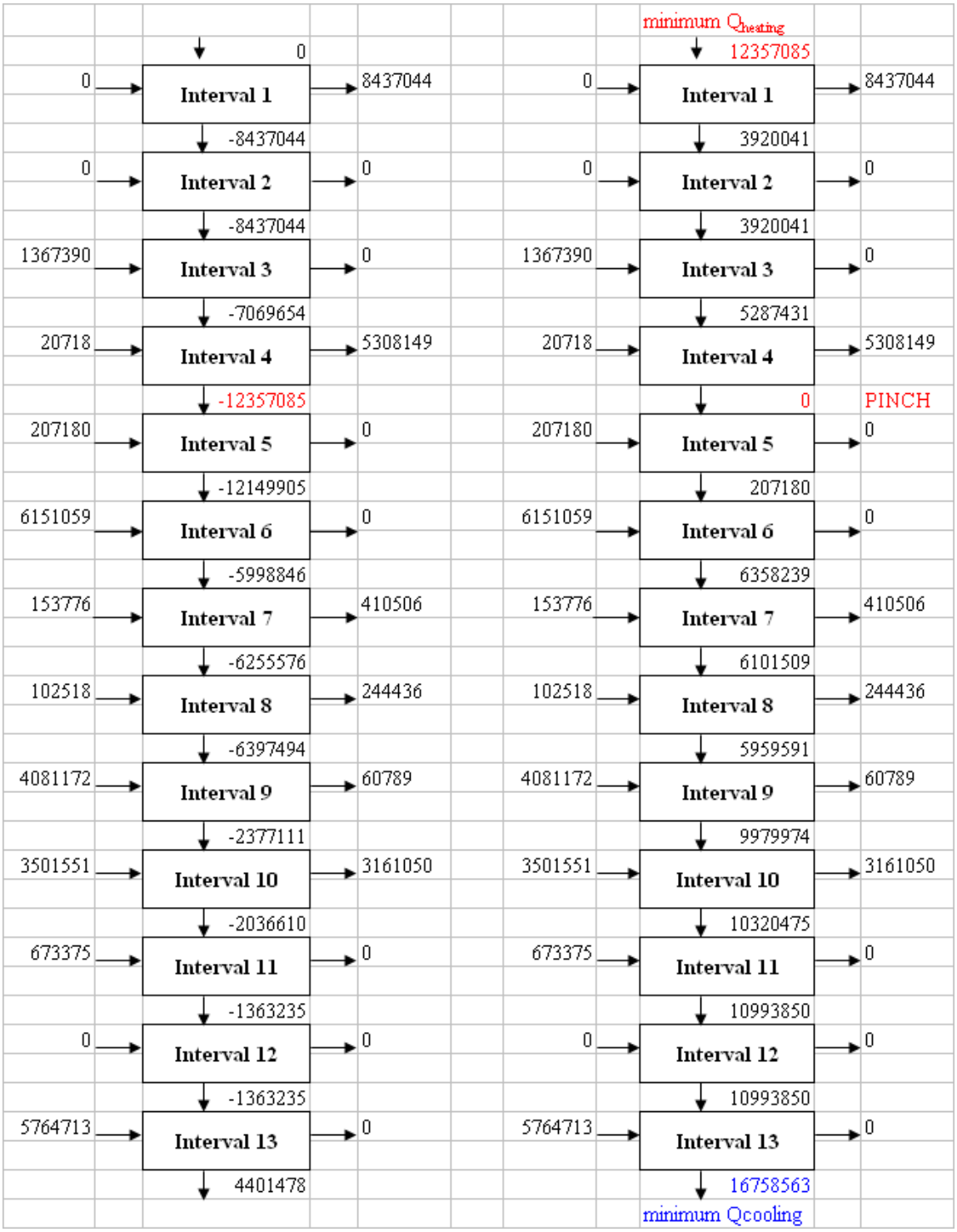

Figure 5.3 Cascade diagram of biodiesel production HEN (heat unit: Btu/hr)

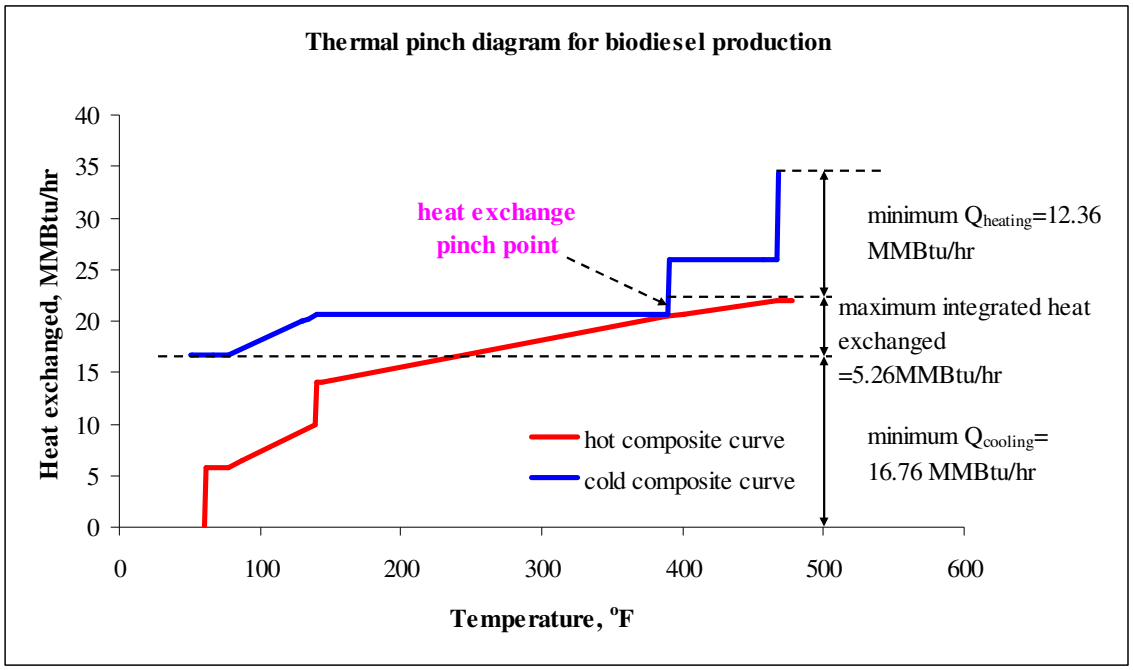

Figure 5.4 Thermal pinch diagram for biodiesel production

Table 5.3 Utility savings of biodiesel production from heat integration

	heating utility	**cooling utility**
utility without integration (Btu/hr)	17621975	22023452
utility after integration (Btu/hr)	12357085	16758563
savings from heat integration (Btu/hr)	5264890	5264889
percentage of savings	**29.9%**	**23.9%**

5.2.2 Heat Integration for ULSD Production

Similarly, heat integration was performed for the ultra low sulfur diesel (ULSD) plant with a feed capacity of 70000 barrel per stream day (BPSD) or 980 million gallon per year (MMGPY) based on 8000 operating hours per year. The cold and hot streams of ULSD production with expected total heating and cooling utilities are shown in Table 5.4. Heat capacity was calculated by net duty / (target temperature-supply temperature).

Table 5.4 Cold and hot streams of ULSD production

	supply temp, ^{o}F	**target temp, ^{o}F**	**net duty (Btu/hr)**	**heat capacity (Btu/hr.^{o}F)**
cold streams				
T-0001 reboiler	522	523	231856905	231856905
total heating utility			**231856905**	
hot streams				
HE-0001	653	550	-111576084	1083263
HE-0002	554	110	-142625321	321228
HE-0003	467	110	-172709725	483781
HE-0004	522	110	-193577134	469847
HE-0005	385	110	-168418.23	612
T-0001 condenser	110	109	-38149075	38149075
total cooling utility			**-658805757**	

The temperature-interval diagram (TID) was constructed based on the cold and hot streams of biodiesel production, as shown in Figure 5.5. Cascade diagram of biodiesel production was then developed, as shown in Figure 5.6. The pinch point was found between the 4th and 5th interval with the most negative residual heat -113213801 Btu/hr. The minimum heating and cooling utility were determined to be 113213801 Btu/hr and 540162653 Btu/hr, respectively. Similarly, these results are consistent with those from the graphic heat integration method as shown in Figure 5.7 and from LINGO linear programming with the set formulations shown in Appendix B. It was shown from the thermal pinch diagram that the integrated heat exchange was maximized at 119.55 MMBtu/hr. Table 5.5 shows that the heating and cooling utility was reduced by 51.2% and 18.0% with heat integration.

intervals	hot streams	°F	°F	cold streams
		653	643	
1		554	544	
2		550	540	
3		533	523	
4		532	522	
5		522	512	
6		467	457	
7		385	375	
8		110	100	
9		109	99	

Figure 5.5 Temperature interval diagram of ULSD production HEN

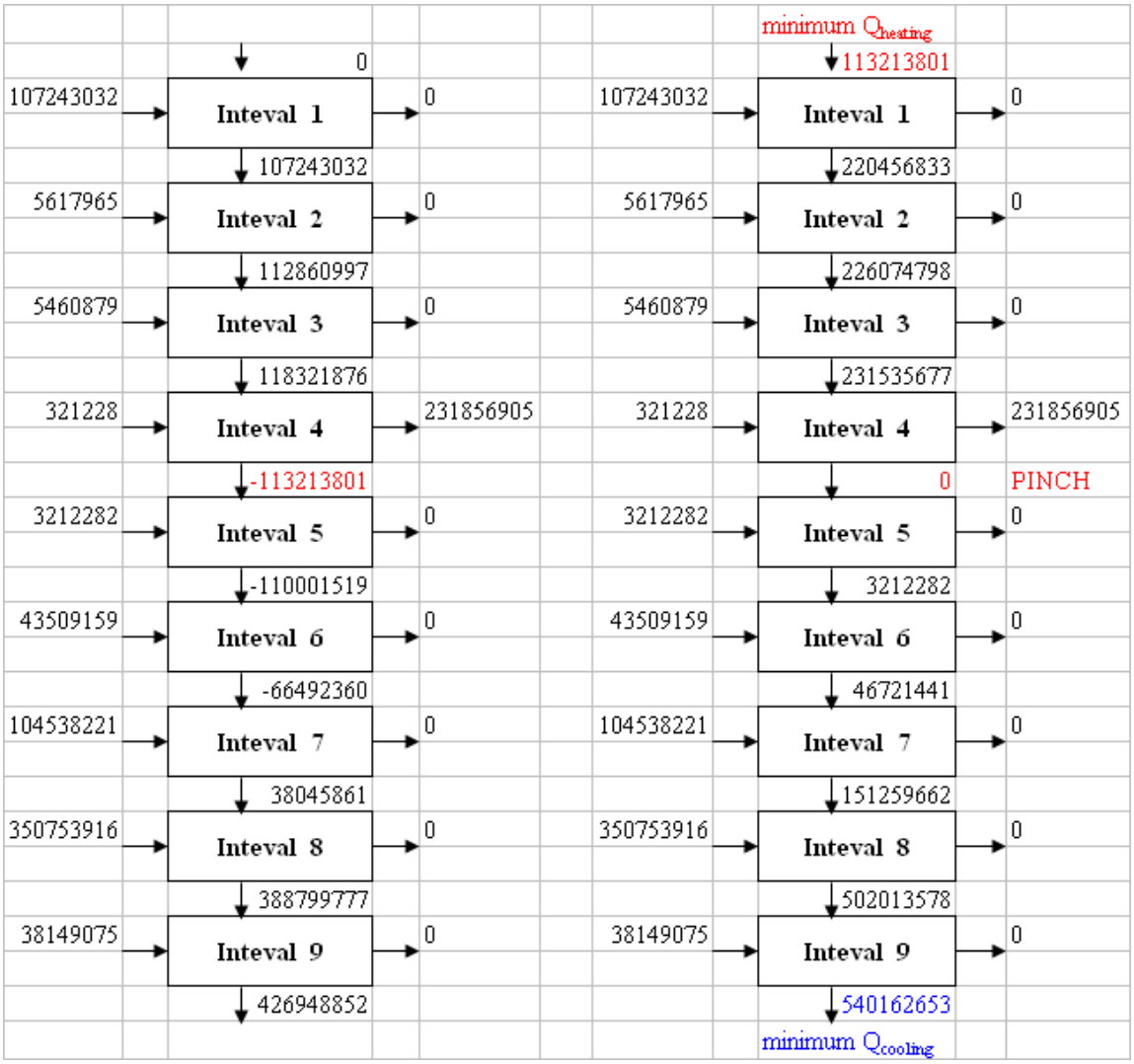

Figure 5.6 Cascade diagram of ULSD production HEN (heat unit: Btu/hr)

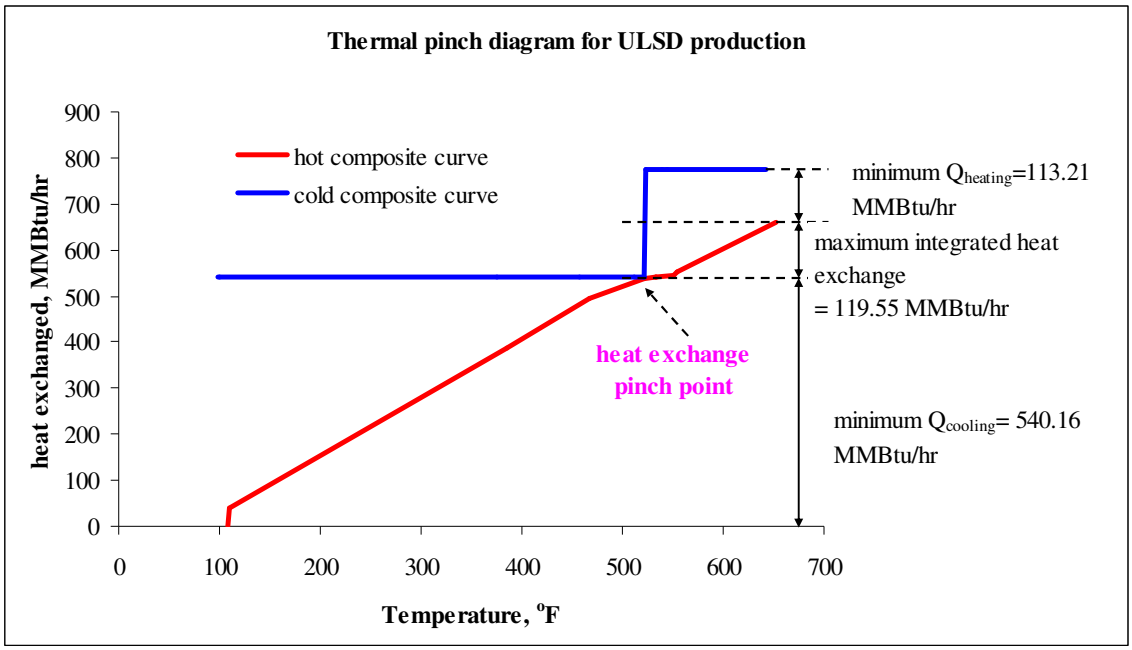

Figure 5.7 Thermal pinch diagram for ULSD production

Table 5.5 Utility savings of ULSD production from heat integration

	heating utility	**cooling utility**
utility without integration (Btu/hr)	231856905	658805757
utility after integration (Btu/hr)	113213801	540162653
savings from heat integration (Btu/hr)	118643104	118643104
percentage of savings	**51.2%**	**18.0%**

5.3 Estimation of Total Capital Investment and Operating Cost

Capital investment is the total amount of money needed to supply the necessary plant and manufacturing facilities plus the amount of money required as working capital for operation of the facilities. Another major component of an economic analysis is the total product cost, which is defined as the total of all costs of operating the plant, selling the products, recovering the capital investment, and contributing to corporate functions such as management and research and development. It is broadly divided into two categories:

manufacturing costs and general expenses. Manufacturing costs are also referred to as operating or production costs (Peters et al., 2003). The structure and components of total capital investment and total product cost are shown in Figures 5.8 and 5.9, respectively. Total capital investment and manufacturing (operating / production) cost were estimated for biodiesel and ULSD production in this work.

5.3.1 Biodiesel Production Cost Estimation

The cost estimation was performed based on the biodiesel production capacity of 40 million gallons per year (MMGPY) or 500 gallons per hour based on 8000 operating hours per year.

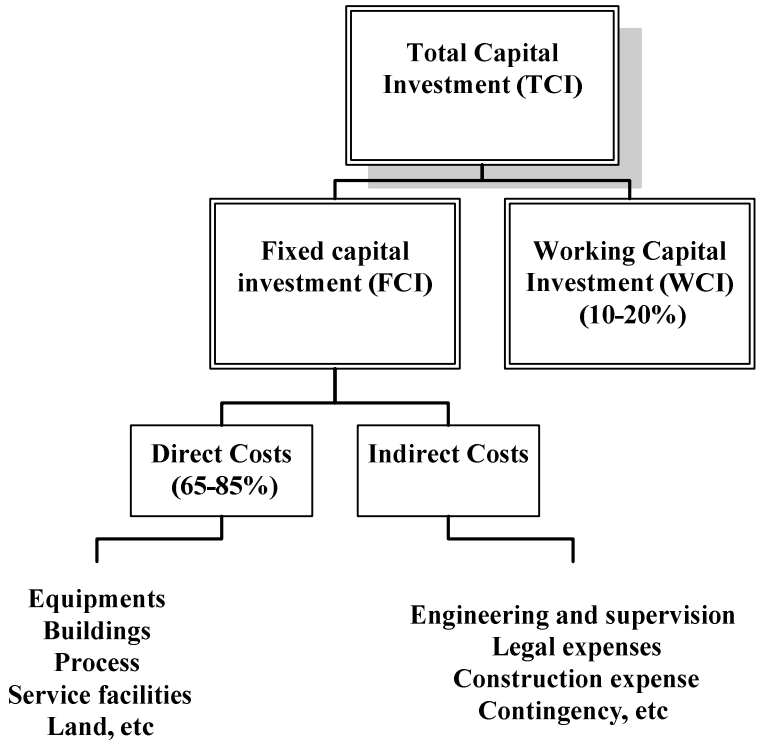

Figure 5.8 Structure and components of total capital investment

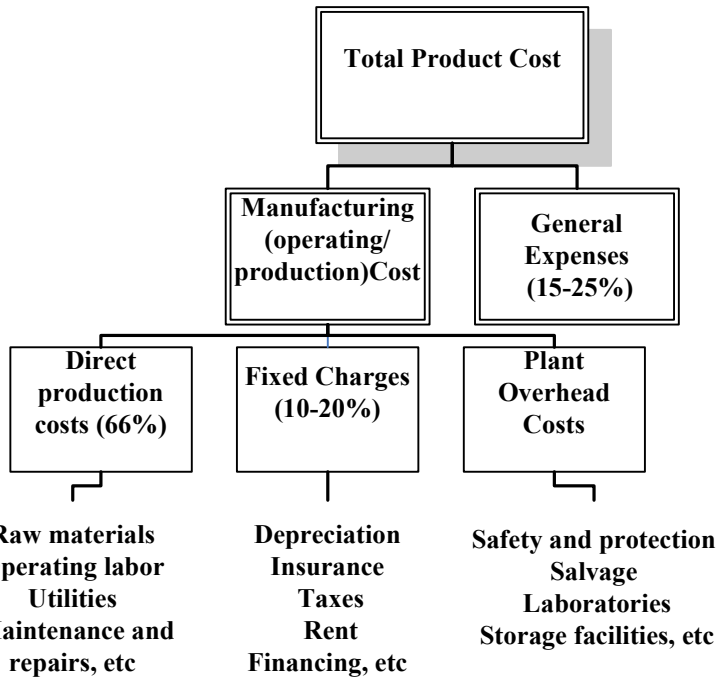

Figure 5.9 Structure and components of total product cost

The Aspen ICARUS Process Evaluator tool was used to estimate the total capital investment. The bulk of the total capital investment resulted from the installed equipment costs and other materials costs such as piping and instrumentation systems. Working capital investment (WCI) was set at 15% of the total capital investment (TCI). It was indicated from Table 5.6 that a large portion of the total capital investment (TCI) is purchasing and installing the equipments. Aspen ICARUS was used to determine the installed equipment costs. Specifications and installed costs for all major pieces of equipments were shown in Table 5.7.

Table 5.6 Total capital investment of biodiesel production

	Total Cost ($)
Purchased Equipment	649,500
Equipment Setting	20,200
Piping	725,800
Civil	144,300
Steel	52,600
Instrumentation	1,066,800
Electrical	396,500
Insulation	305,700
Paint	40,700
Other	3,489,800
Subcontracts	0
G and A Overheads	144,200
Contract Fee	369,100
Escalation	0
Contingencies	1,332,900
Special Charges	0
Fixed Capital Investment	8,738,100
Working Capital Investment	1,542,000
Total Capital Investment	**10,280,100**

Table 5.7 Total equipment cost of biodiesel production

Equipment Name	Equipment Type	Total Direct Cost ($)	Equipment Cost ($)
Decanters			
DECANT1	DVT CYLINDER	74,800	12,600
DECANT2	DVT CYLINDER	92,900	15,700
DECANT3	DVT CYLINDER	92,900	15,700
DECANT4	DVT CYLINDER	92,900	15,700
Heat exchangers			
HEX1	DHE FLOAT HEAD	57,500	23,900
HEX10	DHE FLOAT HEAD	75,200	16,700
HEX11	DHE FLOAT HEAD	64,700	16,600
HEX2	DHE FLOAT HEAD	64,900	16,300
HEX3	DHE FLOAT HEAD	57,700	24,100
HEX4	DHE FLOAT HEAD	77,200	17,900
HEX5	DHE FLOAT HEAD	64,600	16,900
HEX6	DHE FLOAT HEAD	64,600	16,900
HEX7	DHE FLOAT HEAD	64,900	16,300
HEX8	DHE FLOAT HEAD	79,600	20,000
HEX9	DHE FLOAT HEAD	64,900	16,300
Distillation columns			
METDIST1-tower	DTW TRAYED	323,600	90,100
METDIST1-cond	DHE FIXED T S	56,500	14,900
METDIST1-cond acc	DHT HORIZ DRUM	66,400	12,400
METDIST1-reflux pump	DCP CENTRIF	21,700	3,600
METDIST1-reb	DRB U TUBE	96,700	23,200
METDIST2-tower	DTW TRAYED	73,700	56,500
METDIST2-cond	DHE FIXED T S	67,600	16,900
METDIST2-cond acc	DHT HORIZ DRUM	53,500	9,000
METDIST2-reflux pump	DCP CENTRIF	22,200	4,100
METDIST2-reb	DRB U TUBE	71,500	17,900
Pumps			
PUMP1	DCP CENTRIF	25,200	3,800
PUMP10	DCP CENTRIF	30,500	4,800
PUMP2	DCP CENTRIF	30,500	4,800
PUMP3	DCP CENTRIF	21,600	3,600
PUMP4	DCP CENTRIF	31,600	5,000
PUMP5	DCP CENTRIF	22,500	3,700
PUMP6	DCP CENTRIF	25,100	3,700
PUMP7	DCP CENTRIF	30,500	4,800
PUMP9	DCP CENTRIF	30,500	4,800
Reactors			
REACT1	DAT REACTOR	177,800	66,500
REACT2	DAT REACTOR	177,800	66,500
	Total	**2,546,300**	**682,200**

Table 5.8 Calculation of annual operating cost of biodiesel production

Items	**annual cost ($/yr)**
Raw materials cost	142,510,500
operating labor cost	480,000
maintenance cost	37,500
supervision	280,000
electricity	37,500
heating and cooling utilities	904,400
Total	**144,249,900**

The annual operating cost of biodiesel production was tabulated, as shown in Table 5.8. The operating labor cost, maintenance cost, supervision and electricity costs were extracted from Aspen ICARUS results. The calculation of raw materials cost and heating and cooling utilities was listed in Table 5.9 and Table 5.10, respectively. The prices per unit for soybean oil and methanol are obtained from online ICIS pricing for chemicals, and those for NaOH, HCl and water are obtained from Lay Myint's biodiesel production results (Myint, 2007). The amount of raw materials used is extracted from biodiesel production ASPEN simulation stream results. The utility unit prices were obtained from the specification of CHEN 426 Plant Design course project by Fluor.

Table 5.9 Costs of raw materials of biodiesel production

Raw materials	**cost per unit ($/lb)**	**units (lb/hr)**	**annual cost ($/yr)**
soy bean oil	0.42	36357.00	122,159,500
methanol	0.26	8253.78	17,167,900
NaOH	1.8	185.42	2,670,000
HCl	0.63	93.70	472,300
water	0.0012	4251.61	40,800
		Total	**142,510,500**

Table 5.10 Costs of heating and cooling utilities of biodiesel production

Heat exchanger	utility	utility flow rate (lb/hr)	utility costs ($/1000lb)	annual utility costs ($/yr)
HEX1	boiling water	2187.96	0.57	10,000
HEX2	boiling water	42397.07	0.57	193,300
HEX3	boiling water	159.50	0.57	700
HEX4	cooling water	36088.83	0.0096	2,800
HEX5	boiling water	15401.73	0.57	70,200
HEX6	boiling water	17887.56	0.57	81,600
HEX7	boiling water	56783.58	0.57	258,900
HEX8	cooling water	200394.48	0.0096	15,400
HEX9	boiling water	58613.04	0.57	267,300
HEX10	cooling water	29737.12	0.0096	2,300
HEX11	cooling water	25025.60	0.0096	1,900
			Total	**904,400**

As shown in Table 5.11, the annual sales of biodiesel product were found to be $137,930,100 /yr, based on the biodiesel production capacity of 40 million gallons per year (MMGPY) and the biodiesel retail price (after-tax) of $3.39/gal (October, 2007, online ICIS pricing). In the biodiesel production process, the byproducts glycerol can be purified for commercialized use, recovered methanol are recycled back as the feed, waster water and soybean oil can be sold or recycled as the feed. Therefore, the sales of glycerol, methanol, recovered water and soybean oil were estimated as well in order to further reduce operating cost. The retail prices of glycerol, methanol and recovered soybean oil were obtained from online ICIS pricing (October, 2007), and that of water was obtained from Myint (2007). The recovered soybean oil with the purity of 99.8 wt% was considered as crude soybean oil, so the crude soybean oil price was used. The annual operating cost and savings after process integration were listed in Table 5.12.

Table 5.11 Sales of biodiesel products and byproducts

Products	purity (wt%)	lb/hr	gal/day	price per unit	annual sales ($/yr)
biodiesel	99.65	36446.40	122062.04	$ 3.39 /gal	137,930,100
glycerol	97.6	3678.52	9736.53	$ 0.60 /gal	1,947,300
glycerol-2	83.9	202.02	518.07	$ 0.07 /gal	12,100
methanol	100	1282.00	4638.93	$ 0.26 / lb	2,666,600
methan-2	99.97	3013.00	10902.56	$ 0.26 / lb	6,267,000
recovered water	97.1	4337.88	14434.21	$ 0.000120 / lb	4,200
recovered soybean oil	99.8	181.70	621.01	$ 0.39 / lb	566,900
				total	**149,394,200**

Table 5.12 Annual operating cost and savings of biodiesel production with process integration

Items	annual cost ($/yr)
Raw materials cost	142,510,500
operating labor cost	480,000
maintenance cost	37,500
supervision	280,000
electricity	37,500
heating and cooling utilities	904,400
total operating cost before process integration	**144,249,900**
savings from process integration	
heat integration	269,100
water recycling	4,200
methanol recycling	8,933,600
glycerol sales	1,959,400
total savings from process integration	11,166,300
total operating cost with process integration	**133,083,600**

5.3.2 Ultra Low Sulfur Diesel (ULSD) Production Cost Estimation

The cost estimation was performed based on the ULSD feed capacity of 70000 barrel per stream day (BPSD) or 980 million gallons per year (MMGPY) based on 8000 operating hours per year.

Similarly to the cost estimation of biodiesel production, the total capital investment was obtained from Aspen ICARUS results with the working capital investment being set at 15% of the total capital investment, as shown in Table 5.13. The installed equipment costs were specified in Table 5.14.

Table 5.13 Total capital investment of ULSD production

	Total Cost ($)
Purchased Equipment	6,617,000
Equipment Setting	96,900
Piping	2,047,200
Civil	300,100
Steel	94,600
Instrumentation	1,138,500
Electrical	423,700
Insulation	670,600
Paint	66,600
Other	4,901,700
Subcontracts	0
G and A Overheads	426,300
Contract Fee	614,400
Escalation	0
Contingencies	3,131,600
Special Charges	0
Fixed Capital Investment	20,529,200
Working Capital Investment	3,622,800
Total Capital Investment	**24,152,000**

Table 5.14 Total equipment cost of biodiesel production

Equipment Name	Equipment Type	Total Direct Cost ($)	Equipment Cost ($)
Compressors			
C-0001	DGC CENTRIF	1,115,300	917,900
C-0002	DGC CENTRIF	1,063,000	960,800
C-0003	DGC CENTRIF	1,361,000	960,100
Heat exchangers			
HE-0001	DHE FLOAT HEAD	124,300	33,900
HE-0002	DHE FLOAT HEAD	263,900	119,400
HE-0003	DHE FLOAT HEAD	328,800	150,000
HE-0004	DHE FLOAT HEAD	329,100	150,300
HE-0005	DHE FLOAT HEAD	57,400	17,400
Pumps			
P-0001	DCP CENTRIF	66,100	17,100
P-0002	DCP CENTRIF	25,200	3,800
P-0005	DCP CENTRIF	84,200	20,700
P-0006	DCP CENTRIF	76,900	20,700
Distillation columns			
T-0001-tower	DTW TRAYED	2,592,600	1,350,800
T-0001-cond	DHE FIXED T S	112,700	32,100
T-0001-cond acc	DHT HORIZ DRUM	84,800	16,100
T-0001-reflux pump	DCP CENTRIF	31,400	4,900
T-0001-reb	DRB U TUBE	1,521,000	1,110,000
T-0002-tower	DTW TRAYED	463,500	276,600
T-0003-tower	DTW TRAYED	101,600	15,200
Flashes			
V-0001-flash vessel	DVT CYLINDER	139,000	25,400
V-0002-flash vessel	DVT CYLINDER	111,500	23,500
Reactors			
Reactors	multiple-stage reactor	757,400	328,100
	Total	**10,810,700**	**6,554,800**

Table 5.15 Calculation of annual operating cost of ULSD production

Items	**annual cost ($/yr)**
Raw materials cost	1,966,912,200
operating labor cost	800,000
maintenance cost	324,000
supervision	280,000
electricity	105,800
heating and cooling utilities	1,388,700
catalysts	1,747,200
Total	**1,971,557,900**

The annual operating cost of ULSD production with a capacity of 70000 barrel per stream day (BPSD) was calculated to be $1,971,557,900. The calculation of raw materials, heating and cooling utility costs was shown in Table 5.16 and Table 5.17. The prices for raw materials H_2 and lean amine, heating and cooling utilities were obtained from the ULSD design project provided by Fluor Daniel. The feedstock FCC LCO & SR diesel price was calculated based on the assumption that the feedstock prices change is proportional to the crude oil change from March, 2005 to October 2007.

Table 5.16 Costs of raw materials of ULSD production

Raw materials	**cost per unit**	**units**	**annual cost ($/yr)**
FCC LCO & SR Diesel	$ 83.46 /BBL	70000 BBL/day	1,947,400,000
Pipeline Make up H_2	$ 5.00 /MSCF	9466.5 MSCF/day	15,777,500
Lean Amine	$ 7.00 /MGAL	1600.6 MGAL/day	3,734,700
		total	**1,966,912,200**

Table 5.17 Costs of heating and cooling utilities of ULSD production

Heat exchanger	utility	utility flow rate (lb/hr)	utility costs ($/1000lb)	annual utility costs ($/yr)
HE-0001	cooling water	2468222.50	0.0096	189,600
HE-0002	cooling water	3465707.01	0.0096	266,200
HE-0003	cooling water	4529413.61	0.0096	347,900
HE-0004	cooling water	7608915.69	0.0096	584,400
HE-0005	cooling water	8400.31	0.0096	600
			Total	**1,388,700**

As Table 5.18 indicated, the sales of diesel and naphtha were found to be $ 3,778,873,700 /yr and $ 110,248,300 /yr, respectively with a retail price of $ 127.93 per barrel and $ 83.08 per barrel (October, 2007, available at EIA crude spot price online). The recovered hydrogen can be sold or recycled back to the hydrotreater in order to facilitate the removal of sulfur in the feedstock. The savings from heat integration and hydrogen recycling were listed in Table 5.19.

Table 5.18 Sales of ULSD products and byproducts

Products	purity (wt%)	cuft/hr	bbl/day	price per unit	annual cost ($/yr)
Diesel	—	20731.15	88615.81	$ 127.93/BBL	3,778,873,700
Naphtha	—	931.34	3981.04	$ 83.08/BBL	110,248,300
recovered H_2	96.5	168060.34	718377.92	$ 2.60/MSCF	3,495,700
				Total	**3,892,617,700**

Table 5.19 Annual operating cost and savings of ULSD production with process integration

Items	**annual cost ($/yr)**
Raw materials cost	1,966,912,200
operating labor cost	800,000
maintenance cost	324,000
supervision	280,000
electricity	105,800
heating and cooling utilities	1,388,700
catalysts	1,747,200
Total operating cost before process integration	**1,971,557,900**
savings from process integration	
heat integration	15,107,500
hydrogen recycling	3,495,700
total savings from process integration	18,603,200
total operating cost with process integration	**1,952,954,700**

5.3.3 Cost Estimation of Base Case LSD Production

Since the base case LSD production was not simulated in our study, the cost of LSD production was estimated by subtracting the incremental costs from the ULSD production during the revamping. The revamping incremental costs of equipments and annual operating costs are summarized in Table 5.20 and Table 5.21, respectively.

Table 5.20 Revamped cost increments for equipment

Equipment Name	Equipment Type	Total Direct Cost ($)	Equipment Cost ($)
C-0001	DGC CENTRIF	1,115,300	917,900
C-0002	DGC CENTRIF	1,063,000	960,800
HE-0005	DHE FLOAT HEAD	57,400	17,400
P-0001	DCP CENTRIF	66,100	17,100
P-0002	DCP CENTRIF	25,200	3,800
T-0002-tower	DTW TRAYED	463,500	276,600
T-0003-tower	DTW TRAYED	101,600	15,200
Reactors	multiple-stage reactor	757,400	328,100
	total	**3,649,500**	**2,536,900**

Table 5.21 Revamped cost increments of annual operating cost

	unit price	amount	total costs	units
catalysts	$ 200 /cuft	21840 cuft	4,368,000	USD
		2.5 year /cycle length	1,747,200	USD/yr
H2 consumption increment	$ 5.00 /MSCF	2533.3MSCF/DAY	4,222,200	USD/yr
Lean Amine	$ 7.00 /MGAL	1600.6 MGAL/day	3,734,700	USD/yr
		total	**9,704,100**	**USD/yr**

The fixed capital investment (FCI) and total capital investment (TCI) of LSD were then calculated by using the Lang Factors method (Peters et al., 2003; El-Halwagi, 2007).

FCI = FCI Lang Factor * equipment cost;

TCI = TCI Lang Factor * equipment cost;

Therefore, $\frac{FCI_{LSD}}{FCI_{ULSD}} = \frac{equipment_{LSD}}{equipment_{ULSD}}$ and $\frac{TCI_{LSD}}{TCI_{ULSD}} = \frac{equipment_{LSD}}{equipment_{ULSD}}$.

The annual operating cost of LSD was calculated by

Annual operating cost of LSD = operating cost of ULSD- revamp operating cost increment.

5.3.4 Cost Comparisons of Biodiesel, ULSD and LSD Production Processes

The process simulation and cost estimation for biodiesel production was performed based on the capacity of 40 million gallon per year (MMGPY) with a useful life cycle of 5 years, while those for ULSD and base case LSD production were based on the capacity of 980 MMGPY with a useful life cycle of 10 years. In order to compare the three processes, the cost estimation results need to be normalized with the same capacity of 40 MMGPY. The cost estimation for the normalized processes was shown in Table 5.22.

Table 5.22 Costs of biodiesel, ULSD and LSD processes based on a 40 MMGPY capacity

	biodiesel	**ULSD**	**LSD**
capacity	40MMGPY	40MMGPY	40MMGPY
useful life period	5 years	10 years	10 years
FCI ($/yr)	8,738,100	3,012,100	1,857,300
TCI ($/yr)	10,280,100	3,543,700	2,185,100
total operating cost before integration($/yr)	144,249,900	80,471,800	80,075,700
total operating cost after integration($/yr)	133,083,600	79,712,400	79,320,100
total production income ($/yr)	149,394,200	158,882,400	--
salvage value ($yr)	873,800	301,200	185,700
Depreciation/annualized fixed cost ($/yr)	1,572,900	271,100	167,200
total annualized cost (TAC) ($/yr)	134,656,500	79,983,500	79,487,300

When the capacity of ULSD and LSD were reduced from 980 MMGPY to 40 MMGPY, the capacity was calculated by the empirical formula (Peters et al., 2003; El-Halwagi, 2007)

$$\frac{FCI_A}{FCI_B} = \left(\frac{Capacity_A}{Capacity_B}\right)^{0.6}$$

Therefore, FCI and the capacity don't have a linear relationship, whereas the operating cost is proportional to the capacity, hence

$$\frac{operating_A}{operating_B} = \frac{Capacity_A}{Capacity_B}$$

Total capital investment (TCI) is the sum of fixed cost investment (FCI) and working cost investment (WCI, 15% of TCI).

Total operating cost after integration of LSD was calculated by assuming

$$\frac{operating_{LSD,after}}{operating_{ULSD,after}} = \frac{operating_{LSD,before}}{operating_{ULSD,before}}$$

Salvage value is set at 10% of the fixed capital investment (FCI) for all the processes. Depreciation is defined as an annual charge which is set aside to recover the fixed cost over the useful life period of the plant due to physical or functional depreciation (El-Halwagi, 2007; Peters et al., 2003). For project estimation purposes, depreciation equals to annualized fixed cost (AFC). Depreciation is calculated by

$$\text{Depreciation} = \frac{\text{Initial plant (or equipment) cost (FCI)} - \text{Salvage value}}{\text{Useful life period}}$$

Total annualized cost (TAC) was the sum of annualized fixed cost (depreciation) and the annual operating cost (El-Halwagi, 2007; Myint, 2007).

5.4 Blending Optimization for Three Blending Options

Three blending options were identified and investigated in this project. The first option was to blend low sulfur diesel (LSD) with biodiesel in order to meet the stringent ultra low sulfur diesel regulations. The second option was to blend ULSD with biodiesel to solve certain issues caused by the production of ULSD. The third option was to add commercial chemical additives into ULSD. The optimum blends of each option were then compared from economic, safety and environmental perspectives and in turn the optimum blending strategy was identified. The components of the three options were shown in Figure 5.10.

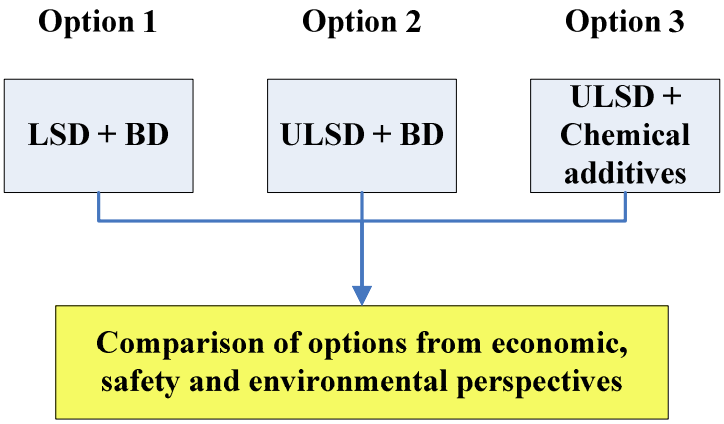

Figure 5.10 Components of three blending options

5.4.1 Blending Optimization for Option 1

This option is to blend low sulfur diesel (LSD, 470 ppmw sulfur) with biodiesel (0 ppmw) in order to keep the overall sulfur content of the blends below 15 ppmw. Since the sulfur content is proportional to fuel amounts, the LSD and biodiesel volume ratio can be determined by $\frac{470V_{LSD} + 0V_{BD}}{V_{LSD} + V_{BD}} = 15$, where V_{LSD} and V_{BD} are the volume of LSD and biodiesel respectively, therefore the blended biodiesel fraction was 96.8 %. The total annualized cost (TAC) was found to be $ 132,931,800 /yr for a 40 MMGPY blend capacity. Total annualized cost (TAC) was the sum of annualized fixed cost (depreciation) and the annual operating cost, as mentioned in Section 5.3.4.

$$TAC = TAC\_BD + TAC\_LSD$$

5.4.2 Blending Optimization for Option 2

Although ULSD produced in our case contained only 8 ppmw sulfur, which was below the ultra low sulfur diesel (15 ppmw) regulation, ULSD normally possesses poor lubricity due to the removal of polar compounds during the desulfurization process and

low cetane number. Blending biodiesel into ULSD could enhance the lubricity and cetane number; however, because of the drawbacks of biodiesel itself such as the prices, NOx emission and energy content, several constraints need to be taken into account for the blending.

The objective function is to minimize the total annualized cost (TAC) of the blends of biodiesel and petrodiesel fuel. The constraints are determined mainly by the existing specifications and regulations of biodiesel and petrodiesel. The variable is the volume percent of biodiesel blended into the petrodiesel, x. It is assumed that the biodiesel and ULSD we produced have similar densities despite the fact that biodiesel is slightly denser than diesel fuel. Therefore, x is also the mass fraction of biodiesel blended into the petrodiesel.

Fixed capital investment (FCI) for similar processes with different capacity is calculated by (El-Halwagi, 2007)

$$\frac{FCI_A}{FCI_B} = \left(\frac{Capacity_A}{Capacity_B}\right)^{0.6}$$

Thus the FCI is not linearly related to the production capacity, while the operating cost is proportional to the production capacity.

The TAC of biodiesel production with a capacity of (40*x) MMGPY

$$TAC\_BD = \frac{8738100x^{0.6}(1-0.1)}{5} + 133083600x$$

The TAC of ULSD production with a capacity of 40*(1-x) MMGPY

$$TAC\_ULSD = \frac{3012100(1-x)^{0.6}(1-0.1)}{10} + 79712400(1-x)$$

The formulation of the objective function based on a 40MMGPY blends production capacity would be

$$TAC = TAC\_BD + TAC\_ULSD$$

$$= \frac{8738100x^{0.6}(1-0.1)}{5} + 133083600x + \frac{3012100(1-x)^{0.6}(1-0.1)}{10} + 79712400(1-x)$$

When it came to the constraint formulations, there were following crucial factors taken into consideration:

- **Lubricity**

It has been widely reported that 2% blends of biodiesel can provide any type of distillate fuel with adequate lubricity (Meadbiofuel, http://www.meadbiofuel.com/blending.htm). Even 2% biodiesel can restore sufficient lubricity to dry fuels such as kerosene or Fischer-Tropsch diesel (DOE, 2006). In US, with a 20% blend of biodiesel with 80% diesel fuel (B20) being more and more common, a considerate amount of experiences in dealing with B20 were acquired and reported. It was suggested that the B20 blends do not require any engine modifications. Although biodiesel (B100) can be used, blends of over 20% biodiesel with diesel fuel should be evaluated on a case-by-case basis until further experience is available (National Biodiesel Board). Therefore, x should lie in the range between 0.02 and 0.2, which is $0.02 < x < 0.2$.

- **Cetane number**

Cetane number of a fuel is defined as "the percentage by volume of normal cetane in a mixture of normal cetane and alpha-methyl naphthalene which has the same ignition delay as the test fuel when combustion is carried out in a standard engine under specified operating conditions" (wikipedia explanation of cetane number, 2008).

Since there are hundreds of components in diesel fuel, with each having a different cetane quality, the overall cetane number of the diesel is the average cetane performance of all the components. As a matter of fact, there is very little actual cetane in diesel fuel (wikipedia explanation of cetane number, 2008). Therefore, we assume that the cetane number has a linear relationship with the volume fraction of the fuels, and the cetane number of the blends is the sum of the cetane number of each fuel in the blends multiplying by its blending fraction.

The cetane number of our ULSD is designated as 40, the minimum requirement of ASTM D 975 for diesel fuel properties, and that of biodiesel is designated as 67, which is the highest cetane number of soybean oil-derived methyl ester according to Gerpen (2008). The target cetane number of the blends is 43, which is required by Engine Manufacturers Association (EMA). The formulation for the cetane constraint would be $40(1-x)+67x \geq 43$

- **NOx emissions and energy content**

It was reported that 20% biodiesel blend (B20) would increase the NOx emission by 2%, and pure biodiesel (B100) increases the emission by 10% (Steve Richardson & Company, LLC, 2008).

The energy content of blends of biodiesel and petrodiesel has a linear relationship with the amount of biodiesel and petrodiesel in the blend and the BTU value of the biodiesel and petrodiesel fuel used to make the blend. Pure biodiesel (B100) has a 12.5% per pound or 8% per gallon less energy content than petrodiesel, while B20 gives rise to 1% loss in fuel economy on average, and changes in torque or power are barely reported (DOE, 2006).

In order to keep the NOx emission and energy content loss as low as possible, the blended biodiesel fraction should be less than 0.2 as well, which is x<0.2.

Therefore, the optimization formulation would be summarized as follows:

$$\min \quad \frac{8738100x^{0.6}(1-0.1)}{5}+133083600x+\frac{3012100(1-x)^{0.6}(1-0.1)}{10}+79712400(1-x)$$

s.t. $0.02 \leq x \leq 0.2$

$40(1-x)+67x \geq 43$

After solving this problem using optimization software LINGO, we get

TAC_{min} = 86, 315,990, and x=0.111

Therefore, the optimal fraction of biodiesel blended into the ULSD is 11.1% (or B11.1) with the minimum total annualized cost of $ 86,315,990 /yr based on a blend production capacity of 40 MMGPY.

5.4.3 Blending Optimization for Option 3

This option is to blend ULSD with commercial chemical additives which can enhance lubricity, with some working as cetane improvers or demulsifiers as well.

The additives investigated in our project were chosen based on the diesel fuel lubricity additives study results by Spicer (2007). In his study, an untreated ULSD fuel with a high HFRR score of 636 microns was utilized as the baseline fuel or control sample for testing all of the additives. All additives tested were evaluated on their ability to restore the lubricity to the fuel by comparing their scores to the control sample. 19 additives were tested with the HFRR scores, blend ratio and blending cost listed. It was suggested that nine of them can improve the untreated ULSD and to meet the ASTM standard of less than 520 microns, and four can meet the Engine Manufacturers Association standard of less than 460 microns. The four additives are the blending candidates for our study, and the performances of them were summarized in Table 5.23.

Table 5.23 Performance of diesel fuel lubricity additives candidates (Spicer, 2007)

ranking	additive	HFRR Score	improvement over base fuel	blend ratio	$ cost per 26-Gal Tank	comments
desired	EMA desired	< 460				desired by the Engine Manufacturers Association
standard	US Standard	< 520				US Lubricity standard for ULSD fuel
baseline	untreated ULSD #2 diesel fuel	636				baseline fuel used in this study
1	2% REG SoyPower Biodiesel	221	415	50:1	market, $1.76	soybean based biodiesel
2	Opti-Lube XPD	317	309	256:1	$4.35	multi-purpose + anti-gel, cetane improver, demulsifier
3	FPPF RV diesel/gas fuel treatment	439	197	640:1	$2.60	gas & diesel - cetane improver, emulsifier
4	Opti-Lube Summer Blend	447	189	3000:1	$0.68	multi-purpose, demulsifier

The performance of lubricity additives candidates showed that the 2% biodiesel significantly increased the lubricity by 65.3%, and the cost is $ 1.76 /26-gal tank ULSD based on a market retail price of $ 3.39/gal, which is more cost-effective than Opti-Lube XPD and FPPF RV diesel/gas fuel treatment but more expensive than Opti-Lube Summer Blend.

The total annualized costs (TAC) for B11.1, B2, B20 and blends of ULSD with additive candidates were calculated, as shown in Table 5.24. The TAC of the optimum blends of option 2, B11.1 was higher than that of the blends with FPPF RV diesel/gas fuel

treatment and Opti-Lube Summer Blend, and slightly lower than that of the blends with Opti-Lube XPD.

Table 5.24 Total annualized cost (TAC) of blends with biodiesel and chemical additives

	total annualized cost (TAC) ($/yr)
B11.1 (optimum for option 2)	86,316,000
B2	81,198,100
B20	91,222,600
Opti-Lube XPD	86,675,800
FPPF RV diesel/gas fuel treatment	83,983,500
Opti-Lube Summer Blend	81,029,700

5.5 Comparison of the Optimum Blends of the Three Options

In order to compare the three blending options from an economic perspective and gain insights of the optimum blending strategies, depreciation, annual net (after-tax) profit, return on investment (ROI) and payback period (PP) were calculated and breakeven point analysis was performed for all the three blending options.

Breakeven occurs when the total annual product cost equals to the total annual sales, as shown in Figure 5.11. The total annual product cost is the sum of the fixed charges (depreciation included), overhead, and general expenses, and the variable production costs. Total annual sales are equivalent to the total income (El-Halwagi, 2007; Peters et al., 2003).

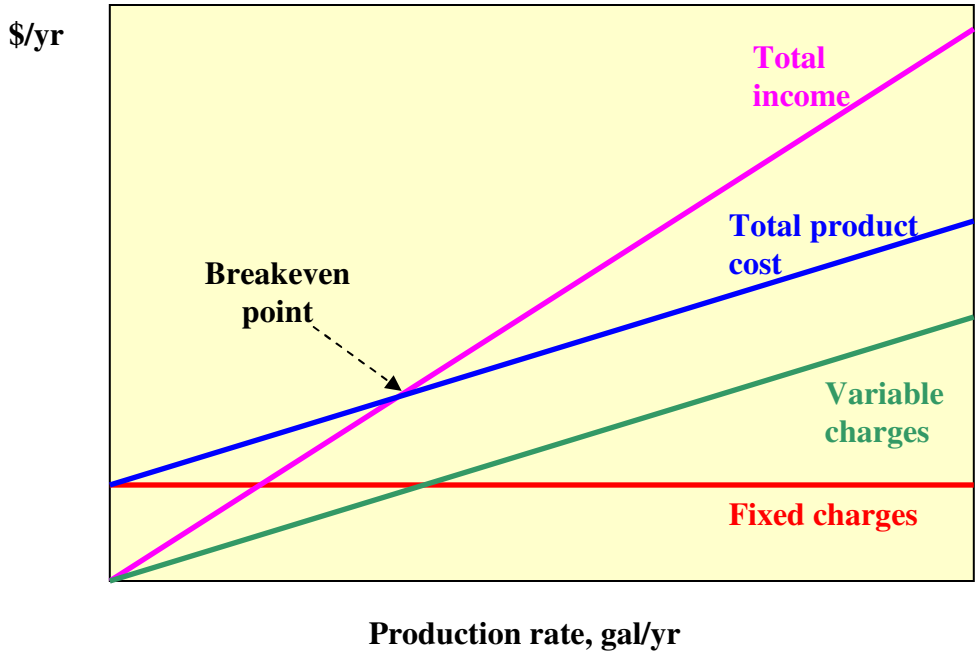

Figure 5.11 Breakeven chart for chemical processing plant (Peters et al., 2003)

For all the three blending options, the annual fixed charges (e.g. depreciation, local taxes, insurance and financing /interest) were assumed to be 15% of the operating costs. Variable charges mainly consist of total operating costs, and thus the total product costs are the sum of total operating costs and total fixed charges. Breakeven production rate x was then determined by solving the equation

fixed charges + total operating cost *x = total income*x.

Return on investment (ROI) is the rate of return obtained from an investment. It is calculated by (El-Halwagi, 2007)

$$\text{ROI} = \frac{\text{Annual Net (After -Tax) Profit}}{\text{Total Capital Investment}}$$

with a unit of fraction per year or % per year.

Annual net (after tax) profit is calculated by (El-Halwagi, 2007)
Annual net (after-tax) profit = Net income per year = Annual after-tax cash flow
= (Annual income – Annual operating cost – Depreciation)*(1-Tax rate) +Depreciation
= (Annual income – Total annualized cost)*(1-Tax rate) + Depreciation
A tax rate of 2% is assumed for the ROI calculation for all the three blending options.

Payback period (PP) or payout period, is the length of time needed for the total return to equal to the capital investment, which is calculated by (El-Halwagi, 2007)

$$\text{Payback period (yrs)} = \frac{\text{Fixed capital investment}}{\text{Annual after-tax cash flow}}$$

Annual after tax cash flow is assumed to equal to the annual net (after-tax) profit.

Table 5.25 Economic comparison of the three options based on a 40 MMGPY capacity

	option 1 LSD+BD	**option 2 B11.1**	**option 3 ULSD+Summer Blend**
capacity	40MMGPY	40MMGPY	40MMGPY
useful life period	5 years	10 years	10 years
FCI ($)	8,804,800	5,143,500	3,012,100
TCI ($)	10,358,600	6,051,200	3,543,700
total operating cost after integration($/yr)	131,368,000	85,636,600	80,758,600
total production income ($/yr)	149,394,200	157,829,200	158,882,400
depreciation/annualized fixed cost ($/yr)	1,563,700	673,200	271,100
annual fixed charges ($/yr)	19,705,200	12,845,500	11,956,900
total annualized cost (TAC) ($/yr)	132,931,800	86,316,000	81,029,700
annual net (after-tax) profit ($/yr)	17,697,000	70,762,200	76,566,700
break even production rate (MMGPY)	43.73	7.12	6.12
ROI	171%	1169%	2161%
payback period (yrs)	0.50	0.07	0.04

The three options have the total annualized cost (TAC) in the order of option 1 > 2 > 3. The break even results from Table 5.25 are consistent with those resulted from the breakeven chart analysis method, as shown in Figure 5.12. The return on investment (ROI) and payback period (PP) as a function of production rate were plotted respectively in order to gain insights of the optimum production capacity with attractive ROI and PP. It was indicated both from Table 5.25 and Figure 5.12 that option 1 need a 6-time more production rate than option 2 and 3 in order to achieve break even. Option 2 and 3 performed much better than option 1 in both ROI and PP analysis. Option 2 has a little lower ROI and longer PP than option 3, but both of them have very attractive ROI and PP, as shown in Figure 5.13 and 5.14.

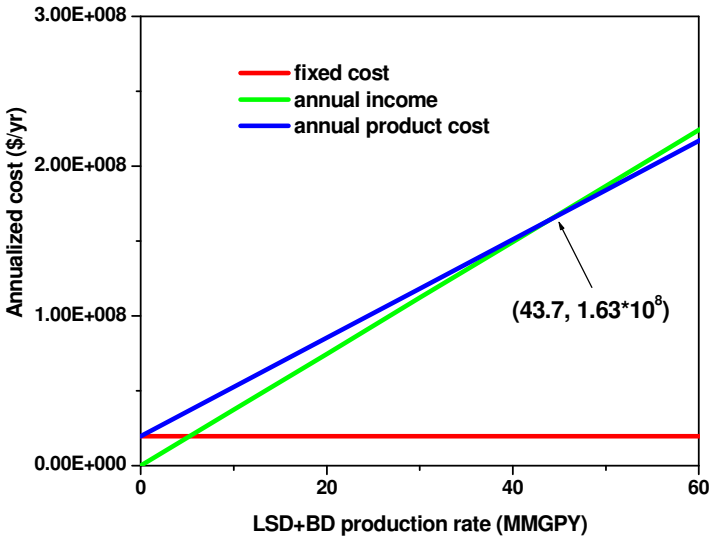

(a)

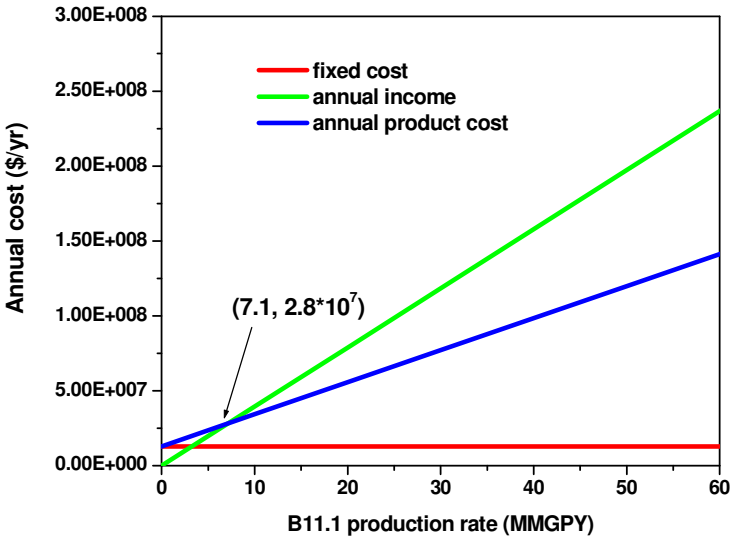

(b)

Figure 5.12 Breakeven chart (a) option 1: LSD+BD (b) option 2: B11.1 (c) option 3: ULSD+Opti-Lube Summer Blend

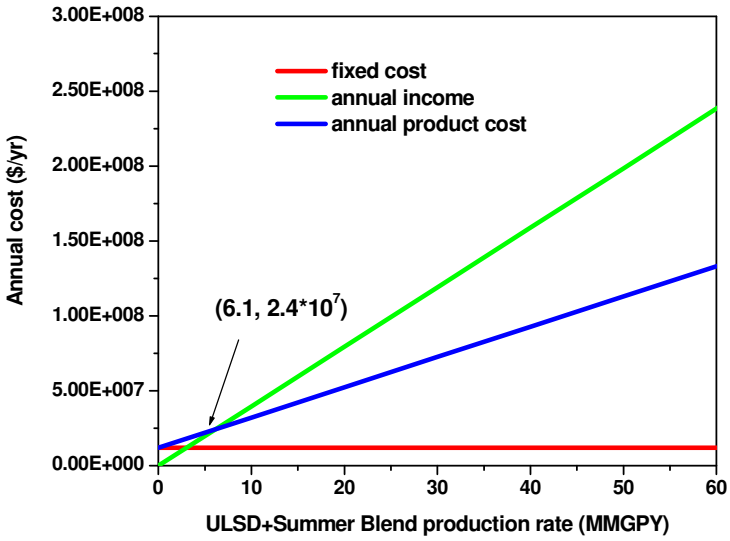

(c)

Figure 5.12 Continued

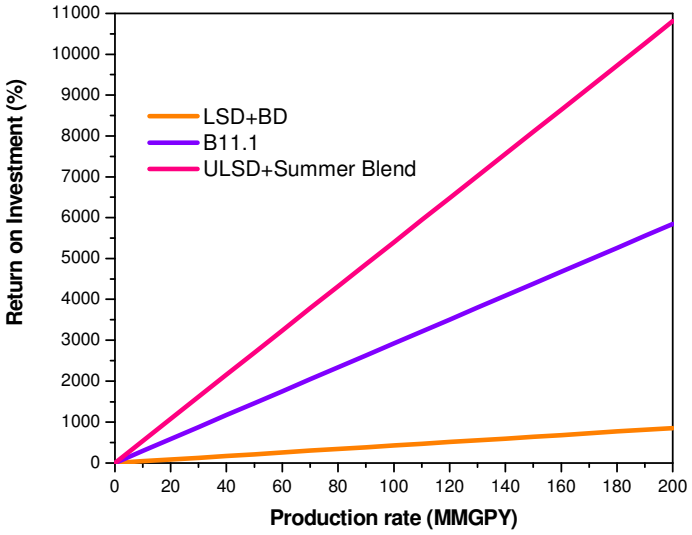

Figure 5.13 Comparison of return on investment (ROI) for the three options

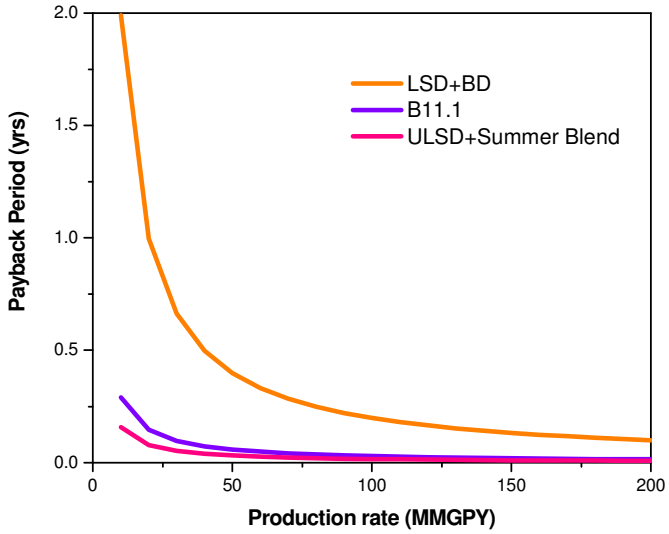

Figure 5.14 Comparison of payback period (PP) for the three options

5.6 Life-Cycle Greenhouse Gas (GHG) Emission Comparison

Although the comparison of total annualized cost (TAC), breakeven analysis, return on investment (ROI) and payback period (PP) indicated that option 3 with Opti-Lube Summer Blend additive was slightly more profitable than the optimum blend B11.1 from option 2, based on an economic perspective, we still argued that the biodiesel blends were superior to the blends with chemical additives such as FPPF RV diesel/gas fuel treatment and Opti-Lube Summer Blend, based on the environmental and safety comparisons.

Life cycle inventories (LCIs) is a comprehensive quantification of all the energy and environmental flows associated with a product from “cradle to grave.” “Cradle to grave” indicates all the steps from the first extraction of raw materials from the environment to the final end-use of the product. LCIs play imperative roles in the overall environmental impacts assessments and comparisons of diverse products. It gives the insights on the following aspects (Sheehan et al., 1998):

- Raw materials extracted from the environment
- Energy resources consumed
- Air, water, and solid waste emissions generated

One of the major purposes of LCIs is to assess overall greenhouse gas emissions from a variety of products, which is currently gaining more and more attentions, due to the global nature of greenhouse gas effects and increasing awareness of the global warming.

The biodiesel can reduce the net CO_2 emission compared to petrodiesel, because the biomass from which biodiesel is derived, can convert CO_2 the biodiesel fuel emits to the atmosphere into carbon-based compounds through photosynthesis. Since the CO_2 is recycled to the fuel, the net effect of biodiesel combustion is thus to reduce the amount of CO_2 in the atmosphere. The LCI model tracks carbon from the point at which it is taken up as biomass via photosynthesis to its final combustion as biodiesel used in vehicles. The biomass-derived carbon that becomes CO_2 leaving the tailpipe is subtracted from the total CO_2 emitted by the vehicles because it is ultimately reused to produce new soybean oil (Sheehan et al., 1998).

Net CO_2 life-cycle emissions for petroleum diesel and biodiesel blends were shown in Figure 5.15. Pure biodiesel has a net CO_2 emission of 136.45 g CO_2/bhp-h, only 21.55 % of that of petroleum diesel. Petroleum diesel has a net CO_2 emission of 633.28 g CO_2/bhp-h, which is assumed to be the same with that of ULSD in our case. A B20 blend emits 15.66% less than petroleum diesel, which suggests the linear relationship between the CO_2 emission and biodiesel composition.

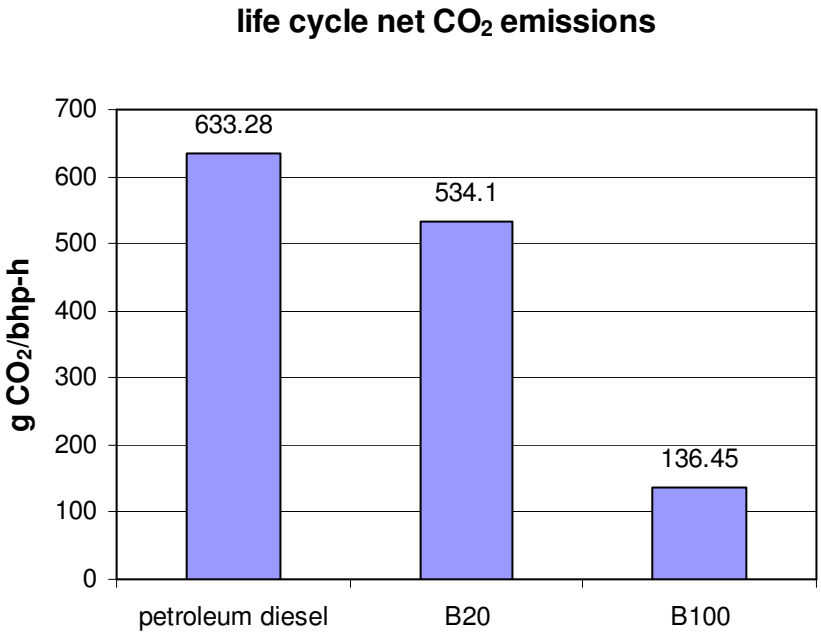

Figure 5.15 Comparison of net CO_2 life-cycle emissions for petroleum diesel and biodiesel blends (Sheehan et al., 1998)

Several assumptions were made in order to identify the net life-cycle CO_2 emissions of chemical additives such as Opti-Lube XPD, FPPF RV diesel/gas fuel treatment and Opti-Lube Summer Blend, due to the insufficient literature information regarding these chemical additives. The assumptions were shown as follows:

- The net life-cycle CO_2 emissions of the three chemical additives were assumed to equal to that of the petroleum naphtha. It was found that the main components were petroleum naphtha (52-63 wt %) and C9 hydrocarbons (trimethylbenzene, 1, 2, 4-trimethylbenzene and 1, 3, 5-trimethylbenzene, 28.8 – 40.1 wt %), from the Material Safety Data Sheet (MSDS of Opti-Lube XPD is available at http://www.opti-lube.com/XPD%20MSDS.pdf). Furthermore, C9 hydrocarbons were also one of the main components of petroleum naphtha.

- All the three chemical additives had very similar net CO_2 emissions since they were all hydrocarbon mixtures with naphtha being the main components.
- Well-to-pump (WTP) greenhouse gas (GHG) emissions for naphtha have an average value of 14 g CO_2/MJ (Wang et al., 2004). A life-cycle (or well-to-wheels, WTW) analysis includes the feedstock, fuel, and vehicle operation stages. The feedstock and fuel stages together are called "well-to-pump" (WTP) or "upstream" stages, and the vehicle operation stage is called the "pump-to-wheels" (PTW) or "downstream" stage (Wang, 2002, 2008). For petroleum diesel, CO_2 emitted from the tailpipe represents 86.54% of the total CO_2 emitted across the entire life cycle of the fuel. For biodiesel, 84.43% of the CO_2 emissions occur at the tailpipe (Sheehan et al., 1998), which means that the emission of PTW phase have an average of 85% of the entire life cycle emission. This was also indicated by the Figure 5-6 in Huo et al.'s paper (2008). Therefore, we assume that WTP emission of naphtha is only 15% of the life-cycle emission, which means $\frac{WTP}{WTP + PTW} = 15\%$. Therefore, the life-cycle net GHG emission of naphtha is 93.3 g CO_2/MJ fuel.
- Theoretically, GHG emissions are CO_2-equivalent emissions of CO_2, CH_4, and N_2O. Emissions of the three GHGs are combined together with their global warming potential (GWP, 1 for CO_2, 21 for CH_4, and 310 for N_2O) to derive CO_2-equivalent GHG emissions (Wang et al., 2002). In our study, only CO_2 emission was considered, as the most important greenhouse gas contributing to global warming is carbon dioxide.

Based on the abovementioned assumptions and literature reviews, the calculation of net CO_2 emissions of biodiesel, ULSD and additives were summarized in Table 5.26. Table 5.27 and Figure 5.16 showed the net CO_2 emission and retailed prices of the optimum B11.1 from option 2 and the blends of ULSD with chemical additives such as Opti-Lube XPD, FPPF RV and Opti-Lube summer blend. The blends of ULSD with FPPF RV and

with Opti-Lube XPD performed worse in both emission and price aspects than B11.1, while the blend of ULSD with Opti-Lube summer blend was slightly cheaper than B11.1 and emit much more CO_2. Therefore, only the ULSD with Opti-Lube summer blend were analyzed and compared with B11.1 in our study.

Table 5.26 Net CO_2 emissions of biodiesel, ULSD and additives

	B100	**ULSD**	**naphtha (additives)**
net CO_2 emission (gCO_2/bhp-h)	136.45	633.28	
net CO_2 emission (gCO_2/MJ fuel)	50.66	235.90	93.30
energy content (MJ/L)	35.10	38.60	35.50
net CO_2 emission (gCO_2/gal)	6731.09	34468.98	12537.85
Retail (after-tax) price ($/gal)	3.3900	3.0460	78.5000

Table 5.27 TAC, net CO_2 emission and blend price of four blends

	ULSD+XPD	**ULSD+FPPF RV**	**ULSD+summer blends**	**B11.1**
total annualized cost (TAC) ($/yr)	86,675,800	83,983,500	81,029,700	86,316,000
net CO_2 emission (gCO_2/gal)	34517.95	34488.57	34473.16	31150.68
blend price ($/gal)	3.2133	3.1460	3.0722	3.0842

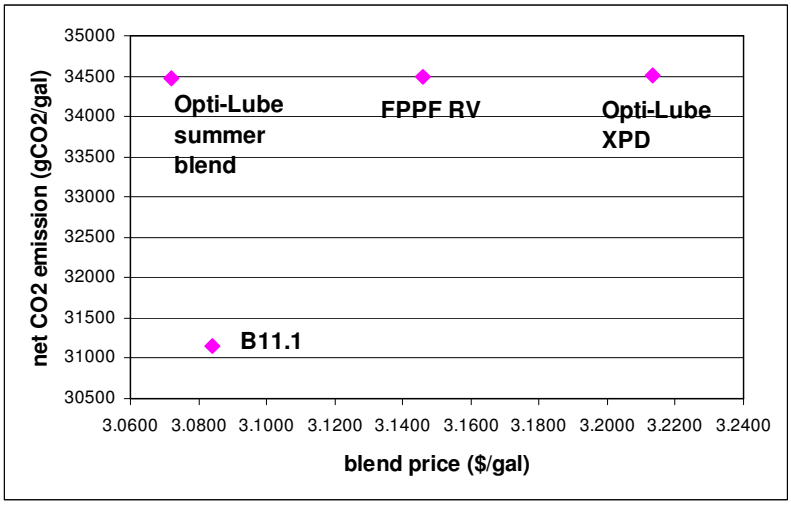

Figure 5.16 Net CO_2 emission vs. blend price of biodiesel blend and blends with chemical additives

As the usage of the petroleum fuels increases significantly, the greenhouse gas (GHG) emissions resulting from the burning of the petroleum fuels increase greatly. Being aware of the necessity of controlling or reducing the emissions, the concept of carbon credit was brought on table. Carbon credits are a critical factor of national and international emissions trading scheme for reducing the GHG emission and mitigating the global warming (wikipedia explanation of carbon credit, 2008). In carbon transactions, one party can pay another party in exchange for a given quantity of GHG emission reductions, either in the form of subsidies or "credits" that the buyer can use to achieve greenhouse gas mitigation. There are a variety of payment methods for emission reductions including cash, debt, and in-kind contributions such as providing technologies to abate GHG emissions (Capoor, K. and Ambrosi, P., 2006).

The carbon credit of biofuels is calculated as the CO_2 saved for the duty forgone (e.g., 20 pence per liter, Turley et al., 2003). For our specific case,

$$\text{Carbon credit} = \frac{\Delta price}{\Delta emissions} = \frac{(B11.1 - ULSDblends)\$/gal}{(ULSDblends - B11.1)gCO2/gal}$$

Because there is currently no market for carbon credits in the United States, the future value of carbon equivalent credits must be estimated (Stephenson et al., 2004). However, almost all biofuels produced in the U.S. today are subsidized. Ethanol suppliers receive, on average, a $0.54 per gallon subsidy (Schneider and McCarl, 2003). The subsidy for biodiesel produced from soybean oil was approximately $2.10 per gallon for the period January 1, 2004 through March 31, 2004 (Green Star Products, Inc., 2004). In addition, on May 15, 2008, the US House Ways and Means Committee approved H.R. 6049, the Energy and Tax Extenders Act of 2008. In H.R. 6049, there is a provision pertaining to biodiesel that the government will provide $1 per gallon incentive for all biodiesel regardless of feedstock (NBB, 2008). In UK, the government currently accepts £19/tonne CO_2 ($ 37/tonne CO_2, Turley et al., 2003).

Table 5.28 Carbon credit calculation of B11.1 and ULSD blend with Opti-Lube Summer Blend

carbon credit	unit
3.62E-06	$ /g CO_2
3.62	$ /ton CO_2
0.11	$ /gal B11.1
1.02	$ /gal B100

Table 5.28 showed the carbon credit results of B11.1 and the ULSD blend with the best chemical additive Opti-Lube Summer Blend. Price per gallon fuels instead of price per fuel energy was calculated, as the energy content of biodiesel and additives were very close (35.10 MJ/L for B100 vs. 35.50 MJ/L for additives, Table 5.26), and only a small portion of biodiesel and additives were blended. It was demonstrated that the US government only have to subsidize or give tax credits of $ 3.62 per tonne of CO_2 emitted, $ 0.11 per gal of B11.1 blended and $ 1.02 per pure biodiesel produced. This carbon credit calculation result matches the congress-approved provision exactly. Since

H.R. 6049, the Energy and Tax Extenders Act of 2008 has approved the $ 1 subsidy for biodiesel production regardless of the feedstock, more and more producers are expected to go for the biodiesel instead of the petrodiesel production, and the life-cycle greenhouse gas emissions are expected to decrease significantly.

5.7 Safety Comparison

Safety issue is also a crucial factor to consider when comparing and handling the biodiesel and chemical additives. Biodiesel contains no hazardous materials and is generally regarded as safe to use (DOE, 2006). As shown in the Material Safety Data Sheet (MSDS), biodiesel (MSDS is available at http://www.biodiesel.org/pdf_files/fuelfactsheets/MSDS.pdf) contains no hazardous ingredients, quite stable with a flash point of 130 ^{o}C, whereas the chemical additive Opti-Lube XPD (MSDS is available at http://www.opti-lube.com/XPD%20MSDS.pdf) as a mixture of hydrocarbons, contains 10 hazardous ingredients such as naphtha, trimethylbezene and naphthalene with stringent exposure limits given by American Conference of Governmental Industrial Hygienists (ACGIH) and Occupational Safety and Health Administration (OSHA). Opti-Lube XPD has a very low flash point of 42^{o}C and can be unstable at elevated temperature and pressures. Moreover, it is considered to be toxic to both human beings and environment. The National Fire Protection Association (NFPA) ratings of biodiesel and chemical additive were listed in Table 5.29.

Table 5.29 National Fire Protection Association (NFPA) ratings

	Health	Flammability	Reactivity	Special
biodiesel	0	1	0	NA
Opti-Lube XPD	2	2	1	NA

(0-least, 1-slight, 2-moderate, 3-high, 4-extreme)

To sum up, based on the economic estimation, carbon credit analysis for greenhouse gas (GHG) emission and safety comparison of biodiesel and chemical additives, it was believed that the blending of ULSD with biodiesel is the optimum strategy, rather than the blending of ULSD with commercial chemical additives, or blending of LSD with biodiesel fuel.

CHAPTER VI

CONCLUSIONS AND RECOMMENDATIONS FOR FUTURE WORK

This work has examined three alternatives for producing ULSD: (a) retrofitting of the refinery (e.g., addition of hydrotreating units), (b) usage of special additives, and (c) blending with biodiesel. For each alternative, process simulation, integration, and optimization tasks were undertaken. The ULSD process was revamped based on an existing LSD process. For blending with biodiesel, a grassroot soybean-oil derived biodiesel process was synthesized and analyzed. Computer-aided simulation using ASPEN Plus was applied to model the synthesized processes and examine key performance characteristics. Sensitivity analyses were performed for both processes in order to identify the optimal operating conditions and to achieve certain specifications of ULSD and biodiesel. After process synthesis and simulation, mass and heat integration activities were performed based on the simulation results. The maximum integrated heat exchange and minimum heating and cooling utilities were identified for biodiesel and ULSD using three methods: graphical (thermal pinch diagram) and algebraic (temperature-interval diagram and cascade diagram), and optimization (LINGO formulations). Economic analysis was performed for each process. Total capital investment estimation was carried out with the help of the software ICARUS Process Evaluator. Other costs such as operating costs and incomes were analyzed based on updated chemical market prices. Operating costs before and after process integration were calculated and compared.

Three blending options (LSD blended with biodiesel, ULSD blended with biodiesel, and ULSD blended with commercial chemical additives) were developed and optimization for each option was performed. Then the identified optimum blends of each option were normalized based on a target capacity of 40 million gallon per year. Economic comparisons were carried out based on several criteria including the total annualized cost, breakeven analysis, return on investment (ROI), and payback period (PP) estimation. The economic comparison indicated that the blending LSD with biodiesel

option was inferior to the other two options. The option of blending chemical additives with ULSD was slightly more profitable than the option of blending biodiesel with ULSD.

Finally, life-cycle greenhouse gas (GHG) emission and safety analysis between the biodiesel blends and commercial additive blends were performed in order to further investigate the pros and cons of the two options. It was determined that for boidiesel blending to be competitive, a carbon tax credit/subsidy of $3.62 per tonne CO_2. Biodiesel producers need to get a subsidy or tax credit of at least $ 1.02 for each gallon of pure biodiesel. This calculation result matches exactly the provision that the government will provide $1 per gallon incentive for all biodiesel regardless of feedstock in H.R. 6049, the Energy and Tax Extenders Act of 2008 approved on May 15, 2008. From the environmental and safety perspectives, the blending of ULSD with biodiesel was found to be superior to the option of blending chemical additives into ULSD. Therefore, the optimum blending strategy was identified to be the blending of ULSD with biodiesel, particularly the ULSD with 11.1% biodiesel blend for the data used in the case study.

The following tasks are recommended for future work:

- To consider biodiesel production from multiple feedstocks
- To conduct detailed and comprehensive modeling and simulation of ULSD production including various catalytic routes for hydrotreating
- To carry out experiments and theoretical analysis for the development and identification of property mixing rules for properties such as sulfur content, cetane number, lubricity and energy content, etc.
- To develop a mixed-integer nonlinear programming (MINLP) formulation as a general technique for optimizing alternative options simultaneously

REFERENCES

Ackerson, M. D., Byars, M. S, Roddey, J. B., 2004. Revamping diesel hydrotreaters for ultra-low sulfur using IsoTherming technology. Presented at 2004 National Petrochemical and Refiners Association (NRPA) annual meeting, AM-04-40.

Anderson, D., Masterson, D., McDonald, B. and Sullivan, L., 2003, August 24-28. Industrial biodiesel plant design and engineering: practical experience. Presented at the Chemistry and Technology Conference, session seven: Renewable Energy Management. International Palm Oil Conference (PIPOC), Putrajaya, Malaysia.

Aspentech, 2001. Aspen Plus 11.1 user guide. Aspen Technology, Inc., Cambridge, MA, USA.

Babich, I.V. and Moulijn, J.A., 2003. Science and technology of novel processes for deep desulfurization of oil refinery streams: a review. Fuel, 82, 607–631.

Baldwin, J., 2008. Gas and petroleum processing. CHEN 459 class notes. Chemical Engineering Department, Texas A&M University.

Bharvani, R. R. and Henderson, R.S., 2002. Revamp your hydrotreater for deep desulfurization. Hydrocarbon Processing, 81(2), 61-64.

Bingham, F. E. and Christensen, P., 2000. Revamping HDS units to meet high quality diesel specifications. Presented at the Asian Pacific Refining Technology Conference. 8-10 March, Kuala Lumpur, Malaysia.

Biodiesel Association of Canada. ASTM D975 diesel fuel specification. Available at http://www.greenfuels.org/biodiesel/tech/ASTM-D975.pdf. Accessed May 22, 2008.

BP explanation on cetane number. Available at http://www.bp.com/sectiongenericarticle.do?categoryId=4005623&contentId=7009145, Accessed May 22. 2008.

Bruno, T. J. and Smith, B. L., 2006. Improvements in the measurements of distillation curves. 1. A composition-explicit approach. Ind. Eng. Chem. Res., 45, 4371-4380.

Capoor, K. and Ambrosi, P., 2006. State and trends of the carbon market 2006. Washington DC. World Bank.

CDTECH. Mid/heavy FCC gasoline treating. Available at http://www.cdtech.com/updates/Publications/Refining%20Papers/FCC%20Gasoline%20HDS%20papers/Mid-Heavy%20FCC%20Gasoline%20treating.pdf, Accessed June 8, 2008.

Courier 4. Commercial ultra-low sulfur diesel production with Albemarle NEBULA catalyst – a success story. Issue 69. Available at http://www.albemarle.com/Products_And_services/Catalysts/Courier/Commercial_ultra-low_sulfur_diesel_prod.pdf. Accessed May 22, 2008.

Courier 11. Ultra low sulfur diesel technology update. Albemarle UD-HDS technology in U.S. commercial applications. Issue 62. Available at http://www.albemarle.com/Products_and_services/Catalysts/Courier/C62_art08_ULSD_technology.pdf. Accessed June 8, 2008.

Connemann, J. and Fischer, J., 1998. Biodiesel in Europe 1998: biodiesel processing technologies. Presented at the International Liquid Biofuels Congress, July 21, Curitiba, Paraná, Brazil.

Department of Energy (DOE), 2006. Biodiesel handling and use guidelines. Third edition, DOE/GO-102006-2358, U.S. Department of Energy, Office of Scientific and Technical Information, Oak Ridge, TN 37831-0062.

Department of the Environment and Heritage, 2004. Measuring cetane number: options for diesel and alternative diesel fuels. National Fuel Quality Standards. Canberra, Australia.

Dunn, R. F. and El-Halwagi, M. M., 2003. Process integration technology review: background and applications in the chemical process industry. Journal of Chemical Technology and Biotechnology, 78, 1011-1021.

El-Halwagi, M. M., 2006. Process integration. Academic Press, New York.

El-Halwagi, M. M., 2007. Process integration, simulation, and economics, CHEN 425 class notes. Chemical Engineering Department, Texas A&M University.

El-Halwagi, M. M., 2008. Chemical engineering optimization, CHEN 661 class notes. Chemical Engineering Department, Texas A&M University.

Encinar, J. M., González, J. F. and Rodríguez-Reinares, A., 2007. Ethanolysis of used frying oil. Biodiesel preparation and characterization. Fuel Processing Technology, 88, 513-522.

Energy Information Administration (EIA), 2001. The transition to ultra-low-sulfur diesel fuel: effects on prices and supply. Office of Integrated Analysis and Forecasting. US Department of Energy. Washington, DC 20585.

Engine Manufacturers Association (EMA). North American ultra low sulfur diesel fuel properties. Available at http://www.enginemanufacturers.org/admin/library/upload/192.pdf, accessed May 15, 2008.

Freedman, B.F., Butterfield, R.O., and Pryde, E.H., 1986. Transesterification kinetics of soybean oil, Journal of the American Oil Chemists' Society, 63, 1375-1380.

Gas Processors Suppliers Association (GPSA), 1998. Engineering data book. FPS version, Section 22, Volume II, Eleventh Edition. Tulsa, OK 74145.

Gerpen, J. V., Cetane number testing of biodiesel. Available at http://www.biodiesel.org/resources/reportsdatabase/reports/gen/19960901_gen-187.pdf. Accessed May 15, 2008.

Gerpen, J. V., Hammond, E. G., Johnson, L. A., Marley, S. J., Yu, L., Lee, I., Monyem, A., 1996. Determining the influence of contaminants on biodiesel properties. Final report prepared for The Iowa Soybean Promotion Board. Iowa State University, Ames, Iowa 50011.

Gerpen, J. V., Shanks, B., Pruszko, R., Clements, D. and Knothe, G., 2004. Biodiesel production technology August 2002- January 2004. NREL/SR-510-36244. National Renewable Energy Laboratory, Golden, Colorado 80401-3393.

Green Star Products, Inc., 2004, March 26. GSPI looks forward to highest USDA biodiesel subsidies in US history. Available at http://www.greenstarusa.com/news/04-03-26.html. Bakersfield, California.

Haas, M. J., McAloon, A. J., Yee, W. C., Foglia, T. A., 2006. A process model to estimate biodiesel production costs. Bioresource Technology, 97, 671-678.

Harwell, L. Thakkar, S., Polcar, S., Palmer, R.E. and Desai, P. H., 2003. Study outline optimum ULSD hydrotreater design. Oil & Gas Journal, 29, 50-56.

Harwell, L. Thakkar, S., Polcar, S., Palmer, R.E. and Desai, P. H., 2003. Study identifies optimum operating conditions for ULSD hydrotreaters. Oil & Gas Journal, 30, 46-51.

Hu, J., Du, Z., Li, C. and Min, E., 2005. Study on the lubrication properties of biodiesel as fuel lubricity enhancers. Fuel, 84, 1601–1606.

Hu, M.C., Ring, Z., Briker, J. and Te, M., 2002. Rigorous hydrotreater simulation. Refining, 85-91.

Huo, H., Wang, M., Bloyd, C., and Putsche, V., 2008. Life-cycle assessment of energy and greenhouse gas effects of soybean-derived biodiesel and renewable fuels. Energy Systems Division. ANL/ESD/08-2. Office of Scientific and Technical Information, US Department of Energy, Oak Ridge, TN 37831-0062.

Knothe, G., Steidley, K. R., 2005. Lubricity of components of biodiesel and petrodiesel. The origin of biodiesel lubricity, Energy & Fuels, 19, 1192-1200.

Knudsen, K. G., Cooper, B. H. and Topsoe, H., 1999. Catalyst and process technologies for ultra low sulfur diesel. Applied Catalysis A: General, 189, 205-215.

Knudsen, K. G. and Cooper, B. H. Ultra deep desulfurization of diesel: how can understanding of the underlying kinetics can reduce investment costs. Available at http://www.kfupm.edu.sa/catsymp/Symp12th/Data%5CHT-2.pdf. Accessed May 15, 2008.

Lee, S.W., Ryu, J. W. and Min, W., 2003. SK hydrodesulfurization (HDS) pretreatment technology for ultra low sulfur diesel (ULSD) production. Catalysis Surveys From Asia, 7 (4), 271-279.

Li, D. and Lee, C. K., 2001. German refiner debottlenecks diesel hydrotreaters for new sulfur specs. Oil & Gas Journal, 99 (37), 68-71.

Ma, F. and Hanna, M.A., 1999. Biodiesel production: a review. Bioresource Technology, 70, 1-15.

Meadbiofuel blending facts. Available at http://www.meadbiofuel.com/blending.htm. Accessed May 15, 2008.

Meher, L. C., Sagar, D. V. and Naik, S. N., 2006. Technical aspects of biodiesel production by transesterification -a review. Renewable and Sustainable Energy Reviews, 10, 248-268.

Myint, L. L., 2007. Process analysis and optimization of biodiesel production from vegetable oils. Master thesis, Chemical Engineering Department, Texas A&M University.

National Biodiesel Board (NBB), 2007. Specification for biodiesel (B100) –ASTM D67451-07b. Available at http://www.biodiesel.org/pdf_files/fuelfactsheets/bdspec.pdf.

National Biodiesel Board (NBB). Biodiesel production. Available at http://www.biodiesel.org/pdf_files/fuelfactsheets/production.pdf. accessed May 15, 2008.

National Biodiesel Board (NBB) news, 2008. Key house committee extends biodiesel tax incentive. May 15, Washington, D.C.

Noureddini, H., and Zhu, D., 1997. Kinetics of transesterification of soybean oil. JAOCS, 74, 1457-1463.

National Petrochemical and Refiners Association (NPRA), 2007. 2007 NPRA Q&A and Technology Forum: Answer Book. October 9-12, Austin, Texas.

Palmer, R. E., Ripperger, G. and Migliavacca, J., 2001. Revamp your hydrotreater to manufacture ultra low sulfur diesel fuel. Presented at the 2001 National Petrochemical and Refiners Association (NPRA) annual meeting. Mustang Engineers and Constructors, Houston, Texas.

Palmer, R. E. and Johnson, J. W., 2004. Review fundamentals when retrofitting for ULSD. Hydrocarbon Processing, 83 (1), 39-41.

Perry, R. H., 1997. Perry's chemical engineers' handbook. Seventh edition, ISBN 0-07-049841-5. McGraw-Hill, New York.

Peters, M. S., Timmerhaus, K. D. and West, R. E., 2003. Plant design and economics for chemical engineers, Fifth Edition, ISBN 0-07-239266-5. McGraw Hill, New York.

Seider, W., Seader, J. D. and Lewin, D. R., 2004. Product & process design principles, synthesis, analysis, and evaluation. Second edition, John Wiley and Sons, Inc. New York.

Sheehan, J., Duffield, J., Shapouri, H., Graboski, M., Camobreco, V., 1998. Life cycle inventory of biodiesel and petroleum diesel for use in an urban bus. Final report prepared for US Department of Energy's Office of Fuels Development and US Department of Agiculture's Office of Energy. National Renewable Energy Laboratory, Golden, Colorado 80401-3393. NREL/SR-580-24089.

Sheehan, J., Duffield, J., Shapouri, H., Graboski, M., Camobreco, V., 1998. An overview of biodiesel and petroleum diesel life cycles. National Renewable Energy Laboratory, Golden, Colorado 80401-3393. NREL/TP-580-24772.

Spicer, A., 2007. Diesel fuel lubricity additives study results. The diesel Place. Available at http://inchoate.harm.org/~halbritt/dodge/Diesel%20Fuel%20Additive%20V3.pdf Accessed August, 2007.

Stephenson, K., Bosch, D. and Groover, G., 2004. Carbon credit potential from intensive rotational grazing under carbon credit certification protocols. Paper prepared for

presentation at the American Agricultural Economics Association Annual meeting, , August 1-4, Denver, Colorado.

Steve Richardson & Company, LLC. Comparison of biodiesel, ULSD and CNG for use in on-road heavy-duty applications. Available at http://www.pinnaclecng.com/pdfs/Biodiesel_ULSD_CNG_Heavy_Duty%20Comparison112904.pdf. Accessed May 15, 2008.

Tanaka, Y., Okabe, A. and Ando, S., 1981. Method for the preparation of a lower alkyl ester of fatty acids. US Patent number: 4303590.

Tapasvi, D., Wiesenborn, D., Gustafson, C., 2005. Process model for biodiesel production from various feedstocks. American Society of Agricultural Engineers, 48, 2215-2221.

Turley, D., Ceddia, G., Bullard, M., 2003. Liquid biofuels – industry support, cost of carbon savings and agricultural implications. Paper prepared for Defra Organic Farming and Industrial Crops Division. Available at http://www.defra.gov.uk/farm/crops/industrial/research/reports/biofuels_industry.pdf.

Wang, M., 2002. Assessment of well-to-wheels energy use and greenhouse gas emissions of Fischer-Tropsch diesel. Prepared for Office of Energy Efficiency and Renewable Energy, U.S. Department of Energy, Washington, DC 20585.

Wang, M., Lee, H., Molburg, J., 2004. Allocation of energy use in petroleum refineries to petroleum products, implications for life-cycle energy use and emission inventory of petroleum transportation fuels. The International Journal of Life Cycle Assessment, 9 (1), 34-44.

Wang, M., 2008, March. Estimation of energy efficiencies of U.S. petroleum refineries. Available at http://www.transportation.anl.gov/software/GREET/pdfs/energy_eff_petroleum_refineries-03-08.pdf..

Westerberg, A. W., 2004. A retrospective on design and process synthesis. Computers and Chemical Engineering, 28, 447-458.

Wikipedia explanation of carbon credit, available at http://en.wikipedia.org/wiki/Carbon_credit, accessed May 15, 2008.

Wikipedia explanation of cetane number. Available at http://en.wikipedia.org/wiki/Cetane_number, accessed May 15, 2008.

Wikipedia explanation of ultra low sulfur diesel. Available at http://en.wikipedia.org/wiki/Ultra-low_sulfur_diesel, accessed May 15, 2008.

Wimmer, T., 1995. Process for the production of fatty acid esters of lower alcohols. US Patent number: 5399731.

Zhang, Y., Dube, M. A., McLean, D. D., Kates, M., 2003. Biodiesel production from waste cooking oil: 1. Process design and technological assessment. Bioresource Technology, 89, 1-16.

APPENDIX A

Appendix A1. ASPEN Plus Flowsheet of ULSD Process

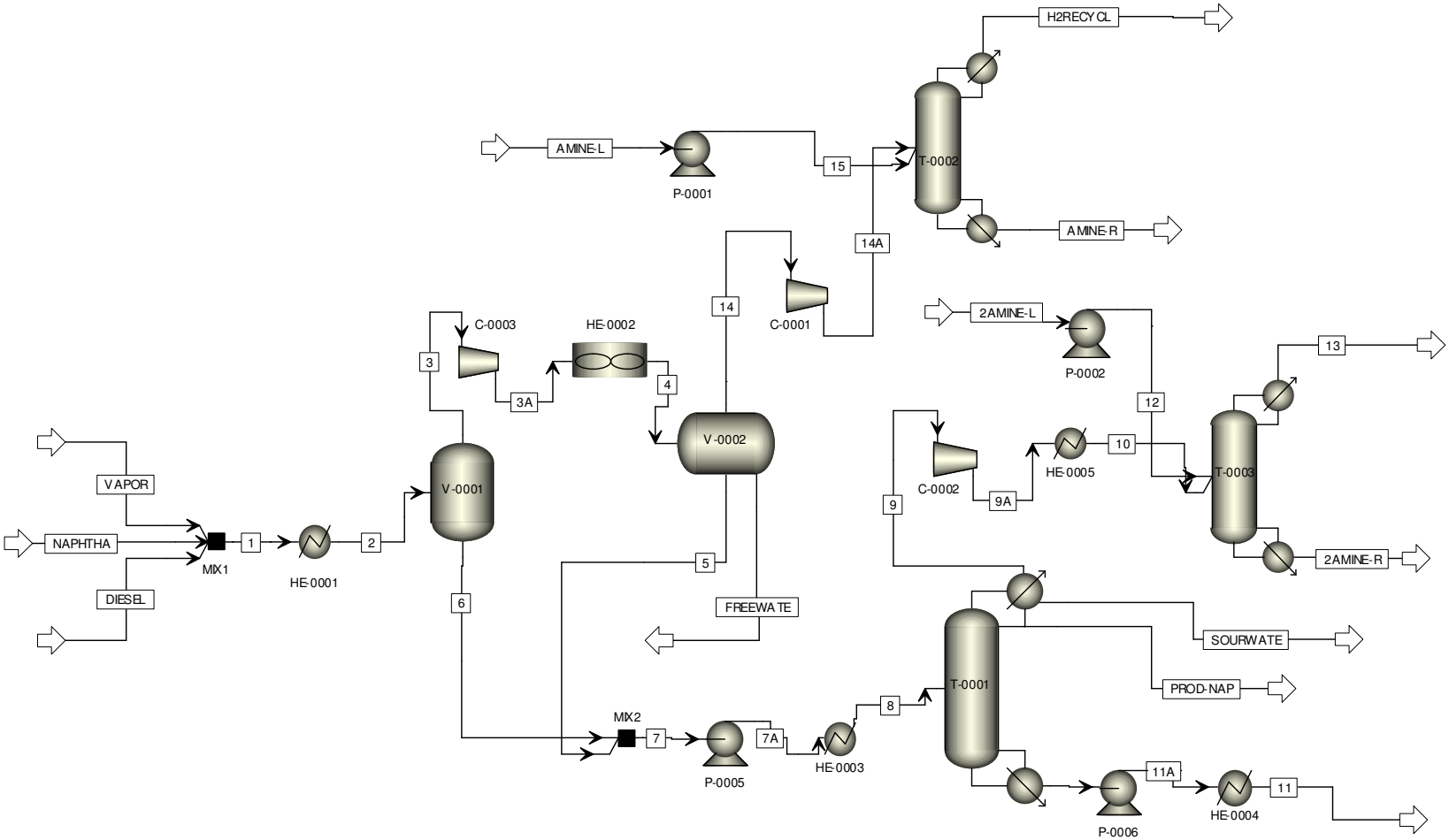

Appendix A2. ASPEN Plus Flowsheet of Biodiesel Process

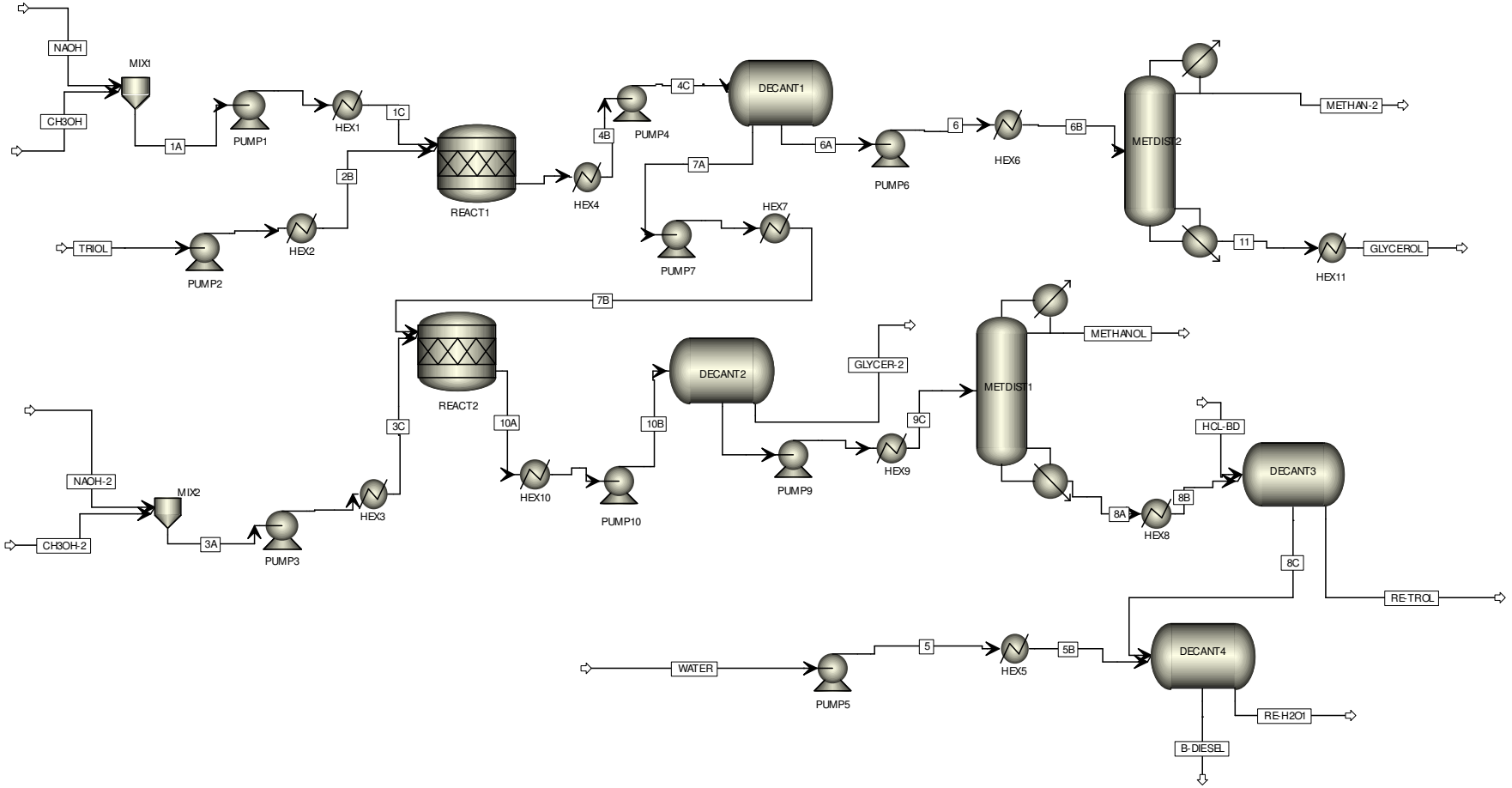

APPENDIX B

Appendix B1. Heat Integration of Biodiesel HEN Using LINGO Set Formulation

```
min=HU1;
SETS:
INTERVAL/1..13/:HOT_LOAD,COLD_LOAD,HOTU_LOAD,COLDU_LOAD,FACTOR_HOTU,FAC
TOR_COLDU,RESIDUAL;
ENDSETS
DATA:
HOT_LOAD=
0
0
1367390
20718
207180
6151059
153776
102518
4081172
3501551
673375
0
5764713
;
COLD_LOAD=
8437044
0
0
5308149
0
0
410506
244436
60789
3161050
0
0
0
;
FACTOR_HOTU=1 0 0 0 0 0 0 0 0 0 0 0 0;
FACTOR_COLDU=0 0 0 0 0 0 0 0 0 0 0 0 1;
ENDDATA
HU1=@SUM(INTERVAL(I):HOTU_LOAD(I)*FACTOR_HOTU(I));
CU1=@SUM(INTERVAL(I):COLDU_LOAD(I)*FACTOR_COLDU(I));
@FOR(INTERVAL(I)|I#GE#2:
         HOT_LOAD(I)+HOTU_LOAD(I)*FACTOR_HOTU(I)+RESIDUAL(I-1)
         =COLD_LOAD(I)+COLDU_LOAD(I)*FACTOR_COLDU(I)+RESIDUAL(I));
!FOR THE 1ST INTERVAL;
```

```
HOT_LOAD(1)+HOTU_LOAD(1)*FACTOR_HOTU(1)=COLD_LOAD(1)+COLDU_LOAD(1)*FACT
OR_COLDU(1)+RESIDUAL(1);
!FOR THE LAST INTERVAL;
HOT_LOAD(13)+HOTU_LOAD(13)*FACTOR_HOTU(13)+RESIDUAL(12)=COLD_LOAD(13)+C
OLDU_LOAD(13)*FACTOR_COLDU(13);
@FOR(INTERVAL(I):RESIDUAL(I)>=0);
END

Global optimal solution found.
  Objective value:                              0.1235708E+08
  Total solver iterations:                              0


                     Variable           Value        Reduced Cost
                          HU1       0.1235708E+08        0.000000
                          CU1       0.1675856E+08        0.000000
                 HOT_LOAD( 1)        0.000000            0.000000
                 HOT_LOAD( 2)        0.000000            0.000000
                 HOT_LOAD( 3)        1367390.            0.000000
                 HOT_LOAD( 4)        20718.00            0.000000
                 HOT_LOAD( 5)        207180.0            0.000000
                 HOT_LOAD( 6)        6151059.            0.000000
                 HOT_LOAD( 7)        153776.0            0.000000
                 HOT_LOAD( 8)        102518.0            0.000000
                 HOT_LOAD( 9)        4081172.            0.000000
                HOT_LOAD( 10)        3501551.            0.000000
                HOT_LOAD( 11)        673375.0            0.000000
                HOT_LOAD( 12)        0.000000            0.000000
                HOT_LOAD( 13)        5764713.            0.000000
                COLD_LOAD( 1)        8437044.            0.000000
                COLD_LOAD( 2)        0.000000            0.000000
                COLD_LOAD( 3)        0.000000            0.000000
                COLD_LOAD( 4)        5308149.            0.000000
                COLD_LOAD( 5)        0.000000            0.000000
                COLD_LOAD( 6)        0.000000            0.000000
                COLD_LOAD( 7)        410506.0            0.000000
                COLD_LOAD( 8)        244436.0            0.000000
                COLD_LOAD( 9)        60789.00            0.000000
               COLD_LOAD( 10)        3161050.            0.000000
               COLD_LOAD( 11)        0.000000            0.000000
               COLD_LOAD( 12)        0.000000            0.000000
               COLD_LOAD( 13)        0.000000            0.000000
                HOTU_LOAD( 1)       0.1235708E+08        0.000000
                HOTU_LOAD( 2)        0.000000            0.000000
                HOTU_LOAD( 3)        0.000000            0.000000
                HOTU_LOAD( 4)        0.000000            0.000000
                HOTU_LOAD( 5)        0.000000            0.000000
                HOTU_LOAD( 6)        0.000000            0.000000
                HOTU_LOAD( 7)        0.000000            0.000000
                HOTU_LOAD( 8)        0.000000            0.000000
                HOTU_LOAD( 9)        0.000000            0.000000
               HOTU_LOAD( 10)        0.000000            0.000000
               HOTU_LOAD( 11)        0.000000            0.000000
```

HOTU_LOAD(12)	0.000000	0.000000
HOTU_LOAD(13)	0.000000	0.000000
COLDU_LOAD(1)	0.000000	0.000000
COLDU_LOAD(2)	0.000000	0.000000
COLDU_LOAD(3)	0.000000	0.000000
COLDU_LOAD(4)	0.000000	0.000000
COLDU_LOAD(5)	0.000000	0.000000
COLDU_LOAD(6)	0.000000	0.000000
COLDU_LOAD(7)	0.000000	0.000000
COLDU_LOAD(8)	0.000000	0.000000
COLDU_LOAD(9)	0.000000	0.000000
COLDU_LOAD(10)	0.000000	0.000000
COLDU_LOAD(11)	0.000000	0.000000
COLDU_LOAD(12)	0.000000	0.000000
COLDU_LOAD(13)	0.1675856E+08	0.000000
FACTOR_HOTU(1)	1.000000	0.000000
FACTOR_HOTU(2)	0.000000	0.000000
FACTOR_HOTU(3)	0.000000	0.000000
FACTOR_HOTU(4)	0.000000	0.000000
FACTOR_HOTU(5)	0.000000	0.000000
FACTOR_HOTU(6)	0.000000	0.000000
FACTOR_HOTU(7)	0.000000	0.000000
FACTOR_HOTU(8)	0.000000	0.000000
FACTOR_HOTU(9)	0.000000	0.000000
FACTOR_HOTU(10)	0.000000	0.000000
FACTOR_HOTU(11)	0.000000	0.000000
FACTOR_HOTU(12)	0.000000	0.000000
FACTOR_HOTU(13)	0.000000	0.000000
FACTOR_COLDU(1)	0.000000	0.000000
FACTOR_COLDU(2)	0.000000	0.000000
FACTOR_COLDU(3)	0.000000	0.000000
FACTOR_COLDU(4)	0.000000	0.000000
FACTOR_COLDU(5)	0.000000	0.000000
FACTOR_COLDU(6)	0.000000	0.000000
FACTOR_COLDU(7)	0.000000	0.000000
FACTOR_COLDU(8)	0.000000	0.000000
FACTOR_COLDU(9)	0.000000	0.000000
FACTOR_COLDU(10)	0.000000	0.000000
FACTOR_COLDU(11)	0.000000	0.000000
FACTOR_COLDU(12)	0.000000	0.000000
FACTOR_COLDU(13)	1.000000	0.000000
RESIDUAL(1)	3920041.	0.000000
RESIDUAL(2)	3920041.	0.000000
RESIDUAL(3)	5287431.	0.000000
RESIDUAL(4)	0.000000	1.000000
RESIDUAL(5)	207180.0	0.000000
RESIDUAL(6)	6358239.	0.000000
RESIDUAL(7)	6101509.	0.000000
RESIDUAL(8)	5959591.	0.000000
RESIDUAL(9)	9979974.	0.000000
RESIDUAL(10)	0.1032048E+08	0.000000
RESIDUAL(11)	0.1099385E+08	0.000000
RESIDUAL(12)	0.1099385E+08	0.000000
RESIDUAL(13)	0.000000	0.000000

Appendix B2. Heat Integration of ULSD HEN Using LINGO Set Formulation

```
min=HU1;
SETS:
INTERVAL/1..9/:HOT_LOAD,COLD_LOAD,HOTU_LOAD,COLDU_LOAD,FACTOR_HOTU,FACT
OR_COLDU,RESIDUAL;
ENDSETS
DATA:
HOT_LOAD=
107243032
5617965
5460879
321228
3212282
43509159
104538221
350753916
38149075
;
COLD_LOAD=
0
0
0
231856905
0
0
0
0
0
;
FACTOR_HOTU=1 0 0 0 0 0 0 0 0;
FACTOR_COLDU=0 0 0 0 0 0 0 0 1;
ENDDATA
HU1=@SUM(INTERVAL(I):HOTU_LOAD(I)*FACTOR_HOTU(I));
CU1=@SUM(INTERVAL(I):COLDU_LOAD(I)*FACTOR_COLDU(I));
@FOR(INTERVAL(I)|I#GE#2:
         HOT_LOAD(I)+HOTU_LOAD(I)*FACTOR_HOTU(I)+RESIDUAL(I-1)
         =COLD_LOAD(I)+COLDU_LOAD(I)*FACTOR_COLDU(I)+RESIDUAL(I));
!FOR THE 1ST INTERVAL;
HOT_LOAD(1)+HOTU_LOAD(1)*FACTOR_HOTU(1)=COLD_LOAD(1)+COLDU_LOAD(1)*FACT
OR_COLDU(1)+RESIDUAL(1);
!FOR THE LAST INTERVAL;
HOT_LOAD(9)+HOTU_LOAD(9)*FACTOR_HOTU(9)+RESIDUAL(8)=COLD_LOAD(9)+COLDU_
LOAD(9)*FACTOR_COLDU(9);
@FOR(INTERVAL(I):RESIDUAL(I)>=0);
END
```

Global optimal solution found.
  Objective value: 0.1132138E+09
  Total solver iterations: 0

Variable	Value	Reduced Cost
HU1	0.1132138E+09	0.000000
CU1	0.5401627E+09	0.000000
HOT_LOAD(1)	0.1072430E+09	0.000000
HOT_LOAD(2)	5617965.	0.000000
HOT_LOAD(3)	5460879.	0.000000
HOT_LOAD(4)	321228.0	0.000000
HOT_LOAD(5)	3212282.	0.000000
HOT_LOAD(6)	0.4350916E+08	0.000000
HOT_LOAD(7)	0.1045382E+09	0.000000
HOT_LOAD(8)	0.3507539E+09	0.000000
HOT_LOAD(9)	0.3814908E+08	0.000000
COLD_LOAD(1)	0.000000	0.000000
COLD_LOAD(2)	0.000000	0.000000
COLD_LOAD(3)	0.000000	0.000000
COLD_LOAD(4)	0.2318569E+09	0.000000
COLD_LOAD(5)	0.000000	0.000000
COLD_LOAD(6)	0.000000	0.000000
COLD_LOAD(7)	0.000000	0.000000
COLD_LOAD(8)	0.000000	0.000000
COLD_LOAD(9)	0.000000	0.000000
HOTU_LOAD(1)	0.1132138E+09	0.000000
HOTU_LOAD(2)	0.000000	0.000000
HOTU_LOAD(3)	0.000000	0.000000
HOTU_LOAD(4)	0.000000	0.000000
HOTU_LOAD(5)	0.000000	0.000000
HOTU_LOAD(6)	0.000000	0.000000
HOTU_LOAD(7)	0.000000	0.000000
HOTU_LOAD(8)	0.000000	0.000000
HOTU_LOAD(9)	0.000000	0.000000
COLDU_LOAD(1)	0.000000	0.000000
COLDU_LOAD(2)	0.000000	0.000000
COLDU_LOAD(3)	0.000000	0.000000
COLDU_LOAD(4)	0.000000	0.000000
COLDU_LOAD(5)	0.000000	0.000000
COLDU_LOAD(6)	0.000000	0.000000
COLDU_LOAD(7)	0.000000	0.000000
COLDU_LOAD(8)	0.000000	0.000000
COLDU_LOAD(9)	0.5401627E+09	0.000000
FACTOR_HOTU(1)	1.000000	0.000000
FACTOR_HOTU(2)	0.000000	0.000000
FACTOR_HOTU(3)	0.000000	0.000000
FACTOR_HOTU(4)	0.000000	0.000000
FACTOR_HOTU(5)	0.000000	0.000000
FACTOR_HOTU(6)	0.000000	0.000000
FACTOR_HOTU(7)	0.000000	0.000000
FACTOR_HOTU(8)	0.000000	0.000000
FACTOR_HOTU(9)	0.000000	0.000000
FACTOR_COLDU(1)	0.000000	0.000000

FACTOR_COLDU(2)	0.000000	0.000000
FACTOR_COLDU(3)	0.000000	0.000000
FACTOR_COLDU(4)	0.000000	0.000000
FACTOR_COLDU(5)	0.000000	0.000000
FACTOR_COLDU(6)	0.000000	0.000000
FACTOR_COLDU(7)	0.000000	0.000000
FACTOR_COLDU(8)	0.000000	0.000000
FACTOR_COLDU(9)	1.000000	0.000000
RESIDUAL(1)	0.2204568E+09	0.000000
RESIDUAL(2)	0.2260748E+09	0.000000
RESIDUAL(3)	0.2315357E+09	0.000000
RESIDUAL(4)	0.000000	1.000000
RESIDUAL(5)	3212282.	0.000000
RESIDUAL(6)	0.4672144E+08	0.000000
RESIDUAL(7)	0.1512597E+09	0.000000
RESIDUAL(8)	0.5020136E+09	0.000000
RESIDUAL(9)	0.000000	0.000000

Appendix B3. LINGO Formulation for Blending Option 2

```
min=8738100*0.9*x^0.6/5+133083600*x+3012100*0.9*
(1-x)^0.6/10+79712400*(1-x);
x>0.02;
x<0.2;
40*(1-x)+67*x>=43;
end
```

with the results:

```
Objective value:                              0.8631599E+08
  Extended solver steps:                                 2
  Total solver iterations:                              13


                     Variable           Value        Reduced Cost
                            X       0.1111111            0.000000
```

VITA

Name:	Ting Wang
Address:	Artie McFerrin Department of Chemical Engineering Texas A&M University College Station, TX 77843-3136
Email address:	wanting426@hotmail.com
Education:	B.S., Biochemical Engineering, 2005 East China University of Science and Technology M.S., Chemical Engineering, 2006 National University of Singapore M.S., Chemical Engineering, 2008 Texas A&M University